Investigating the Role of KRAS Mutation in Peritoneal Carcinomatosis

by

Hande Süer

A Dissertation Submitted to the
Graduate School of Health Sciences
in Partial Fulfilment of the Requirements for the
Degree of
Doctor of Philosophy

in

Cellular and Molecular Medicine

KOÇ ÜNİVERSİTESİ

January 13, 2022

Investigating the Role of KRAS Mutation in Peritoneal Carcinomatosis

Koç University

Graduate School of Health Sciences

This is to certify that I have examined this copy of a doctoral dissertation by

Hande Süer

and have found that it is complete and satisfactory in all respects,
and that any and all revisions required by the final
examining committee have been made.

Committee Members:

Prof. Dr. Nazmi Volkan Adsay (Advisor)

Prof. Dr. Yasemin Gürsoy Özdemir (Co-advisor)

Prof. Dr. Özgür Öktem

Prof. Dr. Murat Akyıldız

Prof. Dr. Murat Mert Erkan

Prof. Dr. Güralp Onur Ceyhan

Date: _____

To my mother and my blended family…

ABSTRACT

Investigating the Role of KRAS Mutation in Peritoneal Carcinomatosis

Hande Süer

Doctor of Philosophy in Cellular and Molecular Medicine
January 13, 2022

The peritoneal carcinomatosis comprises a sequence of complex events starting from tumour detachment from its primary site, surviving in the peritoneal cavity, adherence to mesothelial surface, penetration, and invasion into submesothelial space where it can form a secondary tumour. Gastrointestinal cancers, particularly pancreatic ductal adenocarcinoma (PDAC) and colorectal carcinoma (CRC), have tendencies to metastasise to the peritoneum, so we investigated the underlying reasons of this proclivity in this project. We formed our hypothesis from a case where a patient had hepatocellular carcinoma (HCC) rupture, tumour spillage was found in the peritoneal cavity, and it was still viable. However, neither by the time of the surgery nor in three-year post-operation follow-up was any peritoneal dissemination observed. With the inspiration of this case, this project focused on the effect of KRAS mutation. Due to its frequency in PDAC and CRC, we transduced KRAS mutation to HCC cell lines, which originally held a wild-type KRAS, and investigated the molecular alterations caused by this mutation. We also examined pre-metastatic niche formation in the form of fibrotic reaction when HCC cells co-cultured with hepatic stellate cells. As a result, we found that HCC cells could proliferate, migrate, or form colonies without needing an additional mutation, which supports our clinical case. We created a screen that includes genes that have a role in peritoneal carcinomatosis, fibrosis and are related to KRAS mutation in general. We did not observe significant changes that KRAS induced in adhesion and penetration steps of peritoneal carcinomatosis. However, we gathered compelling information about gene expression patterns that differ in diverse co-culture conditions. This could help us understand tumour-stromal cell crosstalk and could be employed as the foundation for further evaluations of tumour premetastatic niche formation.

ÖZETÇE

Periton karsinomatozunda KRAS Mutasyonunun Rolünün Araştırılması

Hande Süer

Hücresel ve Moleküler Tıp, Doktora
Ocak 13, 2022

Periton karsinomozu, tümörün birincil konumundan kopmasıyla başlayan ve daha sonra periton yüzeyine tutunup, submezotelyal tabakaya sızmasıyla ikincil lokasyonunu oluşturana kadar olan süreci kapsamaktadır. Pankreatik duktal adenokarsinom (PDAK) ve kolorektal karsinom (KRK) başta olmak üzere gastrointestinal kanserler periton metastazına yatkınlık göstermektedirler. Söz konusu projenin hipotezi klinik bir vaka üzerinden şekillendirilmiştir. Bu vakada hepatoselüler karsinomlu (HSK) bir hastada tümör büyümesinden kaynaklı rüptür tespit edilmiştir. Ameliyat esnasında karın boşluğuna dökülmüş canlı tümör parçalarına rastlanmış, ancak hastada ne ameliyat esnasında ne de üç yıllık ameliyat sonrası takibinde peritonal yayılım gözlenmemiştir. Bu klinik durumdan yola çıkıp ve PDAK ve KRK'nin peritona metastaza yatkınlığı da göze önünde bulundurarak, çalışmamızda KRAS mutasyonunun periton karsinomatozundaki rolünün araştırmasına karar verilmiştir. KRAS mutasyonu PDAK ve KRK'de sıklıkla görülen bir mutasyon olup, HSK hücreleri KRAS wild- type'tır. Bundan dolayı HSK hücre hatlarına KRAS mutasyonu viral transdüksiyon yoluyla entegre edildikten sonra HSK hücrelerindeki moleküler değişiklikler incelenmiş, daha sonra bu hücreler insan hepatik stellate hücreleriyle birlikte ko-kültür edilerek oluşan fibrozis formunda ön metastatik niş oluşumları araştırılmıştır. Elde edilen sonuçlara göre HSK hücrelerinin ek mutasyona ihtiyaçları olmaksızın çoğalabildikleri, göç edebildikleri ve yumuşak agarozda koloni oluşturabildikleri gözlemlenmiş olup, bu veri hipotezin oluşmasında temel alınan klinik vakayı desteklemektedir. İkinci aşamada moleküler değişikliklerin incelenmesi amacıyla periton metastazında ve fibroziste ön plana çıkan genlerin bulunduğu bir panel oluşturulmuştur. Oluşturulan panel, ko-kültür yapılan hücrelere uygulandığında, her ne kadar KRAS mutasyonunun direkt olarak etkilediği anlamlı bir hedefe rastlanmadıysa da farklı ko-kültür ortamlarında mutasyondan bağımsız olarak kanser hücrelerinde değişiklik gösteren gen ifadelerine rastlanmıştır. Bulunan farklılıklar tümör- stroma arasındaki ilişkinin aydınlanmasında yardımcı olurken, aynı zamanda bu tümörlerin ön metastatik niş oluşturması ile ilgili yapacağımız araştırmaların da temelini oluşturacağı düşünülmektedir.

ACKNOWLEDGMENTS

First and foremost, I would like to thank my advisor Prof. Dr. Murat Mert Erkan for seeing my potential and including me in his team. When you introduced me to your research area, I knew that I was exactly where I was meant to be from day one. You saw that I was the person who likes challenges, and you provided me the window of independence in my research, respected my ideas and patiently waited to see how things turned out. You taught me how to fish, so now let us have some fish pies.

I would also like to thank Prof. Dr. Nazmi Volkan Adsay. He was there for me when things went a little unexpected. Your support along the way was invaluable. He always spared me some of his time, even when he was in a rush, trying to make the world of pathology a better place. I hope we continue working together in the future.

I am also very thankful for my committee members, who were there when they were most needed. Your comments about my work only encouraged me for the better. I would also like to thank for KUTTAM supporting my thesis financially and providing me with the best environment to conduct my research.

Being in the lab is my whole life, but without you, Burge Ulukan, what kind of life would that be. I think you are the best thing that happened to me in my PhD years. You are the best labmate and roommate, but essentially the best friend. You are the smartest, wittiest, and most competent person I have known. Thank you for being there when I had several breakdowns and things went -really- south. I am the happiest when I am with you, no matter what. I appreciate you, truly. Dr. Noushin Zibandeh, you deserve great things in life. Your love for science is inspirational. So far, nothing has been served us on a silver platter; we always had to go and grab it, but this definitely made us better at what we are doing. I believe in you and thank you for believing me. And lastly, Francesko Hela, my little brother, you are smart (maybe a little too smart), you are worthy, and you are just so annoying sometimes, goodness me. You can, and will, just do great things. Life can get overwhelming sometimes for all of us, but here we are to face it, together…

Throughout my PhD, lots of unexpected things happened, good and bad, but the most unexpected thing happened by the end of it. Nathan Ross Mickler, you and your little, the most joyful baggage are the best things that ever happened to me. Your love and support, the way you calm me down when I am frustrated, the way you care are… I have no words for it… and I never run out of words. Thank you for being in my life. I love our little blended family. I cannot wait to see what the future holds for us.

Lastly, but most importantly, I want to thank my mother; without her unconditional love and support, I would not be able to accomplish anything. She single-handedly brought me up and sacrificed everything so that I could have a better life. She is the strongest, smartest, and most wonderful and capable woman I have ever seen. Even though she complains about the amount of studying from time to time, I always know she is so proud of me. My accomplishments are your accomplishments, mummy. I love you with all my heart. Thank you for being my mother.

TABLE OF CONTENTS

LIST OF TABLES

LIST OF FIGURES

ABBREVIATIONS

α-sma	Alpha-smooth muscle actin
ANGPTN1	angiopoietin 1
c-MET	MET proto-oncogene, receptor tyrosine kinase
CD44	Cluster of differentiation 44
Col1α1	collagen type I alpha 1 chain
Col4α2	collagen type IV alpha 2 chain
CRC	Colorectal cancer
CTGF	connective tissue growth factor
CXCL12	C-X-C Motif Chemokine Ligand 12
CXCR4	C-X-C Motif Chemokine Receptor 4
DMEM	Dulbecco's Modified Eagle
DMEM-F12	Dulbecco's Modified Eagle and Ham's F12 medium
DMSO	Dimethyl sulfoxide
dPBS	Distilled phosphate buffered saline
ECL	Enhanced chemiluminescent
EDTA	Ethylenediaminetetraacetic acid
EMT	Epithelial-to-mesenchymal transition
EpCAM	epithelial cell adhesion molecule
FAK	Focal adhesion kinase/ protein tyrosine kinase 2
FBS	Foetal Bovine Serum
FGF	fibroblast growth factors
FN1	Fibronectin 1
GAP	GTPase-activating protein
GAPDH	glyceraldehyde-3-phosphate dehydrogenase
GDP	guanosine diphosphate
GFAP	Glial fibrillary acidic protein
Gli1	GLI family zinc finger 1
GOI	Gene of Interest
GTPase	guanosine triphosphatases
G12C	Glycine-to-cysteine
G12D	Glycine-to-Aspartic acid Codon 12
G12V	Glycine-to-Valine Codon 12
G13D	Glycine-to-Aspartic acid Codon 13
HAS1	hyaluronan synthase 1
HCC	Hepatocellular carcinoma
HGF	hepatocyte growth factor
HSC	Primary human hepatic stellate cell
ICAM1	Intercellular adhesion protein 1
ITGA	integrin subunit alpha
ITGB	integrin subunit beta
IL-1α	Interleukin 1 alpha
IL-1β	Interleukin 1 beta
IL-6	Interleukin 6
IL-8	C-X-C motif chemokine ligand 8

KRAS	Kristen rat sarcoma virus
LM	Low melting
L1CAM	L1 cell adhesion molecule
MAPK/ERK	Mitogen-activated protein kinase/ extracellular signal-regulated kinase
MMP	Matrix metallopeptidase
MTT	(3-(4,5-dimethylthiazol-2-yl)-2,5-diiphenyltetrazolium bromide)
MUC	Mucin
NSCLC	non-small cell lung cancer
P/S	Penicillin/Streptomycin
PBS-T	dPBS containing 0.1% Tween 20
PDAC	pancreatic ductal adenocarcinoma
PDGF	platelet-derived growth factor
PI3K/AKT/mTOR	phosphoinositide 3-kinase/protein kinase B and mechanistic target of rapamycin
Q61L/H	Glutamine-to-Leucine or Histidine codon 61
RAS	Rat sarcoma virus
RNAseq	RNA sequencing
RT	Room temperature
SDS-PAGE	Sodium dodecyl sulphate–polyacrylamide gel electrophoresis
SHH	sonic hedgehog signalling molecule
SURV	baculoviral IAP repeat containing 5
TBS-T	Tris buffered saline containing 0.1% Tween-20
TGF-β	transforming growth factor- β
TNF-α	Tumour Necrosis Factor alpha
VCAM1	Vascular cell adhesion protein 1
VEGF	vascular endothelial growth factor A
XIAP	X-linked inhibitor of apoptosis

Chapter 1

INTRODUCTION

1.1. The Peritoneum

The peritoneum is a serous membrane with a mesodermal origin. It forms the abdominal cavity lining, provides lubrication and frictionless movements of the viscera, and defends organs from infections[1]. There are three serous membranes in the body similar to the peritoneum, such as the pleura covering the thoracic cavity and lungs and the pericardium, which lines the heart. Yet, the peritoneum has the most extensive surface area, almost the equivalent of skin[2]. It divides into two categories (Figure 1.1A): parietal peritoneum that covers the walls of the abdomen and pelvis; visceral peritoneum that lines intraabdominal organs. The space between these two layers is called the peritoneal cavity, which is filled with peritoneal fluid that washes the contents of the cavity with various chemical and cellular modulators in a continuous manner.

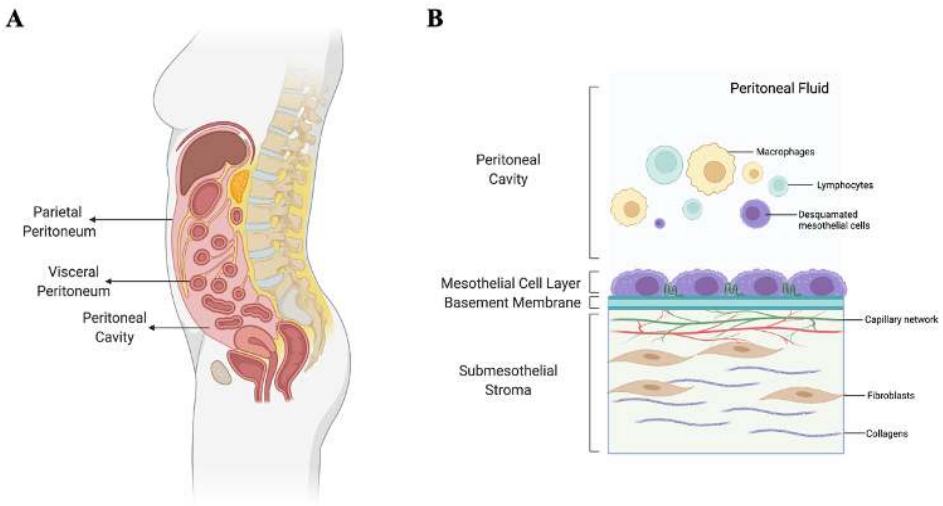

Figure 1.1: Peritoneal anatomy (A) and physiology (B)

The peritoneum contains cellular and acellular compartments: mesothelium and stroma[1] (Figure 1.1B). Mesothelium constitutes a single layer of mesothelial cells, which are mesenchymal-epithelial cells resting on a basement membrane that is responsible for providing lubrication by secreting hyaluronic acid proteoglycans and phospholipids, maintaining homeostasis and tissue repair[3]. Mesothelial cells and the basement membrane constitute the first line of defence against bacterial peritonitis and act as a barrier to macromolecules entering the submesothelial layer[4,5]. Underneath the basement membrane, there is the stroma, which is a loose connective tissue containing cellular elements, such as fibroblasts and immune cells, and acellular elements, including glycoproteins, proteoglycans, and collagens. Blood and lymphatic vessels are found in the deep collagenous layer below the stromal compartment. The capillary network of blood and lymphatics extends to the surface of the peritoneum, which makes the peritoneum rich in blood and lymphatics[2]. Due to the hydrostatic pressure gradient between plasma and peritoneum, the peritoneal fluid contains a high level of plasma proteins, approximately 50% of the plasma concentration. Peritoneal fluid also includes a variety of immune cells such as macrophages, lymphocytes, mast cells and polymorphonuclear cells, and desquamated mesothelial cells, which are also mesothelial cells with squamous form that can differentiate into fibroblastic phenotype in the presence of inflammation and contribute the tissue repair process[2].

1.2. Peritoneal Carcinomatosis

The peritoneum can be a suitable host for metastatic cells due to its broad surface area and the presence of dynamic peritoneal fluid. Peritoneal carcinomatosis, also known as peritoneal metastasis or peritoneal dissemination, is mainly considered as locoregional cancer spread as cancers from extraperitoneal origins such as breast and lung cancer rarely metastasise to peritoneum[6]. It is frequently observed in ovarian and gastrointestinal cancers such as pancreatic, colorectal, gastric cancer. Peritoneal involvement is considered a sign of disease recurrence, particularly for gastrointestinal cancer[5]. It is associated with shorter overall survival, poor prognosis, and disease progression[7]. However, not all intraabdominal cancers have the same proclivity for peritoneal dissemination[6]. For example, it is a rare event for hepatocellular carcinoma (HCC) even though the liver is in proximity to the peritoneum.

Therefore, the underlying reason for cancer cells' tendency to the peritoneum remains elusive.

Peritoneal metastasis refers to a complex sequence of events. It is different from hematogenous metastasis, where the tumour cells travel to their secondary site through systemic circulation; peritoneal metastasis originates mainly by the exfoliation of the cells from the primary tumour site and spread transcoelomically. Exfoliation can be spontaneous, as tumour ruptures due to its increased size, or iatrogenically, resulting from incomplete resection of the primary lesion or cancerous cell efflux from dissected blood and lymph channels[8]. Other factors that may initiate exfoliation are high interstitial pressure caused by fibrosis and the stiffness of the interstitial matrix, increased osmotic pressure due to anaerobic glycolysis and leakage of plasma proteins[9]. These proceedings are more applicable to gastrointestinal cancers; as for ovarian cancer, intraperitoneal seeding could mostly occur directly as peritoneal mesothelial cells constitute a continuity with ovarian epithelium[1].

In literature, the events in peritoneal carcinomatosis are evaluated in four stages known as peritoneal metastatic cascade[8] (Figure 1.2). As the first step, the individual cells or clumps of cells need to break free from the primary tumour and gain access to the abdominal cavity. The cells are carried by the peritoneal fluid, which is shown as not only a passive carrier but also an active contributor to the disease progression via creating a pro-inflammatory environment[1]. Nevertheless, not all free-floating cells could implant in the peritoneum; therefore, adhesion to the surface of the mesothelium is a necessity. In fact, the adhesion is the most crucial step, which presumably causes the different tendencies of different cancers to the peritoneum[10]. Once a successful attachment occurs, the cancer cells penetrate the mesothelial cell layer and reach the growth factor-rich stroma. The last step of this cascade is the invasion of the tissue and angiogenesis to support the growth of the tumour in its secondary location.

Intraperitoneal formation of metastasis is orchestrated by reciprocal interaction between cancer cells and all populations of cells that reside in the peritoneum. Paracrine and autocrine mediators play a significant role in this interaction.

It is one of the reasons that different cancer cells have the distinctive inclination and colonisation capabilities to the peritoneum. Starting from the exfoliation from the primary tumour, free-floating cells or clumps go through various biological changes. For instance, the cells that lost cell-cell contact express a low level of E-cadherin, which is a glycoprotein located at cell adherence junctions and known as a suppressor of metastasis due to its role in maintaining cell attachment to its basement membrane[11,12]. Loss of E-cadherin is considered a hallmark of epithelial-to-mesenchymal transition (EMT) and increase cell motility and invasiveness[12]. Cells that gain motility also acquire resistance to anoikis to survive in the peritoneal fluid until they find an appropriate surface to attach[13]. Loss of E-cadherin and anoikis resistance is relatively common in metastatic cancer cells, so it is not particularly a determining step for successful implantation to peritoneum[14]. However, the EMT process is shown to induce adherence markers such as integrins on metastatic cell surfaces[11]. Ostensibly at this stage, cancer cells acquire a predisposition for attachment to the peritoneal surface.

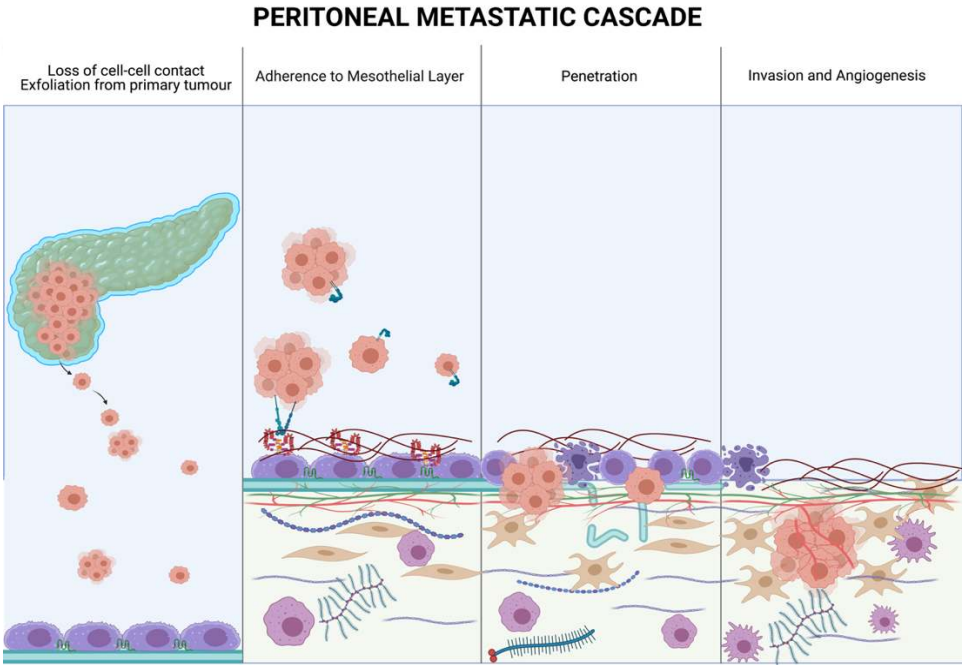

Figure 1.2: Metastatic cascade to the peritoneum. It is a multi-step process starting from tumour cells gaining access to the peritoneal cavity and spreading transcoelomic along with the peritoneal fluid, adhering to the mesothelial surface and invading the submesothelial compartment and creating a niche to nourish[5].

According to Paget's "seed and soil" concept, the primary tumour has a predisposition to specific organs, so the metastasis could not be a random event[15]. This concept has been supported by many researchers, so now it is believed that cancer cells could create an environment for themselves before arrival by altering target sites' surface receptors, recruiting cells that would secrete mitogenic factors so that would help cancer cells to nourish in the environment. In the case of peritoneal carcinomatosis, cancer cells, before encountering mesothelial cells, make mesothelial cells prepare their surface suitable for attachment in a paracrine manner. Mesothelial cells, due to their role in defence, generate chemotactic gradients to recruit immune cells to the area in case of an infection, express vascular cell adhesion protein 1 (VCAM1) and intercellular adhesion protein 1 (ICAM1) on their surface to provide leukocyte migration and secrete hyaluronan to provide a hydrophobic mechanical barrier on the surface[6]. Cancer cells that could successfully attach to mesothelial surfaces are able to alter the expression of these adhesion molecules to their favour or modify their own surface receptors to make a suitable environment for themselves. It has been seen that gastric and colon cancer cells, which successfully implanted to the mesothelium, overexpress a hyaluronan receptor cluster of differentiation 44 (CD44) on their surface[3,16]. Yasumoto et al. reported that C-X-C Motif Chemokine Receptor 4/ C-X-C Motif Chemokine Ligand 12 (CXCR4/CXCL12) axis also plays a role in attracting cancer cells to the peritoneum. They have observed that CXCR4 expressing gastric cancer are more likely to metastasise peritoneum. Later they found that its ligand, CXCL12, is highly present on mesothelial surfaces but not in liver or lymph nodes; therefore, the cancer cells are particularly drawn to the peritoneum due to CXCR4/CXCL12 attraction[17]. Other prominent players in peritoneal disseminations are integrins, which are the family of heterodimeric receptors that mediate adhesion ECM components, consisting of α and β subunits, which can assemble various combinations for ligand specificity[18]. For instance, the $\beta 1$ family of cell adhesion molecules were found to be involved in peritoneum dissemination of gastric and colorectal cancer (CRC)[19,20]. In comparison, $\alpha 5$ integrins are found to be critical for ovarian cancer attachment to peritoneum[11]. Moreover, inflammation and wound healing could make the environment more suitable for cancer cell adhesion.

Proinflammatory cytokines such as tumour necrosis factor alpha (TNF-α), interleukin 1 beta (IL-1β) and interleukin 6 (IL-6) are demonstrated to be markers of surgical trauma are known to increase adhesion via escalating the expression of ICAM-1 in mesothelial surface[9,21].

Following the adhesion step, penetration and invasion are also essential for cancer to successfully create its niche and proliferate. At this stage, matrix metallopeptidases (MMPs) have roles in breaching the basement membrane and invading neighbouring stromal tissue. Furthermore, it is shown that when the cancer cells encounter the mesothelial layer, they can induce physical changes and apoptosis. Yonemura et al. found that mesothelial cells, when contacted with cancer cells *in vitro,* undergo morphological changes and contractions, which results in cells becoming more round and separated from each other[22]. Disruption of the continuity of the mesothelial layer promotes the interaction of cancer cells with the submesothelial compartment and pave the way to penetration. It is also shown that CRC cells induce apoptosis when co-cultured with mesothelial cells through FAS-FAS ligand interaction[23]. So once the integrity of the mesothelial basement membrane is breached, cancer cells can slide into the stromal compartment. When they have access to the stromal compartment of the peritoneum, they interact with fibroblasts and initiate transdifferentiation of fibroblasts to ECM-secreting myofibroblasts. Myofibroblasts secrete various factors that induce inflammation, angiogenesis as a wound healing response which indirectly helps cancer cells to nourish in this environment.

1.3. Oncogenic KRAS

1.3.1. The role of KRAS protein:

Kristen rat sarcoma virus (KRAS) belongs to a family of rat sarcoma virus (RAS) proteins which are small guanosine triphosphatases (GTPase) with a role as a metabolic switch for various cellular processes. It is the interconnection of cell membrane growth factor receptors to intracellular signalling pathways and transcription factors[24]. KRAS protein is known as signal transducers and works in "on" and "off" manner when bound to GTP and guanosine diphosphate (GDP), respectively.

Mutation in KRAS obstructs the binding of GTPase-activating proteins (GAP), which hydrolyse GTP; therefore, the switch cannot be "off", and KRAS stays constitutively active in cells. Commonly seen mutation occurs in codon 12 with the replacement of glycine to valine (G12V) or glycine to aspartic acid (G12D), which prevent forming van der Waals bonds between KRAS protein and GAP and obstruct GTP hydrolysis. Other mutations also occur in codon 13 glycine to aspartic acid (G13D) and in codon 61 glutamine to leucine or histidine (Q61L/H), but these mutations are less common and, according to several studies, not as aggressive[25]. Even though all mutations are assumed to have a similar effect on tumour metabolisms, accumulating evidence shows that they can have different impacts on downstream pathways[25,26].

Activated KRAS interacts with more than 80 downstream effector proteins and signalling pathways, including mitogen-activated protein kinase/ extracellular signal-regulated kinase (MAPK/ERK) pathway, which has a diverse role in cellular proliferation, differentiation, inflammatory responses and cell death, phosphoinositide 3-kinase/protein kinase B and mechanistic target of rapamycin (PI3K/AKT/mTOR) pathway which is essential for proliferation and apoptosis, angiogenesis, and cell metabolism.

1.3.2. KRAS mutation in cancers

Mutation in KRAS supports cancer survival by increasing proliferation, inhibition of apoptosis, increased glucose uptake and a shift from oxidative phosphorylation to anaerobic glycolysis (Warburg effect), increased mobility and invasion capabilities either directly or via mediators they induce or suppress[27]. It is frequently seen in pancreatic ductal adenocarcinoma (PDAC) (95%), CRC (70%), and non-small cell lung cancer (NSCLC) (35%)[26].

PDAC is the most common type of pancreatic cancer. Activating point-mutation in KRAS occur is an initiating event in the majority of PDAC cases[28]. KRAS mutation influences the interaction between cancer cells and the surrounding microenvironment in PDAC in a paracrine manner[28]. KRAS modulates the Hedgehog signalling pathway and other inflammatory mediators such as IL-6, which both have roles in pancreatic stellate cell activation and desmoplasia[29-31].

Mutation in KRAS predicts the resistance of the therapies that target epidermal growth factor receptors and is associated with a higher risk of recurrence and death in CRC[32,33]. It is seen that the presence of this mutation increases the aggressiveness and metastatic potential of the tumour[25,33]. Raparia and colleagues reported that KRAS glycine-to-cysteine (G12C) mutation, which is the most seen mutation in lung cancer, is more likely to invade visceral pleura[33]. Another report showed that KRAS mutation caused malignant pleural effusion upon pleural dissemination, and the mutant KRAS is essential for malignant pleural effusion development[34]. KRAS mutation also affects the integrin profile in cancer cells[35]. It has been shown that integrin $\alpha1\beta1$, which is a collagen IV receptor, works hand in hand with KRAS mutation and promote tumour growth in NSCLC[36]. KRAS G12V mutation is found to upregulate $\alpha6$ integrin expression, which introduces cells to a more stem-cell-like phenotype, including anchorage-dependent growth and resistance to anoikis[37]

1.4. Tissue Desmoplasia and Premetastatic Niche Formation

Tissue homeostasis is maintained by normal stroma through a fine-tuned ECM synthesis, tissue remodelling and degradation[38]. When there is acute damage, stromal cells get activated via inflammatory responses and induce tissue repair. However, when the injury is chronic like cancer, which is known that a wound that never heals, then the balance between synthesis/degradation gets disrupted. It results in excess deposition of ECM components and tissue desmoplasia, which is similar to fibrosis and has been shown to lead to enhanced tumour progression. Key mediators of fibrosis are collagen-secreting myofibroblasts which are the activated form of resident fibroblasts or fibroblast-like cells. There are many inflammatory and growth factors that are secreted either from cancer cells or myofibroblasts themselves to activate ECM-secreting myofibroblasts in a paracrine and autocrine fashion. The most potent stimulants are fibroblast growth factors (FGF), transforming growth factor-β (TGF-β), platelet-derived growth factor (PDGF), connective tissue growth factor (CTGF) [39-41]. These mitogenic factors create a loop that can attract tumour cells and contribute to their survival and proliferation, and at the same time, expand desmoplasia.

It has been shown that tumours can prepare their future metastasis sites before they arrive in a manner resembling the development of fibrosis[38]. In a way that preparing a premetastatic niche by inducing collagen and fibronectin secretion in the host tissue and the recruitment of bone marrow-derived cells to form new blood vessels and create a permissive environment[38]. So, there is a high degree of overlap in mechanisms of premetastatic niche formation and development of fibrosis.

1.5. Research Proposal, Aim and Objectives

1.5.1. Clinical observation

The main idea underlying this study was based on clinical observation. Patient age of 57 admitted to hospital and diagnosed with hepatocellular carcinoma. His computed tomography results showed that the tumour ruptured and encountered peritoneum. During his surgery, tumour spillage is observed adjacent to the peritoneum. The viability of this tissue is investigated during the surgery as fresh frozen and viable tumour cells are observed within necrotic tissue. The timeline between the rupture being detected and the surgery being performed was longer than four weeks. Following the surgery, the patient was followed up for three years; however, no peritoneal metastasis was detected.

1.5.2. Hypothesis

Knowledge about the cellular and molecular determinants of peritoneal carcinomatosis still lack evidence. In PDAC and CRC, peritoneal dissemination is frequently observed. However, the same does not apply to HCC even though a viable tumour was floated in the abdominal cavity due to a rupture. Peritoneal metastasis is known as a high risk of disease recurrence, yet in the abovementioned clinical case, no seeding was observed for three years following the removal of the tumour mass. Since oncogenic KRAS is commonly seen in PDAC and CRC, we hypothesise that KRAS mutation may have a role in adherence to mesothelial cells for successful implantation. Therefore, the presence of KRAS mutation might be one of the initiating events to form a premetastatic niche in the peritoneum, and the lack of this mutation in HCC cells might avert them from forming a secondary tumour in the peritoneum.

1.5.3. Aim and objectives

This project aims to investigate the effects of the presence of KRAS mutation in HCC cells. Following the steps that occurred in our clinical case and considering the peritoneal metastatic cascade steps, the objectives to fulfil our aim in this project as follows:

Since HCC itself is a very aggressive tumour and according to the clinical case observed detachment from the primary tumour and free-floating could happen naturally, our first objective is to investigate the effect of KRAS mutation on the HCC cells' growth, spheroids forming capabilities and resistance to anoikis.

Our second objective is to examine genes that play a significant role in peritoneal metastatic cascade in KRAS mutation transduced HCC cells with or without the presence of HSCs.

Our final objective is to examine whether the KRAS mutation-induced HCCs differentially expressed genes/proteins that could potentially induce or perpetuate fibrosis when co-cultured with primary human hepatic stellate cells (HSCs).

1.5.4. Significance

To our knowledge, there is no study investigating the KRAS mutation's role in peritoneal carcinomatosis. There is some information about the impacts of KRAS mutation on adhesion molecules, ECM modifications, premetastatic niche formation but none of this can be truly applied to peritoneal dissemination. Recently there are some clinical predictions have been made that KRAS mutation may play a role in pleural infusion in lung cancer, but these predictions have not been supported by scientific research yet. Moreover, KRAS G12C mutation is frequently seen form in NSCLC, which is not a common mutation in gastrointestinal cancers. Therefore, this study's outcomes will be the first to establish the biological changes caused by the presence of KRAS mutation in HCC cell lines and their possible impacts on peritoneal dissemination.

Chapter 2

MATERIALS AND METHODS

2.1. Study design and Methodology

The study design is summarised in Figure 2.1 below. As the first step, KRAS mutation was introduced to HepG2 and Huh7 cells. Once the selection was completed, the effects of KRAS mutation that might have been caused in tumour cells were investigated. Later co-culture experiments were performed to see cellular interactions between KRAS mutation containing tumour cells and HSCs. Lastly, the gene expression screen revealed the differentially expressed gene profiles in diverse culture conditions.

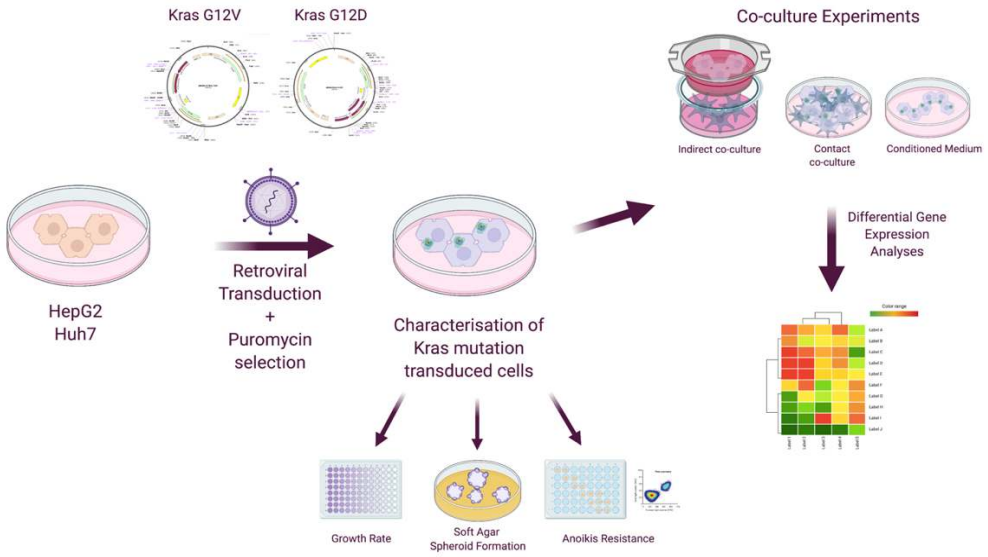

Figure 2.1: Study design illustration.

2.2. Retroviral Transduction

Human HCC cell lines, Huh7, and HepG2, used in these experiments were kindly provided by Assoc. Prof. Müjdat Zeybel. They were grown in high glucose (4.5g/l) Dulbecco's Modified Eagle Medium (DMEM) (Sigma-Aldrich, USA) with 10% foetal bovine serum (FBS) and 1% Penicillin/Streptomycin (P/S). For retroviral transduction, plasmids were purchased from Addgene (Table 2.1). Once delivered, bacteria were taken from agar stab with a loop and spread onto a pre-heated (37°C) agar plate containing 0.1% ampicillin, a selection marker for plasmid containing bacteria. Petri dishes were incubated in a 37°C incubator for 24h. A single colony was selected and mixed with 50ml LB Broth with 0.1% ampicillin. Single clone bacteria were incubated on a shaker incubator at 37°C at 2000rpm overnight. Plasmids were isolated MN Midi Plasmid DNA isolation kit. DNA concentration was measured at Nanodrop (Thermo Scientific, USA) and stored at -20°C.

Prior to viral transduction, DNA sequencing was performed to be sure that the plasmid DNAs contain KRAS mutation and HepG2 and Huh7 have wild-type KRAS. HepG2 and Huh7 genomic DNA were isolated using Quick-DNA Miniprep kit (Zymo Scientific, USA), and all the DNA samples were purified using MN Nucleospin Gel and PCR Clean-up Mini kit (Macherey- Nagel, USA) according to manufacturer's instructions for sequencing. Sanger sequencing was performed at KUISCID, Koç University, Turkey. KRAS amplified using forward primer 5’GCCTGCTGAAAATGACTGAATATA-3'.

$1x10^6$ HEK293T cells were seeded in a 10cm Petri dish overnight, and transfection was performed the next day with 2500ng gene of Interest (GOI) which are the plasmid DNAs 2500ng pumVC and 500ng pVSV-G. Plasmid DNAs were mixed with 1:5 diluted FuGENE transfection reagent in a serum-free DMEM and introduced to the cells dropwise. Plasmid DNA containing medium was discarded in 24h, and medium containing viral particles were collected following 24h and 48h. Dead cells were filtered through a 0.45µ filter, and viral particles were aliquoted as 1 ml. HepG2 and Huh7 cells were seeded one day prior to viral transduction at 250.000 cells/ 6well plate.

The following day, their medium was discarded, and the serum-free DMEM containing 8ug/ml protamine sulphate was added onto the cells and incubated for 2h; then, the virus was added to the culture dropwise. After incubation for 48h, the virus-containing medium was discarded, and a complete DMEM medium was added to the culture and left for recovery for another 48h. Following the recovery, cell mediums were changed to 2µg/ml and 2.5µg/ml puromycin (selection marker) containing complete DMEM for HepG2 and Huh7, respectively. The selection took approximately 7-10 days until the cells in negative control died utterly. Four independent transductions were performed for HepG2 cell lines (n=4) and three for Huh7 cell lines (n=3).

Table 2.1: Retroviral plasmid maps and specifics

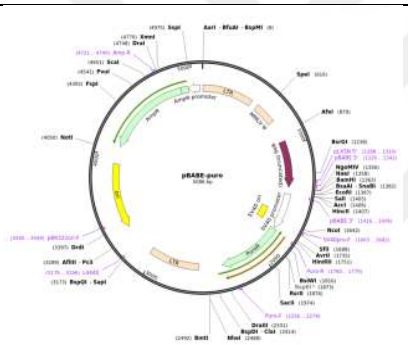	**Backbone:** pBABE-puro (Plasmid #46745) Bacterial Resistance: Ampicillin Vector Type: Mammalian Expression, Retroviral Selectable Markers: Puromycin
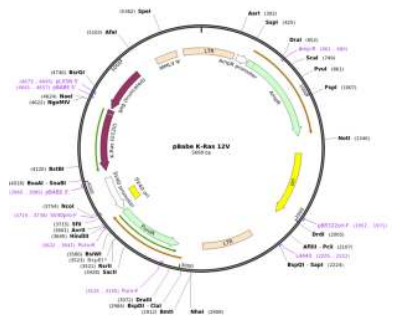	**KRAS G12V:** pBABE-G12V (Plasmid #46746) Bacterial Resistance: Ampicillin Vector Type: Mammalian Expression, Retroviral Selectable Markers: Puromycin
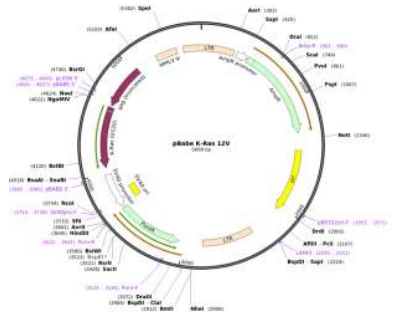	**KRAS G12D:** pBABE-G12D (Plasmid #58902) Bacterial Resistance: Ampicillin Vector Type: Mammalian Expression, Retroviral Selectable Markers: Puromycin

Retroviral particles were produced in HEK293T cell lines. 1.10^6 HEK293T were seeded on a 10 cm petri dish. Upon attachment, plasmid DNAs of GOI (pBABE backbone, pBABE KRAS G12V and pBABE KRAS G12D) were mixed with pUMVC (Plasmid #8449) DNA for viral packaging and envelop pVSV-G DNA (Plasmid #138479) in the ratio of 1:1:0.2 respectively and introduced in FUGENE Transfection Reagent (Promega, USA) and serum-free DMEM (1:4 ratio). Viral particles were collected at 48h and 72h after a medium change in the 24h time. HepG2 and Huh7 cells were seeded as 250.000 cells /6 well plate, and after 24h incubation, viral particles were introduced to cells with 8 µg/ml protamine sulphate solution. 48h of virus incubation was performed in 37°C 5% CO_2 virus incubator, and the virus-containing mediums was discarded after this incubation. The plate setup can be seen in Figure 4.

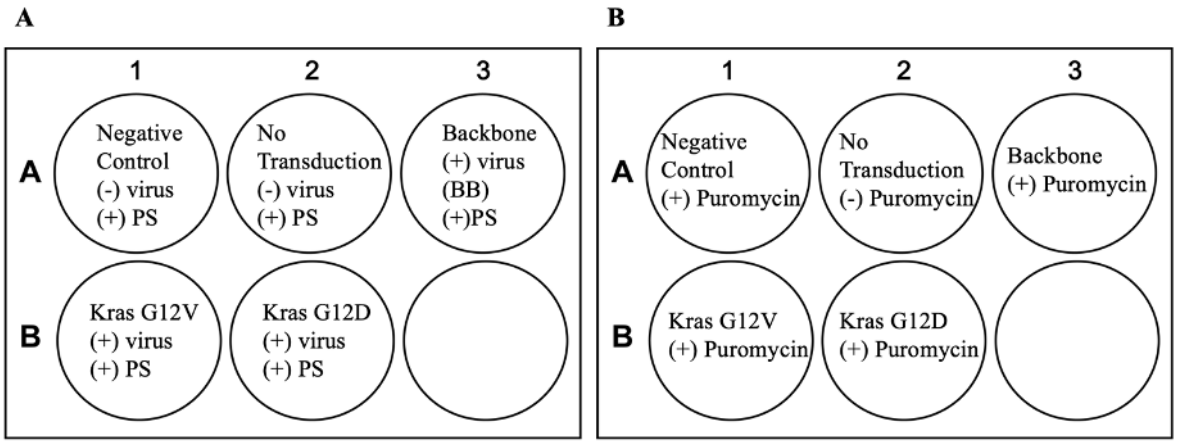

Figure 2.2: Plate setup for retroviral transduction. A. Transduction setup, B. Selection setup.

Antibiotic selection started after 24h of recovery in a complete DMEM medium. 2µg/ml and 2.5µg/ml puromycin were added to the standard DMEM medium to prepare selection mediums for HepG2 and Huh7 cell lines, respectively. The selection was terminated once the cells in the negative control (Figure 2.2B) died entirely. Cells were passaged after the termination of the selection, and half of the cells were separated as pellets for RNA isolation to check the success of the transduction.

2.3. Growth Rate: MTT (3-(4,5-dimethylthiazol-2-yl)-2,5-diiphenyltetrazolium Bromide) Assay

Huh7 and HepG2 cells were seeded to three 96 well plates as 5000 cells/well density in 100µl medium for 0h, 24h and 48h. 0h measurements were used to determine the number of cells when they all adhere to the plastic surface. 24h and 48h were to determine their growth rate. 10x MTT reagent (Invitrogen, USA) was prepared according to the manufacturer's instructions and diluted to 1x in the medium before use. On the day of analyses growth medium was removed and 100µl 1x MTT medium added to the wells and incubated for 2h in 37°C 5% CO_2 incubator. Later 75µl 1x MTT medium was removed, and 100µl Dimethyl sulfoxide (DMSO): Isopropanol mix (1:1) was added to wells to dissolve formazan crystals. Following 10 min incubation, in a 37°C oven, the plate will be read at 570 nm. The absorbance at 0h plate was accepted as zero per cent growth, and the absorbance at 24h and 48h was determined accordingly.

2.4. Soft Agar Spheroid Formation

Two different densities of 2x low-melting (LM) agarose solutions were prepared (Top and bottom). Bottom layer 2x LM agarose was 1.2% (w/v) and top layer was 0.6% (w/v) density. Both agarose solutions were stored at 4°C, liquified in the microwave before use, and then cooled down in a 42°C water bath. Prior to plating, both top and bottom layer agarose mixtures were diluted with 2x DMEM-F12 to 1x. 750µl bottom layer agarose was poured to a 12-well plate carefully avoiding air bubbles and left to solidify at room temperature (RT) for 30 min. The cell suspension was added to 1x top layer agarose as 2500 cells/ well density. 750µl of the cell containing agarose mixture were poured onto the bottom layer of agarose and left to solidify at RT for 30min before placing in the incubator. 200µl medium was added every week for three weeks, and ultimately spheroids were stained 0.01% crystal violet to determine the colonies.

2.5. Anoikis Resistance

The objective of this experiment was to investigate if KRAS mutation has any effects on the anoikis resistance of HCC cells. A low attachment surface was created on a regular cell culture plate. 48well plates were coated with 0.5% (w/v) agar-agar solution, which was prepared by mixing agar-agar with distilled water. Agar-agar mixture was then autoclaved for sterilisation as well as homogenisation. Agar-agar mixture was also stored at 4°C, microwaved and cooled down to 42°C in a water bath before use. 100µl 0.5% agar-agar solution was coated on the bottom of the plate, and the plate was incubated at RT for 30 min. 10.000 or 25.000 HCC cells were suspended in 200µl complete DMEM and added onto agar-agar coated wells. Cells clusters were collected weekly, and cell death was analysed by flow cytometry. Their medium was refreshed every five days for three weeks.

To prepare clusters for flow cytometry, cell clusters were broken into smaller clumps with ice-cold distilled phosphate-buffered saline (dPBS) with 1x ethylenediaminetetraacetic acid (EDTA) and mixed well. The cell suspension was then forced through 70µ mesh to separate clusters as single cells and washed twice with FACS buffer (1x dPBS with 1% FBS and 1x EDTA). Dead cells were then stained with BD Fixable viability stain with Pacific Blue fluorescence dye (BD Biosciences, USA), as 1µl viability stain per 1ml cell suspension. Cell suspension incubated for 10mins at RT in the dark. 1ml FACS buffer was added to the cell suspension by the end of the incubation and centrifuged at 2000 rpm for 5 min. The cells were re-suspended in 500µl of FACS buffer, and cell death was determined with flow cytometry.

Every sample had unstained controls to eliminate autofluorescence and determine the gating strategy (Figure 2.3). Cells were first gated according to their size and granulation (R1). The next gate was to eliminate small clusters, so the gating strategy was the height of the cells vs the area of the cells (R2). Finally, pacific blue-stained cells were separated from the whole population (R3-R4). 5000 and 10.000 cells were analysed for HepG2 and Huh7, respectively. Values shown in histograms were considered the percentage of cell death.

Cell viability percentage was calculated as "100% - cell death (%)". In this setting, viable cells in a low attachment environment were considered resistant to anoikis.

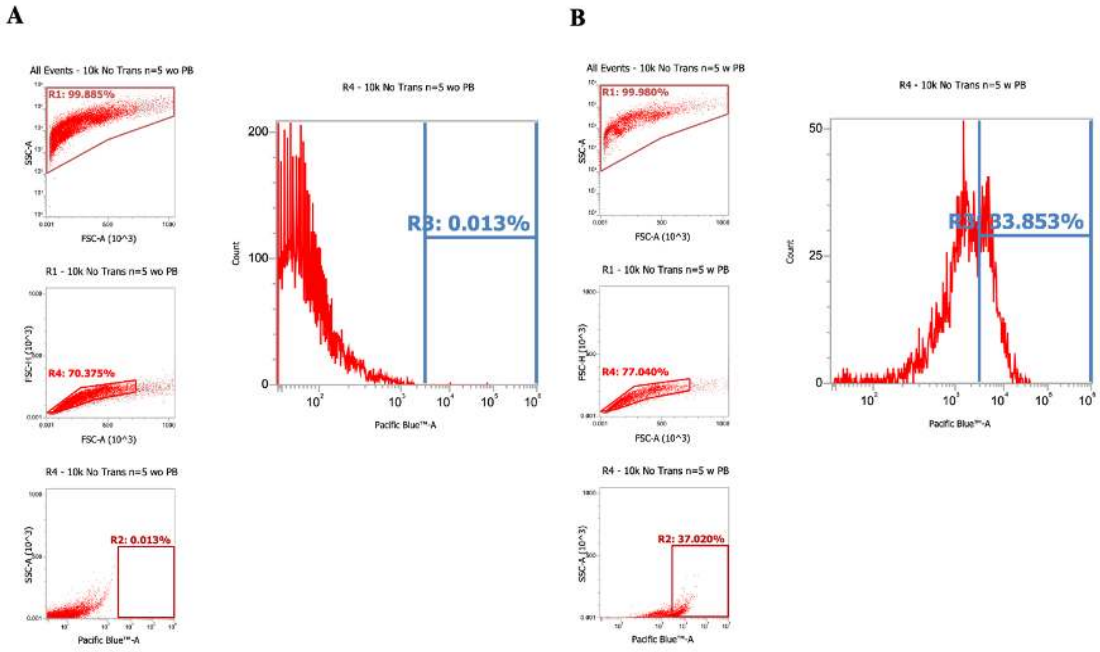

Figure 2.3: Flow cytometry gating strategy to analyse cell death.

2.6. Wound-healing Assay

The purpose of this assay was to investigate if KRAS mutation affects the mobility of the cells. HepG2 and Huh7 cells were seeded as 200.000 cells/ 12 well. 48h later, when the cells fully attached and reached confluency, a straight scratch was made in the middle of the well with a 100-1000µl pipette tip. Cell migration was recorded in 0h, 12h, 24h, 36h, 48h, 72h and 96h.

2.7. HSC Isolation, Culture, and Characterisation

HSCs were isolated from tumour-free human liver tissue from patients who underwent surgery for the removal of hydatid cysts caused by *Echinococcosis granulosus* infection (Ethics Approval number: 2017.085.IRB2.026). The ethics committee approval document can be found in Appendix A.

HSC were isolated using the Nycodenz density gradient centrifugation method (Detailed protocol for primary human stellate cells isolation protocol can be found in Appendix B) and characterised prior to cryopreservation at passage two. HSCs were cultured in DMEM-F12 with 20% FBS with 1% P/S and 1% Amphotericin B.

2.7.1. Immunofluorescence

HSCs are characterised using the immunofluorescence method. Prior to cryopreservation, cells were seeded onto 13mm glass slides. When they reached 50% confluency, the growth medium was discarded, washed with dPBS three times, and fixed with 4% paraformaldehyde for 20min at RT. Cells were permeabilised using 0.1% Triton-X100 in 1x dPBS for 7min at RT and washed three times. Blocking was performed using SuperBlock protein blocking reagent (ScyTek Laboratories, USA) for 10 min at RT.

Table 2.2: Primary and secondary antibodies used for HSC characterisation

Antibodies		**Host**	**Reactivity**	**Brand**
Primary Antibodies				
α-sma	Monoclonal	Mouse	Human	Abcam
Vimentin	Monoclonal	Rabbit	Human	Abcam
GFAP	Polyclonal	Rabbit	Human	Abcam
Nestin	Polyclonal	Rabbit	Human	Abcam
Fibronectin	Polyclonal	Rabbit	Human	Abcam
Collagen III	Polyclonal	Rabbit	Human	Abcam
Secondary Antibodies				
Goat anti Mouse IgG- FITC conjugated	Polyclonal	Goat	Mouse	Jackson Immunoresearch
Goat anti Rabbit IgG-AF488 conjugated	Polyclonal	Goat	Rabbit	Thermo Fischer
Goat anti Rabbit IgG-Cy3 conjugated	Polyclonal	Goat	Rabbit	Jackson Immunoresearch
Nucleus Dye: Fluoroshield Mounting Medium with DAPI (Abcam)				

Slides were washed three times with dPBS containing 0.1% Tween 20 (PBS-T) then incubated with 5µl 1:50 diluted primary antibodies (Table 2.2) in 37°C incubator for 90 min in a humidity chamber. Following three washes, 1:100 diluted secondary antibody was added to slides and incubated at 37°C for 90min. Glass slides were mounted with Fluoroshield DAPI containing mounting medium (Abcam, USA) and analysed with Leica Live-cell imaging fluorescence microscope.

2.8. Co-culture Assays

The purpose of these co-culture experiments was to investigate cellular interactions when they have different degrees of contact between the cell types[42]. One-sided interaction on the tumour cells was examined by conditioned medium examined they exposed to HSCs secretomes. By applying the contact culture technique, the investigation of juxtacrine communication between two types of cells was made possible. Lastly, with an indirect co-culture system, which incorporates a physical separation between cell types with a semi-permeable membrane that only enables signalling via secretome, we were able to investigate two-sided interactions between two cell types.

2.8.1. HSC conditioned medium incubation

HSCs were seeded in a T25 flask; when they reach 80-85% confluency, they have medium refreshments. Cells continued to grow in this medium for 72h, and then they were collected into vials and centrifuged at 2000 rpm for 5min to separate dead cells and debris. HepG2 and Huh7 cells were seeded as 100.000 cells/ 12-well plate 24h before the medium collection from HSCs. After centrifugation of the conditioned medium, it was given to tumour cells and incubated for 72h. After incubation, the supernatant was discarded, cells washed two times with 1x dPBS, trypsinised and pellet was collected for RNA isolation.

2.8.2. Contact culture

HSCs were cultured in 24-well plates until 80-85% confluency. Once they reached the required confluency, 50.000 HepG2 or Huh7 cells were seeded directly onto the HSCs and cultured together for 72h.

After incubation, the supernatant was discarded, cells washed two times with 1x dPBS, trypsinised and pellet was collected for RNA isolation.

2.8.3. Indirect co-culture

HSCs were cultured in 24-well plates until 80-85% confluency. Huh7 and HepG2 cells were seeded onto 0.4µ pore sized 24-well plate cell culture inserts (Sarstedt, Germany) as 50.000 cells/ insert density following an hour priming of inserts with a medium at 37°C. 24h later, both tumour cells and HSCs were primed by serum-free DMEM and DMEM-F12, respectively, for 2h to eliminate the possible effects of instant serum starvation. Priming was followed by medium refreshments (500ul DMEM-F12 to HSCs and 200ul DMEM to HCC cells) and placing inserts onto HSC cells. The co-culture system was incubated for 72h in 37°C 5% CO_2 incubator, then the experiment was terminated, and both tumour and HSC cells were trypsinised and stored as pellets for RNA isolation. The supernatant was also collected to evaluate secreted collagen and fibronectin detection by western blot.

2.8.3.1. Secreted ECM protein detection: Western Blot

Supernatants were collected and stored at 80°C until the analyses. 30µl supernatant was mixed with 4x Laemmli sample buffer with 2-beta-mercaptoethanol and boiled at 95°C for 10 min. Proteins were separated using sodium dodecyl sulphate–polyacrylamide gel electrophoresis (SDS-PAGE) method with 4-20% Mini-PROTEAN TGX Precast Protein gel (10-well, 50µl) (BIORAD, USA) at 90V for 1.5h. Then the proteins were transferred to a PVDF membrane using wet transfer with Transblot Criterion blotter (BIORAD, USA) 250mA for 90min on ice. After the transfer, the membranes were blocked with 5% skimmed milk (BIORAD, USA) in Tris buffered saline containing 0.1% Tween-20 (TBS-T) for 1h, followed by overnight incubation of 1:2500 diluted Goat polyclonal Col1α1 antibody (Santa Cruz, Germany). After washing the membrane three times with TBS-T for 5min each, the membrane was incubated with HRP conjugated rabbit anti-goat antibody (1:5000) (Santa Cruz, Germany) in 5% skimmed milk for 1h at RT.

After three washes with TBS-T, SuperSignal West Femto maximum sensitivity substrate (Thermo Scientific, USA), which contain an enhanced chemiluminescent (ECL) substrate detection kit, was added onto the membrane, and bands were detected in ChemiDoc Imaging Systems (BIORAD, USA) immediately. Following detection, membranes were stripped with mild stripping buffer pH:2.0, two times for 10min, washed with TBS-T three times for 5min, and blocked with 5% non-fat milk for 1h. Stripped membranes were incubated with 1:5000 Rabbit Polyclonal Fibronectin antibody (Abcam, USA) in 3% BSA with 0.001% NaAzide overnight. Following three washes, the membranes were incubated with HRP conjugated goat anti-rabbit antibody (1:5000) (Cell Signalling, USA) for 1h at RT. After three washes with TBS-T, ECL was added to the membranes and bands were detected immediately after.

2.10. Gene Expression Screens: RT-PCR

Total RNA isolation was performed using either Quick-RNA Miniprep Kit or Microprep kit (Zymo Research, USA), depending on the cell pellet. RNA amount and quality was measured with IMPLEN Nanophotometer (IMPLEN, Germany). 1000ng RNA was reverse transcribed to cDNA using iScript (BIORAD, USA) according to manufacturer's instructions, and cDNA volume topped up to100 µL with nuclease-free water to get the final volume of 10ng/µl.

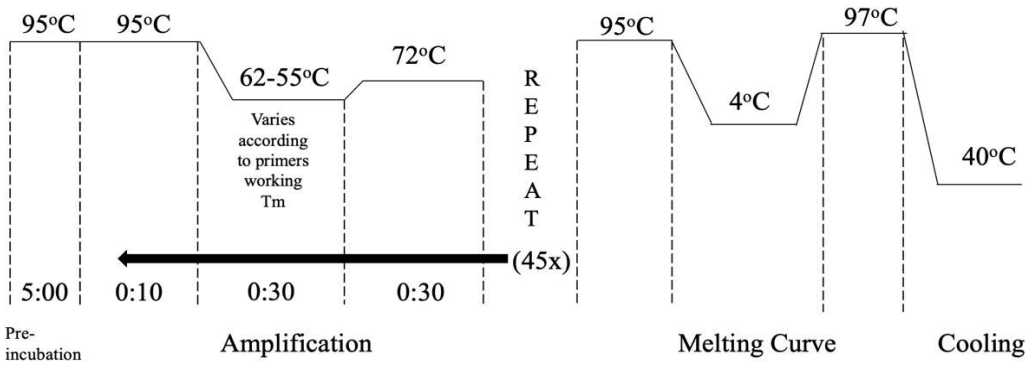

Figure 2.4: RT-PCR working protocol

RT-PCR was performed in duplicates with Lightcycler 480 SYBR Green I Master (Roche Diagnostics, USA) in QuantStudio 7 Flex Real-Time PCR System (Applied Biosystems, USA) with 10µl reaction volume containing 10ng cDNA. The amplification protocol can be seen in Figure 2.4 below. Ct values were normalised to internal control GAPDH gene expression (deltaCT), and gene expression values will be calculated 2^-delta CT method.

Screening primers were purchased from Sentromer, Turkey, and melting temperatures were optimised. First, a gradient PCR was performed to find the best working temperature, and then the serial dilution of the DNA was amplified to calculate amplification efficiency. Amplification efficiency was measured by =100*(1-10^(-1/m), where m is referred to as the slope of the line that is created as the result of serial dilution. The amplification efficiency of the primers that are used in screening experiments were over 90%. Table 2.3 shows the sequences, amplicon sizes and optimised working Tm's of the primers that are used in the experiments

Table 2.3: Genes for screening, and primer sequences for RT-PCR

	Gene Name and primer sequences	Amplicon Size	Working Tm
1	Homo sapiens glyceraldehyde-3-phosphate dehydrogenase (GAPDH)	203bp	50- 65°C
	FWD: AGGGCTGCTTTTAACTCTGGT		
	REV: CCCCACTTGATTTTGGAGGGA		
2	Homo sapiens hepatocyte growth factor (HGF)	156bp	55°C
	FWD: CCTTGCTCCTCCCTTCCTTAC		
	REV: AGTTTGGTCACCCACATGGT		
3	Homo sapiens MET proto-oncogene, receptor tyrosine kinase (c-MET)	111bp	60°C
	FWD: TGGTGCAGAGGAGCAATGG		
	REV: CATTCTGGATGGGTGTTTCCG		
4	Homo sapiens epithelial cell adhesion molecule (EpCAM)	103bp	60°C
	FWD: TGATCCTGACTGCGATGAGAG		
	REV: CTTGTCTGTTCTTCTGACCCC		
5	Homo sapiens cadherin 1 (CDH1) (E-Cadherin)	93bp	60°C
	FWD: AGTGGGCACAGATGGTGTGA		
	REV: TAGGTGGAGTCCCAGGCGTA		
6	Homo sapiens cadherin 2 (CDH2) (N-Cadherin)	293bp	60°C
	FWD: GCGTCTGTAGAGGCTTCTGG		
	REV: GCCACTTGCCACTTTTCCTG		
7	Homo sapiens vimentin	213bp	60°C
	FWD: CCAGGCAAAGCAGGAGTC		
	REV: CGAAGGTGACGAGCCATT		
8	Homo sapiens protein tyrosine kinase 2 (PTK2 or FAK)	106bp	60°C
	FWD: CAACCACCTGGGCCAGTATTATC		
	REV: CCATAGCAGGCCACATGCTTTA		
9	Homo sapiens sonic hedgehog signalling molecule (SHH)	180bp	60°C
	FWD: GCTCGGTGAAAGCAGAGAACT		
	REV: CCAGGAAAGTGAGGAAGTCG		
10	Homo sapiens GLI family zinc finger 1 (GLI1)	100bp	62°C
	FWD: ATCCTTACCTCCCAACCTCTGT		
	REV: CCAACTTCTGGCTCTTCCTGTA		

Table 2.3 continues:

11	Homo sapiens X-linked inhibitor of apoptosis (XIAP)	284bp	60°C
	FWD: GCGGTGCTTTAGTTGTCAT		
	REV: TCGGGTATATGGTGTCTGATA		
12	Homo sapiens baculoviral IAP repeat containing 5 (SURV)	408bp	60°C
	FWD: CTGTCAGCCCAACCTTCACA		
	REV: CAAACAGGTCTGGGGTTCGT		
13	Homo sapiens mucin 1, cell surface associated (MUC1)	114bp	60°C
	FWD: AGAGAAGTTCAGTGCCCAGC		
	REV: TGACATCCTGTCCCTGAGTG		
14	Homo sapiens mucin 5B, oligomeric mucus/gel-forming (MUC5B)	322bp	60°C
	FWD: TCAAGTCCGCATCAACACGA		
	REV: ACGTTCTCAGACAGCAGTGG		
15	Homo sapiens mucin 16, cell surface associated (MUC16),	161bp	60°C
	FWD: CCAGTCCTACATCTTCGGTTGT		
	REV: AGGGTAGTTCCTAGAGGGAGTT		
16	Homo sapiens collagen type I alpha 1 chain (COL1A1)	119bp	60°C
	FWD: GTGCGATGACGTGATCTGTGA		
	REV: CGGTGGTTTCTTGGTCGGT		
17	Homo sapiens actin alpha 2, smooth muscle α-sma)	109bp	60°C
	FWD: GTGTTGCCCCTGAAGAGCAT		
	REV: GCTGGGACATTGAAAGTCTCA		
18	Homo sapiens fibronectin 1 (FN1)	451bp	60°C
	FWD: TGGAACTTCTACCAGTGCCAC		
	REV: TGTCTTCCCATCATCATAACAC		
19	Homo sapiens collagen type IV alpha 2 chain (COL4A2),	139bp	60°C
	FWD: GGACAGACGAGACAACAGCA		
	REV: GAGCTGGCATAACATTGGCG		
20	Homo sapiens matrix metallopeptidase 1 (MMP1)	428bp	60°C w 2.5% DMSO
	FWD: CTGAAGGTGATGAAGCAGCC		
	REV: AGTCCAAGAGAATGGCCGAG		
21	Homo sapiens matrix metallopeptidase 2 (MMP2)	390bp	60°C
	FWD: GCGACAAGAAGTATGGCTTC		
	REV: TGCCAAGGTCAATGTCAGGA		

Table 2.3 continues:

22	Homo sapiens matrix metallopeptidase 3 (MMP3)	156bp	60°C
	FWD: CACTCACAGACCTGACTCGGTT		
	REV: AAGCAGGATCACAGTTGGCTGG		
23	Homo sapiens matrix metallopeptidase 7 (MMP7)	144bp	60°C
	FWD: CATGATTGGCTTTGCGCGAG		
	REV: CTACCATCCGTCCAGCGTTC		
24	Homo sapiens interleukin 1 beta (IL-1B)	188bp	55°C
	FWD: CTCTCTCACCTCTCCTACTCAC		
	REV: ACACTGCTACTTCTTGCCCC		
25	Homo sapiens interleukin 1 alpha (IL-1A)	160bp	62°C
	FWD: TTCTGGGAAACTCACGGCAC		
	REV: TGAGACTCCAGACCTACGCC		
26	Homo sapiens interleukin 6 (IL-6)	104bp	60°C
	FWD: AGTGGCTGCAGGACATGACA		
	REV: TCTGAGGTGCCCATGCTACA		
27	Homo sapiens C-X-C motif chemokine ligand 8 (IL-8)	490bp	60°C w 2.5% DMSO
	FWD: AGTCCTTGTTCCACTGTGCC		
	REV: CACAGCACTACCAACACAGC		
28	Homo sapiens tumour necrosis factor (TNF)	126bp	62°C
	FWD: CTGGGGCCTACAGCTTTGAT		
	REV: GGCCTAAGGTCCACTTGTGT		
29	Homo sapiens transforming growth factor beta 1 (TGFB1)	133bp	60°C
	FWD: CGCATCCTAGACCCTTTCTCCTC		
	REV: GGTGTCTCAGTATCCCACGGAAAT		
30	Homo sapiens C-X-C motif chemokine receptor 4 (CXCR4)	227bp	60°C
	FWD: GGTGGTCTATGTTGGCGTCT		
	REV: TGGAGTGTGACAGCTTGGAG		
31	Homo sapiens C-X-C motif chemokine ligand 12 (CXCL12)	232bp	62°C
	FWD: CGCACTTTCACTCTCCGTCA		
	REV: TGAGATGCTTGACGTTGGCT		
32	Homo sapiens CD44 molecule (Indian blood group) (CD44)	195bp	60°C
	FWD: CCGCTATGTCCAGAAAGGA		
	REV: CTGTCTGTGCTGTCGGTGAT		

Table 2.3 continues:

33	Homo sapiens L1 cell adhesion molecule (L1CAM)	149bp	60°C
	FWD: ACGAGGGATGGTGTCCACTTCAAA		
	REV: TTATTGCTGGCAAAGCAGCGGTAG		
34	Homo sapiens hyaluronan synthase 1 (HAS1)	355bp	62°C w 2.5% DMSO
	FWD: GTGAGTGGCTGTACAACGCG		
	REV: AGAGGGACGTAGTTAGCGGC		
35	Homo sapiens vascular cell adhesion molecule 1 (VCAM1)	243bp	60°C
	FWD: CTGCAAGGTTCCTAGCGTGT		
	REV: AGTGTTTGCGTACTCTGCCT		
36	Homo sapiens intercellular adhesion molecule 1 (ICAM1)	418bp	60°C
	FWD: CGACTGGACGAGAGGGATTG		
	REV: GATAGGTTCAGGGAGGCGTG		
37	Homo sapiens integrin subunit alpha 1 (ITGA1)	353bp	60°C w 2.5% DMSO
	FWD: GGGAAGCTGCCAGTGAGATT		
	REV: GCAGCAGCGTAGAACAACAG		
38	Homo sapiens integrin subunit alpha 2 (ITGA2)	397bp	60°C
	FWD: CTTCCACACCCCATCTTGCT		
	REV: CCGCTGGAGAGAAAGTCAGG		
39	Homo sapiens integrin subunit alpha 4 (ITGA4)	131bp	60°C
	FWD: GCTTCTCAGATCTGCTCGTG		
	REV: GTCACTTCCAACGAGGTTTG		
40	Homo sapiens integrin subunit alpha 5 (ITGA5)	454bp	60°C
	FWD: CTTCAACTTAGACGCGGAGG		
	REV: GCAGGGTGCATACTCCAGAA		
41	Homo sapiens integrin subunit alpha 6 (ITGA6)	404bp	60°C
	FWD: GGGAGGGTGGTTCAACAAAGA		
	REV: GAGGATCACCTACATAGAGCG		
42	Homo sapiens integrin subunit alpha 7 (ITGA7)	164bp	55°C
	FWD: CCTTTGATGGTGATGGGAAA		
	REV: CAGCAGGTCAGGGTATTGGT		
43	Homo sapiens integrin subunit alpha 8 (ITGA8)	100bp	62°C
	FWD: CCTCAGGAAACTGGCAGGAG		
	REV: CCCAGTAAACTCCCCAGCAG		

Table 2.3 continues:

44	Homo sapiens integrin subunit alpha 9 (ITGA9)	163bp	60°C
	FWD: TCTCCGCTGGAAAAAGGGAC		
	REV: CTTCACAGCCCCCAAAGCTA		
45	Homo sapiens integrin subunit alpha 10 (ITGA10)	167bp	60°C
	FWD: CCCAGAACAAGGAAACAGGA		
	REV: CACAGCCACATCAGCAAAAC		
46	Homo sapiens integrin subunit alpha V (ITGAV),	248bp	60°C
	FWD: TTAACCAGTTCACGCCTGCT		
	REV: ATTGTTTCGGACAACCCCGA		
47	Homo sapiens integrin subunit beta 1 (ITGB1)	96bp	60°C
	FWD: CCAAATGGGACACGGGTGAA		
	REV: TTTGCACGGGCAGTACTCAT		
48	Homo sapiens integrin subunit beta 2 (ITGB2)	275bp	60°C w 2.5% DMSO
	FWD: AACAACATCCAGCCCATCTTC		
	REV: ATCTGCACGCCATCACAGTC		
49	Homo sapiens integrin subunit beta 3 (ITGB3)	208bp	60°C
	FWD: ACCAGTAACCTGCGGATTGG		
	REV: TCCGTGACACACTCTGCTTC		
50	Homo sapiens integrin subunit beta 4 (ITGB4)	106bp	60°C
	FWD: TGTCCATCCCCATCATCCCT		
	REV: CCCGATGGAGAGCGTAGAAC		
51	Homo sapiens integrin subunit beta 5 (ITGB5)	176bp	60°C
	FWD: GTGGGGGTCACCTACAACTG		
	REV: CACAGGTTCTGGTACACGCT		
52	Homo sapiens integrin subunit beta 6 (ITGB6)	224bp	60°C
	FWD: CGGTACCCTCTTCCAACACC		
	REV: TCCCGTGGTGACATTTGGAG		
53	Homo sapiens integrin subunit beta 8 (ITGB8)	402bp	60°C w 2.5% DMSO
	FWD: CACTGAGGCGAAAAGGACAAG		
	REV: TGGGTGATGCTGGATCTGTG		
54	Homo sapiens angiopoietin 1 (ANGPT1)	361bp	55°C
	FWD: CAACTGGAGCTGATGGACACA		
	REV: ACTGCCTCTGACTGGTAATGG		

Table 2.3 continues:

55	Homo sapiens platelet derived growth factor subunit B (PDGFB)	126bp	62°C w 2.5% DMSO
	FWD: ACTGATGGGGTCGCTCTTTG		
	REV: CAGGGATCAGGCAGGCTATG		
56	Homo sapiens vascular endothelial growth factor A (VEGFA)	218bp	60°C
	FWD: GGGCAGAATCATCACGAAGT		
	REV: ATCTGCATGGTGATGTTGGA		

Chapter 3

RESULTS

3.1. HSC Characterisation

Figure 3.1. below shows the morphology of isolated HSCs. They exhibit activated star-shaped phenotypes upon attachment to the plastic surface. Their size and morphology indicate that the longer they spend time in the culture they acquire longer projections and become more fibrotic.

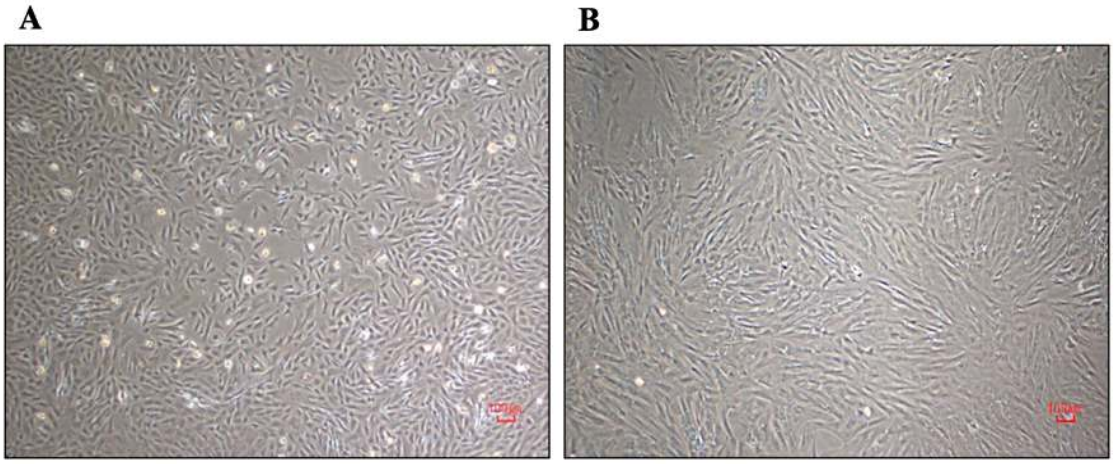

Figure 3.1: Isolated HSCs morphologies (A) P0, pre-passage, (B) P1, pre-stock

HSCs display both mesenchymal and neuronal cell features by expressing vimentin (Fig. 3.2A), Glial fibrillary acidic protein (GFAP) (Fig. 3.2E) and nestin (Fig. 3.2D). Upon activation, they transdifferentiate into myofibroblastic phenotype and start expressing alpha-smooth muscle actin (α-sma) (Fig 3.2B-E) and produce ECM proteins like collagen (Fig 3.2C) and fibronectin (Fig. 3.2F).

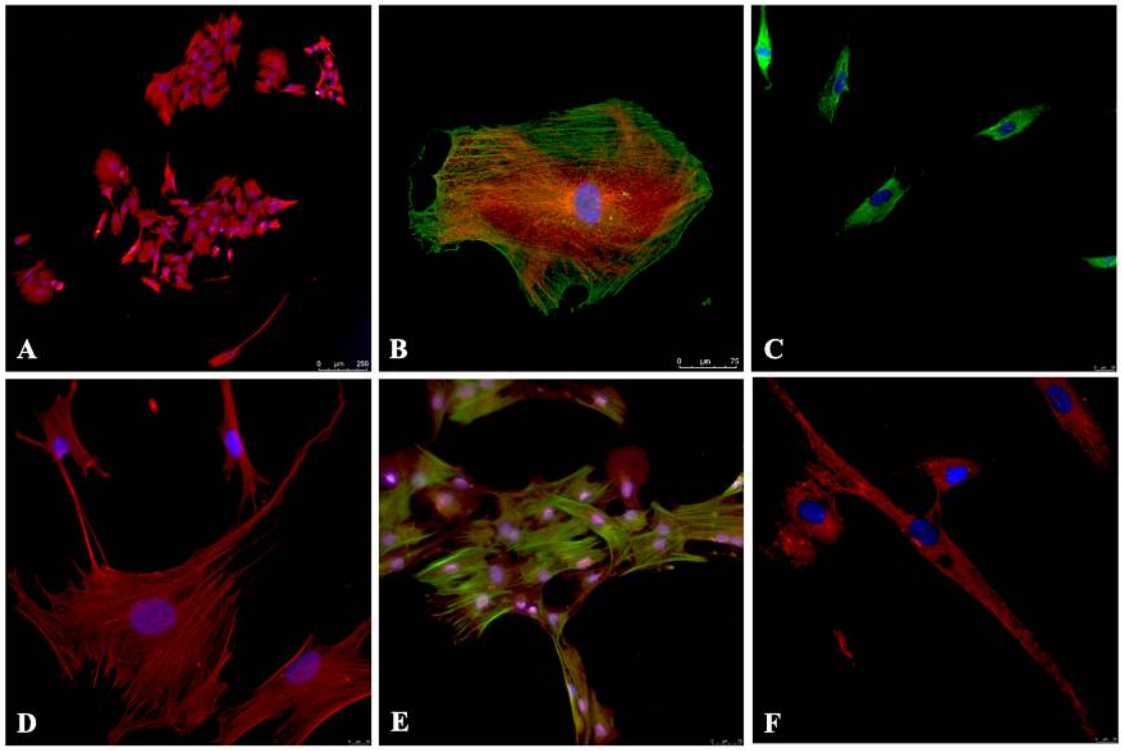

Figure 3.2: HSC characterisation immunofluorescence staining. (A) Vimentin (Cy3), nucleus (DAPI), (B) α-sma (FITC) + vimentin (Cy3) double-staining, nucleus (DAPI), (C) Collagen III (FITC), nucleus (DAPI), (D) Nestin (Cy3), nucleus (DAPI), (E) α-sma (FITC), GFAP (Cy3), nucleus (DAPI), (F) Fibronectin (Cy3), nucleus (DAPI).

3.2. KRAS Status Determination in HepG2 and Huh7 Cells

The sequence data is shown in Table 3.1 below. KRAS is confirmed to be GTT (Valine) in the G12V plasmid and GAC (Aspartic acid) in the G12D plasmid. It is also confirmed that HepG2 and Huh7 have the wild type (GGT, glycine) KRAS.

Table 3.1: Sequencing results of KRAS gene in plasmid and cell lines

KRAS G12V	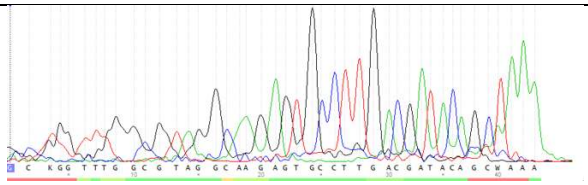 …GTTTGGCGTAGGCAAGAGTGCCTTGACGATACAGCWAAA (Valine)
KRAS G12D	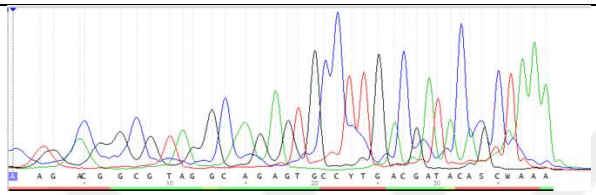 ...AAGACGGCGTAGGC-AGAGTGCCYTGACGATACASCWAAA (Aspartic acid)
HepG2	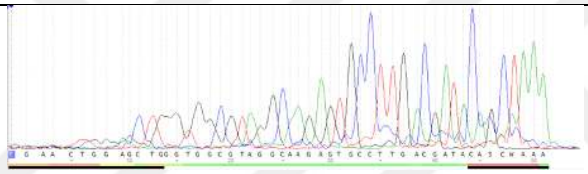 …AGCTGGGTGGCGTAGGCAAGAGTGCCTTGACGATACASCWAA (Glycine)
Huh7	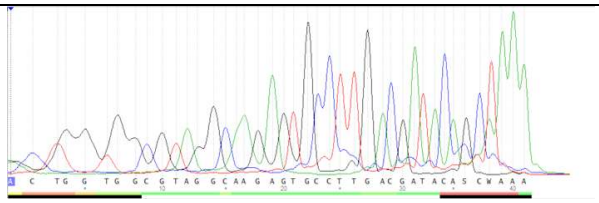 ACTGGTGGCGTAGGCAAGAGTGCCTTGACGATACASCWAAA (Glycine)

3.3. Retroviral Transduction

Figure 3.2. shows KRAS mRNA expression levels in both cell lines. Two-way ANOVA was performed to compare KRAS expression level in no transduction to transduced cells. Total KRAS expression is found significantly higher in KRAS G12D mutation-induced HepG2 (HepG2 G12D) and Huh7 (Huh7 G12D) cells (p-values: 0.0022 and 0.0049, respectively).

Although KRAS expression is higher in KRAS G12V induced cells (HepG2 G12V, Huh7 G12V) than no transduced counterparts, it has failed to reach the significance for both cell lines (p-value: 0.6723 for HepG2 G12V and 0.2254 for Huh7 G12V). Yet, since there was an increase in the expression of KRAS, which comes from the transduced mutation, these cells were used in further experiments. Backbone (HepG2 BB, Huh7 BB), which only contains the plasmid backbone and puromycin resistance gene, did not show any significant change in KRAS expression compared to no transduction in either cell line.

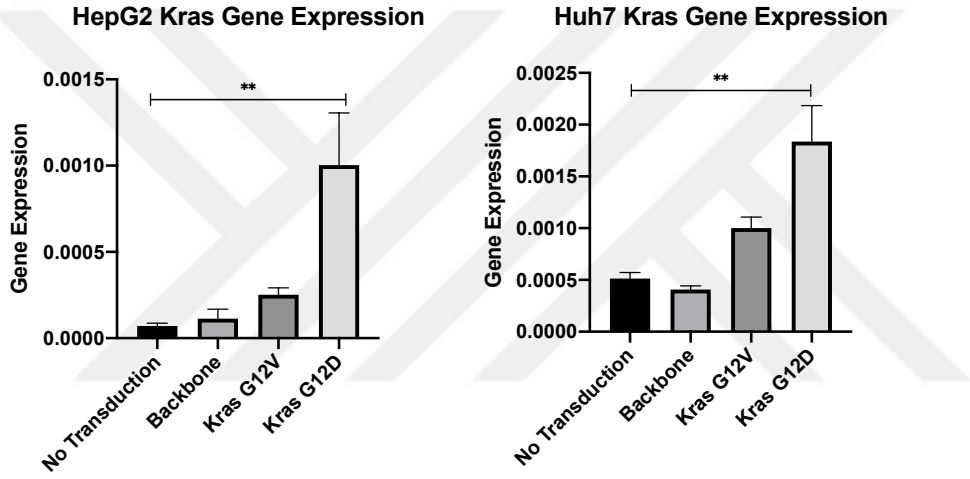

Figure 3.3: KRAS gene expression in HepG2 (n=4) and Huh7 cell lines (n=3).

3.4. The Effect of KRAS Mutation on Cell Proliferation Rate:

This experiment aimed to determine if the KRAS mutation affects the proliferation rate of Huh7 and HepG2. MTT, a colourimetric assay to assess the metabolic activity that directly reveals the viable cells in the well, was used for this purpose. Two-way ANOVA is performed to compare proliferation in no transduced vs transduced cells. Proliferation rates at 24 and 48h can be seen in Figure 3.4. While the transduction of KRAS mutation did not affect proliferation in Huh7 cells, transduction itself seems to increase the proliferation in HepG2 cell lines at 48h significantly (p values of Backbone, KRAS G12V KRAS G12D are 0.0013, 0.0017, 0.0259, respectively).

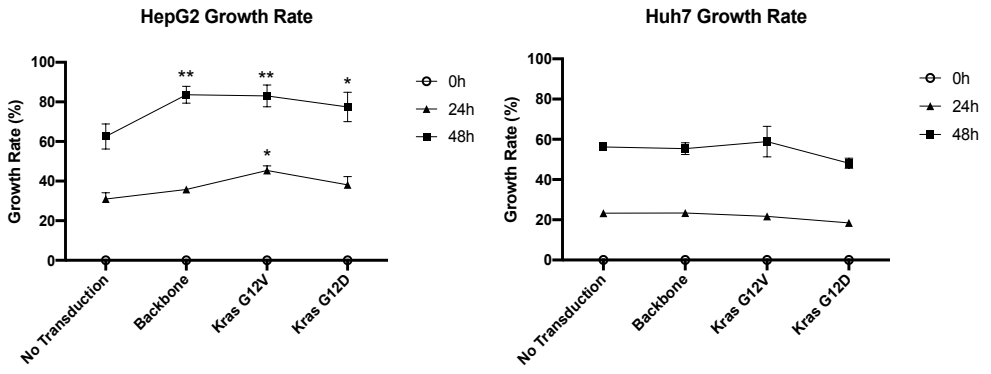

Figure 3.4: Proliferation rates at 24 and 48h for HepG2 and Huh7 cell lines. (p values, * <0.05; ** <0.01).

3.5. Anoikis Resistance

Cells started to form clusters starting from Day 1 and were incubated for three weeks (Figure 3.5). Clusters are collected weekly to analyse cell death in flow cytometry.

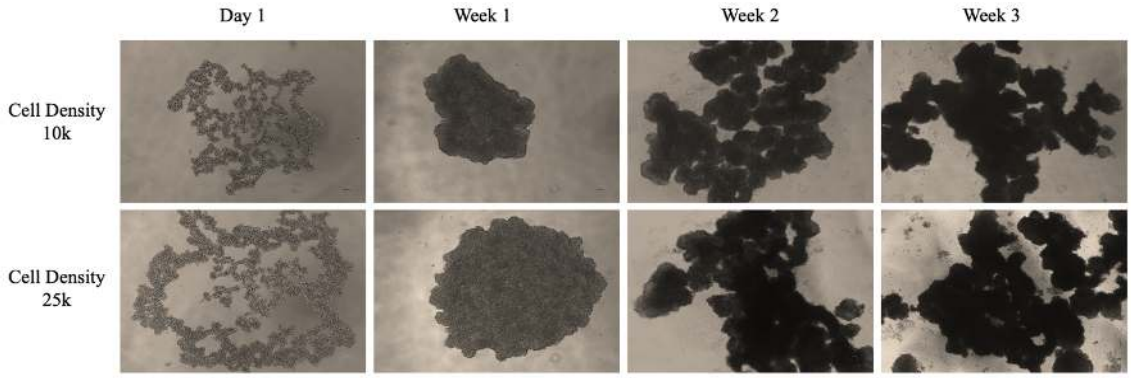

Figure 3.5: Cell clusters in the low-attachment surface.

Gate R1 has covered almost 99% of the cell population. Gate R2 has included around 70-80% of the entire population. Two-way ANOVA is performed to analyse the data that is collected from R4, which is the histogram results of the stained cells. The analyses can be seen in Figure 3.6 and corresponding p values in Table 3.2 below. Cell viability rate is significantly higher in no transduced controls compared to transduced HepG2 cells. However, this effect seems to be independent from the presence of the mutation and more likely the impact of transduction itself.

Conversely, transduced cells did not show a similar pattern of cell viability in Huh7 cells. Yet a decline in the viability rate is observed on the third week of culture, mainly in Huh7 G12D compared to no transduction control.

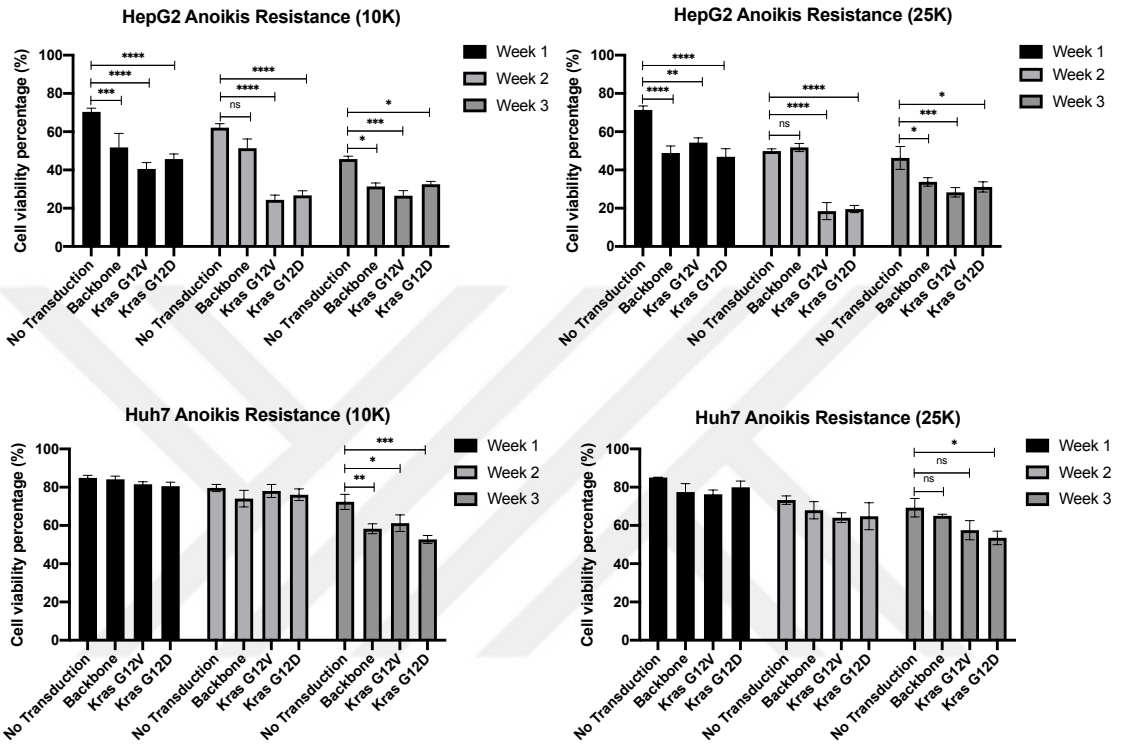

Figure 3.6: Cell viability in HepG2 and Huh7 clusters

In our clinical case, the tumour was viable for over three weeks in the peritoneal cavity. This experiment has been performed for three weeks to mimic exfoliated cells/clumps viability in a low attachment environment. It can be seen in Figure 3.7 and corresponding p-value table 3.3 that cells are more viable on the first week, and viability decreases following weeks in every condition in both cell lines. However, declined viability seems to be independent of the presence of KRAS mutation.

Table 3.2: p-values of cell viability analyses in HepG2 and Huh7 clusters (Figure 3.6) (p values, * <0.05; ** <0.01; *** <0.001; ****<0.0001).

		Week 1		Week 2		Week 3	
		10k	25k	10k	25k	10k	25k
HepG2	BB	0.0009 (***)	<0.0001 (****)	0.0680 (ns)	0.9519 (ns)	0.0109 (*)	0.0255 (*)
	G12V	<0.0001 (****)	0.0019 (**)	<0.0001 (****)	<0.0001 (****)	0.0007 (***)	0.0011 (**)
	G12D	<0.0001 (****)	<0.0001 (****)	<0.0001 (****)	<0.0001 (****)	0.0206 (*)	0.0057 (**)
Huh7	BB	0.9949 (ns)	0.3870 (ns)	0.3993 (ns)	0.6510 (ns)	0.0057 (**)	0.7805 (ns)
	G12V	0.7419 (ns)	0.2769 (ns)	0.9647 (ns)	0.2422 (ns)	0.0297 (*)	0.1042 (ns)
	G12D	0.5813 (ns)	0.6807 (ns)	0.7216 (ns)	0.3025 (ns)	0.0002 (***)	0.0217 (*)

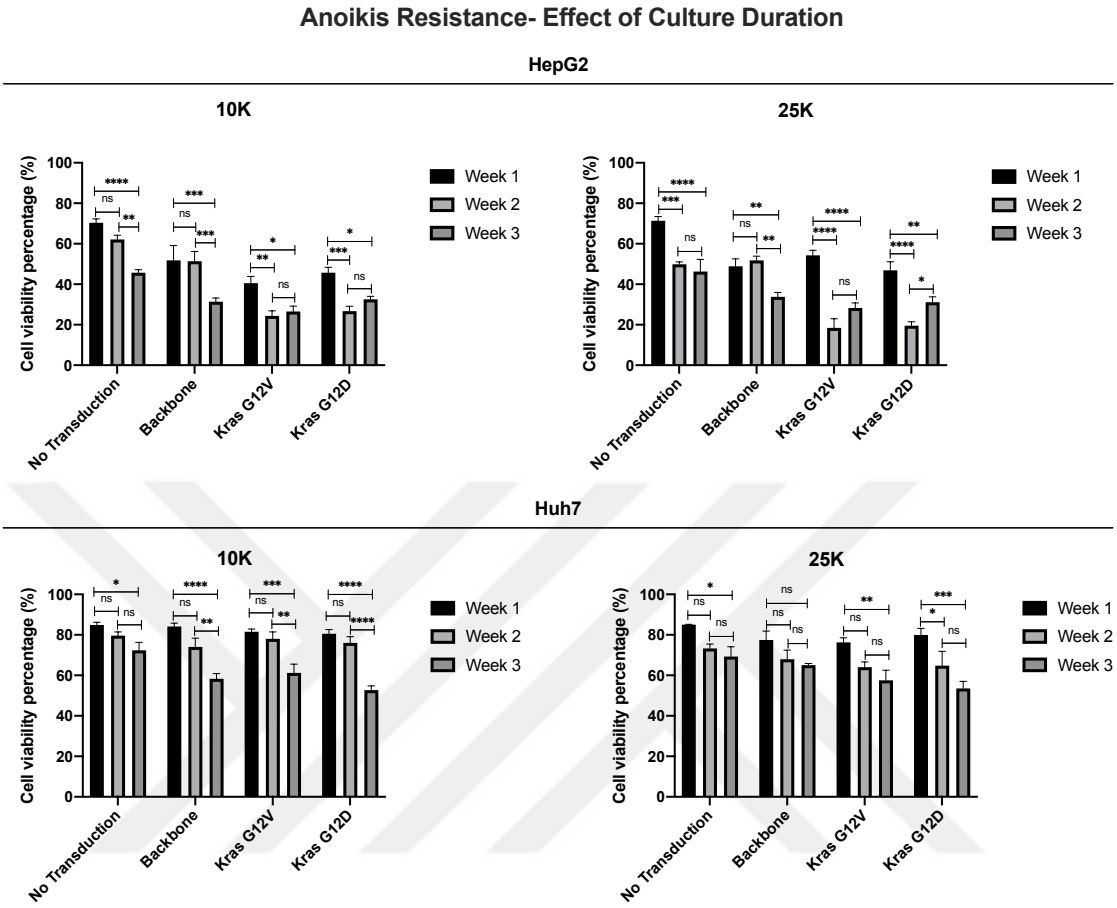

Figure 3.7: Weekly comparison of cell viability in HepG2 and Huh7 clusters (p values: ns >0.05; * <0.05; ** <0.01; *** <0.001; ****<0.0001).

Table 3.3: p-values of cell viability analyses in HepG2 and Huh7 clusters, weekly comparison (Figure 3.7)

		Week 1 vs Week 2		**Week 1 vs Week 3**		**Week 2 vs Week 3**	
		10k	25k	10k	25k	10k	25k
HepG2	No Transduction	0.1952 (ns)	0.0001 (***)	<0.0001 (****)	<0.0001 (****)	0.0032 (**)	0.7173 (ns)
	BB	0.9944 (ns)	0.8073 (ns)	0.0003 (***)	0.0058 (**)	0.0004 (***)	0.0010 (**)
	G12V	0.0037 (**)	<0.0001 (****)	0.0127 (*)	<0.0001 (****)	0.8889 (ns)	0.0939 (ns)
	G12D	0.0007 (***)	<0.0001 (****)	0.0197 (*)	0.0040 (**)	0.4291 (ns)	0.0422 (*)
Huh7	No Transduction	0.4034 (ns)	0.0997 (ns)	0.0132 (*)	0.0211 (*)	0.1963 (ns)	0.7453 (ns)
	BB	0.0517 (ns)	0.2109 (ns)	<0.0001 (****)	0.0782 (ns)	0.0020 (**)	0.8534 (ns)
	G12V	0.6746 (ns)	0.0850 (ns)	0.0001 (***)	0.0059 (**)	0.0010 (**)	0.4658 (ns)
	G12D	0.5223 (ns)	0.0272 (*)	<0.0001 (****)	0.0002 (***)	<0.0001 (****)	0.1173 (ns)

We also checked that the density of cells affects anoikis resistance to see if competing for resources affects the viability of the cells. Therefore, cells were seeded in two different densities, 10k and 25k. However, seeding density did not significantly affect cell density in neither condition (Figure 3.8).

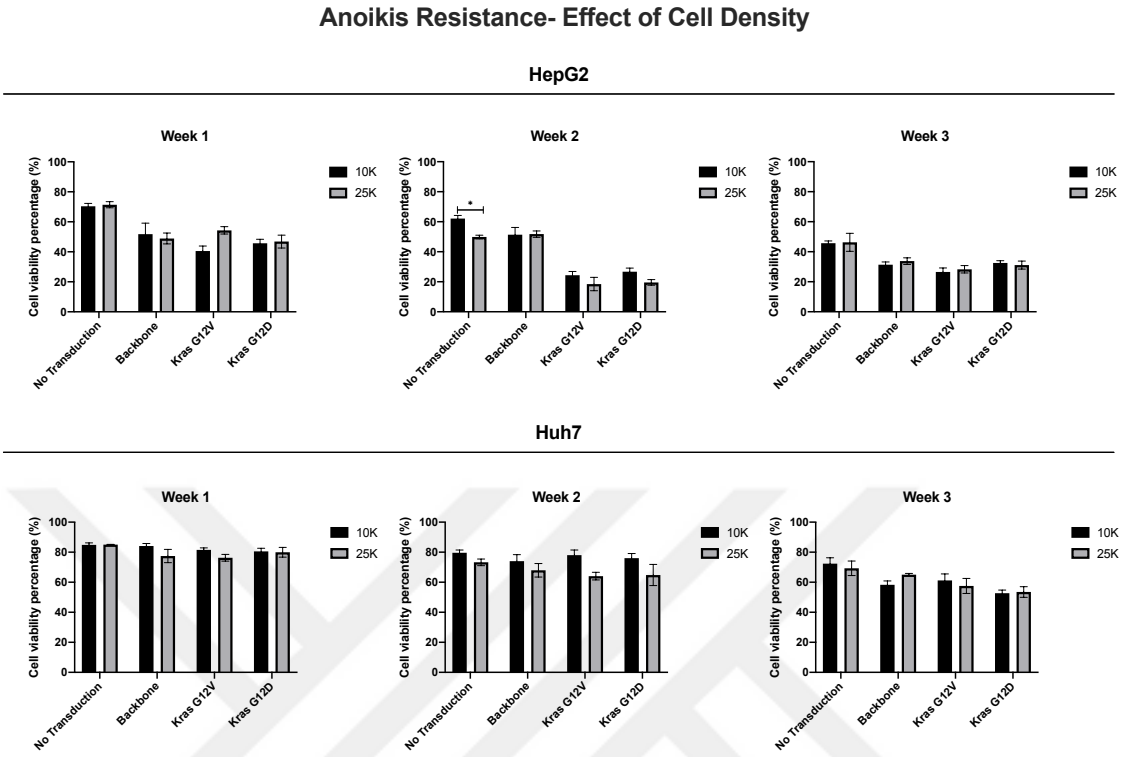

Figure 3.8: Cell viability percentage in HepG2 and Huh7 clusters, comparison of seeding density (p values, * <0.05).

3.6. Soft Agar Colony Formation:

The main aim of this experiment was to show if the transduction of KRAS mutation has any effects on the spheroid formation capacity of Huh7 and HepG2 cell lines. Though Huh7 cells are failed to form colonies due to their growth pattern as monolayers, HepG2 cells formed gradually enlarging colonies in soft agar (Figure 3.9). Colonies are counted, and their sizes are measured using ImageJ software. Comparison analyses were done with two-way ANOVA test. As a result, we did not observe any significant difference in either the size or the number of colonies in HepG2 cells (Figure 3.10).

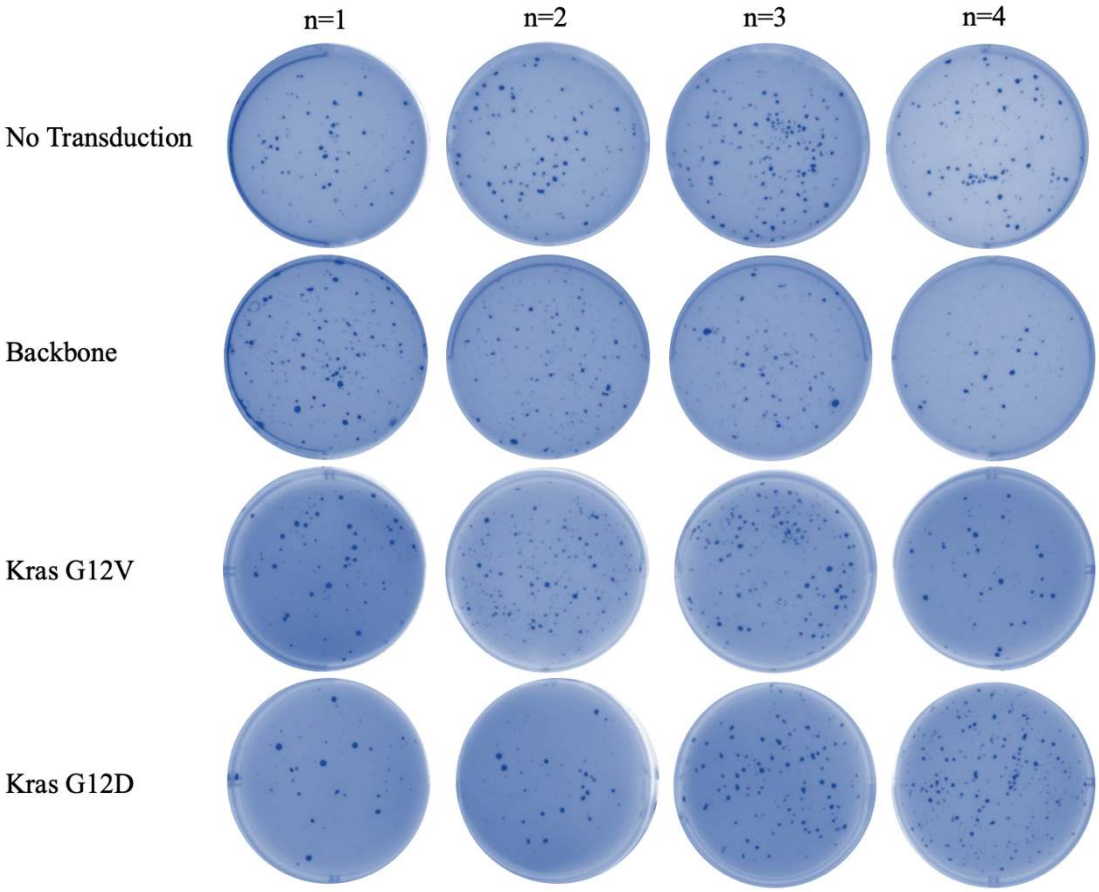

Figure 3.9: HepG2 colony formation in soft agar after crystal violet staining.

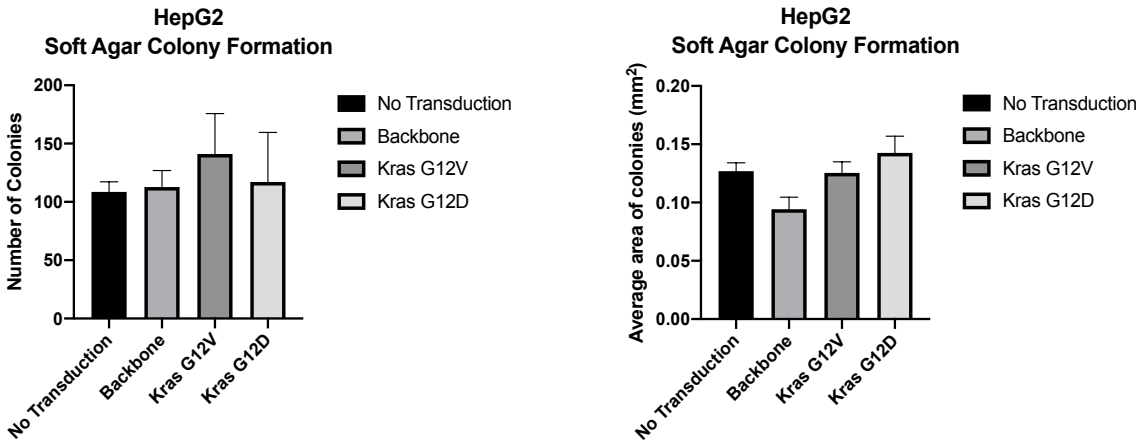

Figure 3.10: HepG2 soft agar colony formation analyses results.

3.7. Wound-healing Assay

The purpose of this assay is to investigate if KRAS mutation affects the mobility of the cells. Wound healing assay could not be performed in HepG2 cells due to their growth pattern as clusters as when they form a proper monolayer for this assay, they get over confluent and start to detach from the surface of the plastic. Therefore, we only performed this assay with Huh7 cells. Cell migration was recorded in 0h, 12h, 24h, 36h, 48h, 72h and 96h (Figure 3.11A). Analyses of wound healing are done in ImageJ using the MRI Wound Healing Tool plug-in, which automatically detects the edges of the scratch and calculates the area automatically (Figure 3.11B).

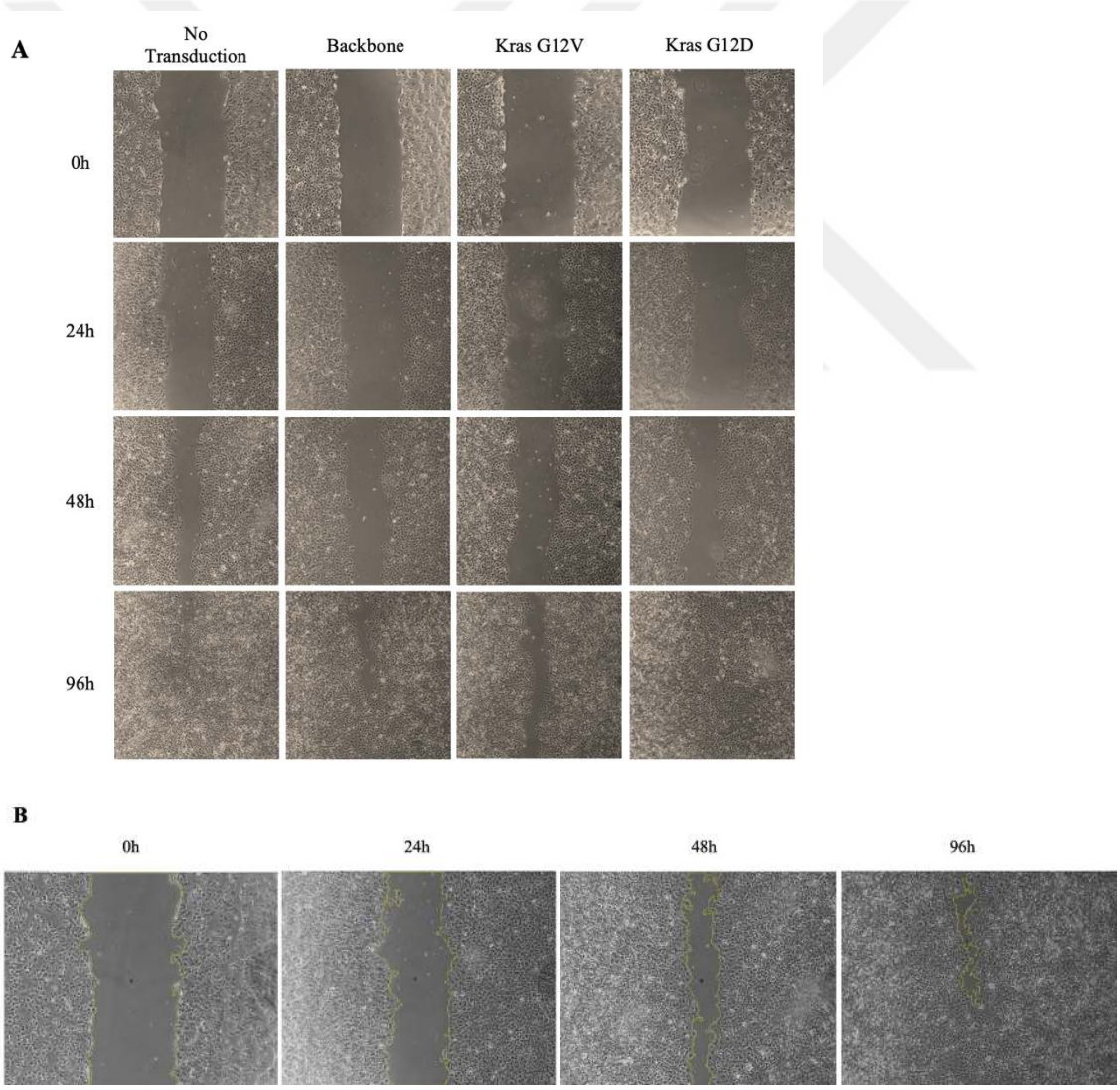

Figure 3.11: Huh7 wound healing assay. (A) Wound healing in times and conditions. (B) ImageJ analysis of the scratch area.

Again, two-way ANOVA test is performed to see if there is any difference between transduced and no transduced cells in their migratory capabilities. As a result, we could not establish any significant difference between no transduced and transduced cells at any time point (Figure 3.12).

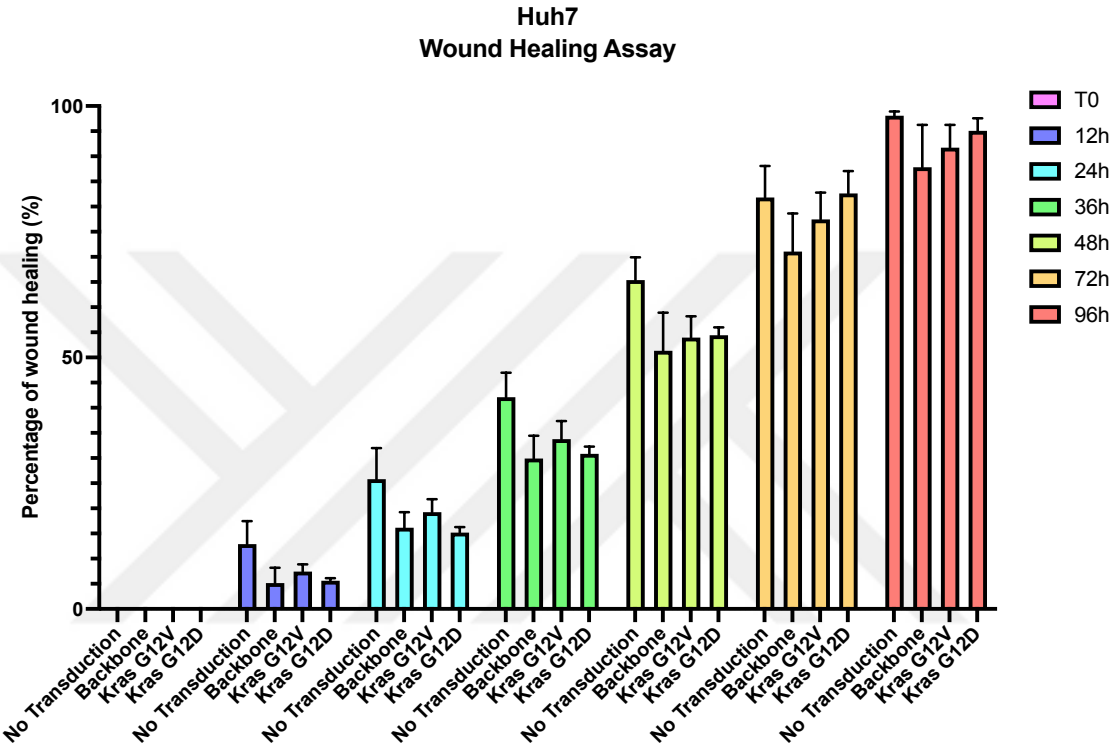

Figure 3.12: Huh7 wound healing analyses results

3.8. HSC: HCC Co-culture Experiments

To understand the nature of normal cell and cancer cell communication in pre-metastatic niche formation, we wanted to evaluate three basic levels of cell-cell interactions: upon their direct physical contact, through the paracrine activity of soluble factors released to the environment, and through reactions mediated by insoluble products of the cell secretome such as ECM constitutes. Therefore, different types of co-culture techniques are employed, and relevant gene expression patterns and ECM components are investigated.

3.8.1. Secreted ECM protein detection: Western blot

This experiment aimed to show if the existence of KRAS mutation in tumour cells induce more collagen and fibronectin secretion of HSCs. All co-culture conditions are compared to the basal level (negative control) of ECM secretion, the condition where the cells are incubated in serum-free DMEM-F12 since activated HSCs can create a fibrotic reaction when there is no stimulant.

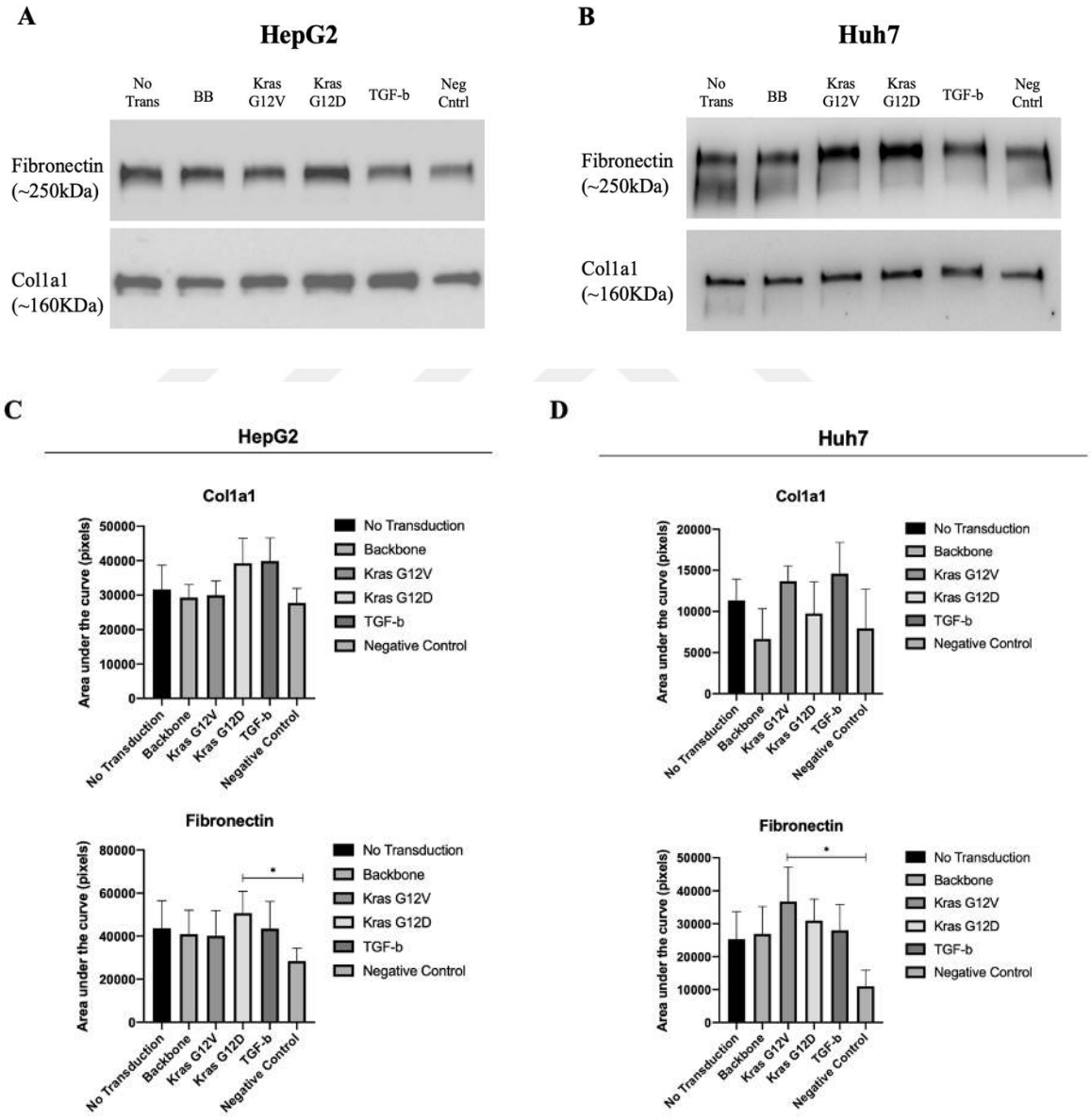

Figure 3.13: Secreted Collagen and Fibronectin. (A, C) Supernatant from HSC indirectly co-cultured with HepG2 (B, D) Supernatant from HSC indirectly co-cultured with Huh7.

TGF-β is used as a positive control, as it is a potent stimulant for ECM secretion in HSCs. HepG2 G12D cells, when co-cultured with HSC, showed increased collagen secretion as much as when cells were exposed to TGF-β; however, compared to the negative control, it failed to reach significance. Nevertheless, fibronectin secretion in both HepG2 and Huh7 is significantly increased with KRAS mutation compared to the negative control (HepG2 G12D p-value: 0.016; Huh7 G12V p-value: 0.0241). However, no significant difference is seen when transduced cells are compared to no transduced cells in either cell line.

3.9. Gene Screening in HCC cell lines and co-culture experiments with HSCs

We aimed to evaluate genes that were found to have a role in the peritoneal carcinomatosis cascade in ovarian and gastrointestinal cancers and genes that play a role in inflammation and desmoplasia. Table 3.4 below shows the genes that play a role in particular parts of this cascade.

Table 3.4. Categorisation of the selected genes for screening.

	Genes selected for evaluation		
	Cancer cells	HSCs	Both
KRAS mutation-induce	MUC1, MUC5B, MUC16		
Desmoplasia, Inflammation	SHH, TGF-β, IL-1β, IL-1α, TNF-α	Col1α1, α-sma, FN-1, Col4α2, HAS1, Gli,	IL-6, IL-8
Exfoliation, EMT, survival	E-Cadherin, N-Cadherin, XIAP, SURV		Vimentin*
Adhesion	FAK, CXCR4, CD44, L1CAM, EpCAM, Integrin family, c-MET	CXCL12, VCAM-1, ICAM-1	HGF
Penetration, invasion, angiogenesis			MMP1, MMP2, MMP3, MMP7, VEGF, ANGPTN1, PDGF-b

*Cancer cells for EMT, HSC for characterisation

Heatmaps in Figure 3.14- Figure 3.15 shows the changes in the expression patterns between different co-culture conditions. Since contact culture contains heterogeneous cell populations containing HSC and HepG2 or Huh7, the gene expression profile is also evaluated separately in comparison with HepG2/Huh7 and HSC controls. HepG2, Huh7 and HSC controls are normal cells that are cultured in their normal condition.

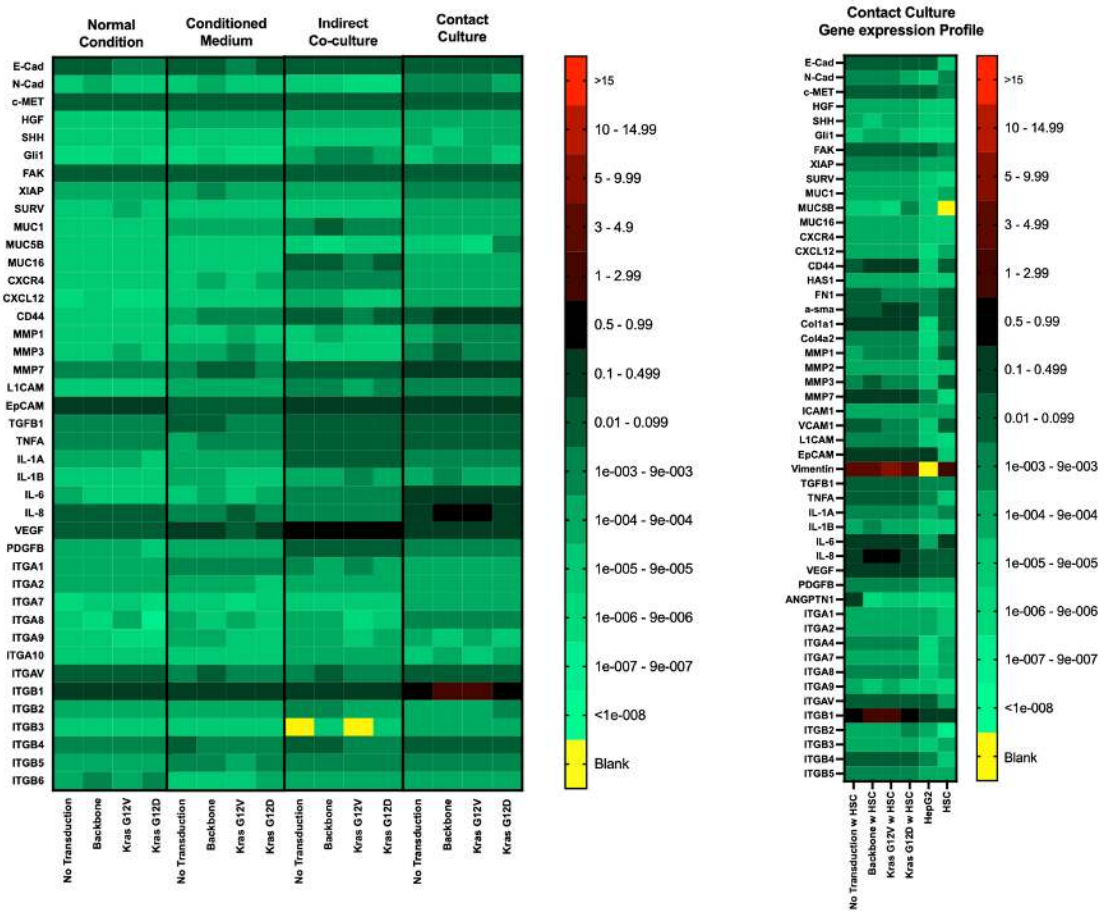

Figure 3.14: HepG2 Heatmap. Dataset on the left contains normal cancer cells (first line) and cancer cells when they are co-cultured with HSC (second to the fourth line). Dataset on the right shows contact culture in comparison with HepG2 cells alone and HSCs under normal culture conditions.

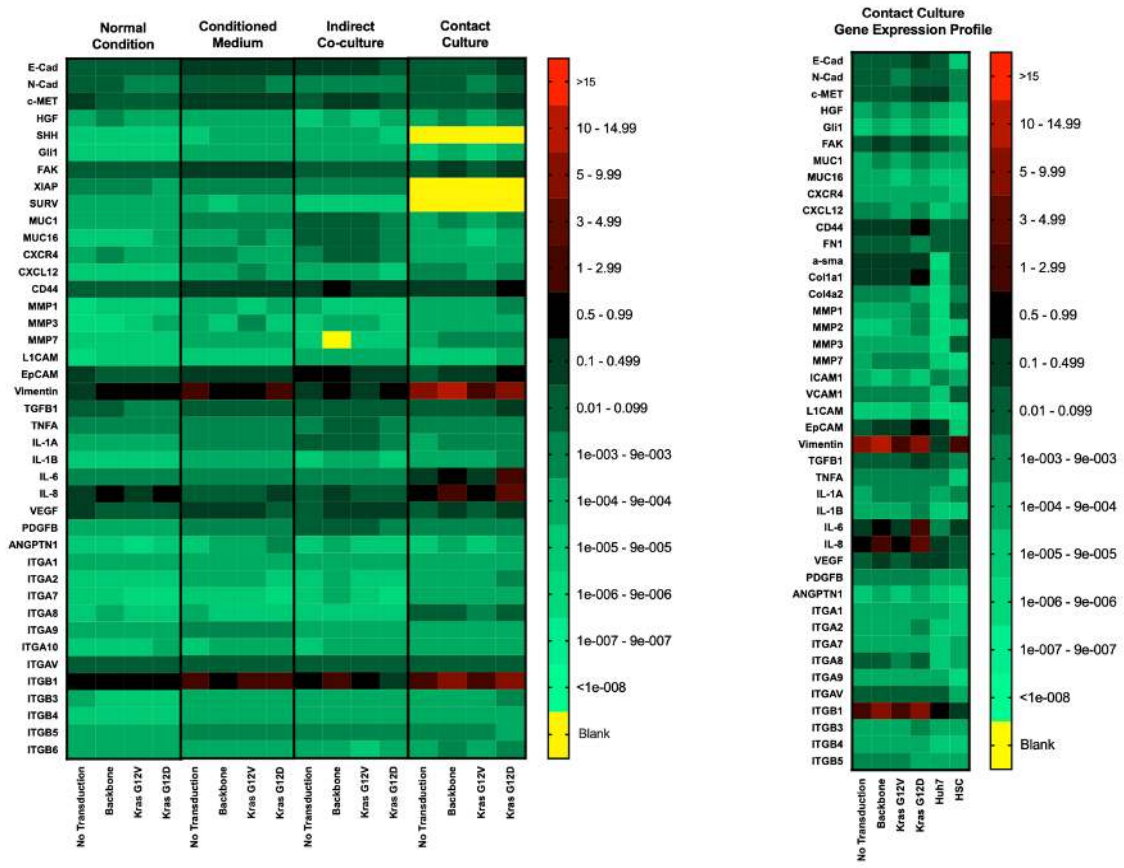

Figure 3.15: Huh7 Heatmap. Dataset on the left contains normal cancer cells (first line) and cancer cells when they are co-cultured with HSC (second to the fourth line). Dataset on the right shows contact culture in comparison with Huh7 cells alone and HSCs under normal culture conditions.

In addition to the heatmap above, gene expressions are shown below (Figure 3.16) as individual graphs in comparison of different conditions and contact culture with HepG2 and HSC under normal culture conditions. To sum up, the results that can be seen in the graphs, E-cadherin (Fig 3.16A) expression is found significantly lower in HepG2 G12V under normal conditions and when co-cultured with HSC secretome. But E-Cadherin expression level is recovered when directly or indirectly co-cultured with HSC. N-Cadherin (Fig 3.16B) expression is found higher in no transduction and HepG2 BB under normal and indirectly co-cultured with HSCs however, this increase is not significant. Since N-cadherin is a mesenchymal marker, we have observed high expression in HSCs. We observed a reduced c-met (Fig 3.16C) expression in HepG2 G12V and HepG2 G12D under normal conditions.

When HepG2 cells were co-cultured with HSC directly or its secretome, no changes in the expression were observed. We have observed an increasing pattern in the expression of c-met in indirect co-culture; however, this seems to be independent of KRAS mutation. Although we found a rising pattern in HGF (Fig 3.16D) when co-cultured with HSC or its secretome. In contact culture condition HepG2 BB and HepG2 G12V express HGF significantly more compared to HepG2 and HSC controls. Gli (Fig 3.16E) expression is altered overall transduced and non-transduced HepG2 when co-cultured with HSC directly and indirectly. Interestingly when HepG2 and HSC are in contact, even though neither of them under normal conditions has high expression of Gli, overall expression increases. On the contrary HepG2 cells do not show any significant changes under any condition with SHH (Fig 3.16F). As the anoikis resistance genes, SURV and XIAP (Fig 3.16 G-H) failed to show any difference under different culture conditions except HepG2 G12V in contact with HSC, which showed significantly higher XIAP expression than HepG2 control. MUC1, MUC5B and MUC16 (Fig 3.16J-L) are investigated in this setting as KRAS mutation could induce mucin genes; however, we failed to see that in our setup. Nevertheless, we observed that MUC1 gene expression seem to increase when the cells are co-cultured with HSC or its secretome. While MUC5B did not show a significant difference between culture conditions, MUC16 seemed to increase in all cells regardless of the mutation when cultured with HSC secretome compared to other culture conditions and when cultured with HSC indirectly; the expression was dropped compared to normal condition. HepG2 cells, regardless of having mutations, showed low expression of CXCR4 (Fig 3.16M) under normal conditions. Yet we have observed that when the cells are co-cultured with HSCs directly or indirectly, CXCR4 expression increases but not when cultured in conditioned medium. In direct contact condition compared to CXCR4 expression in normal HSC and HepG2, there is a slight increase, but it is not significant. CXCL12 is a CXCR4 ligand expressed in mesenchymal cells, in this case in HSCs, as it can be seen in Fig 3.16N, there is a very low expression in cancer cells even though the expression slightly increases when they are cultured with HSC.

As an important receptor for the adhesion on peritoneal metastasis CD44 (Fig 3.16O) showed minimal expression in cells at normal condition; however, when it is co-cultured with HSCs or its secretome, CD44 seem to increase dramatically even though this increase is independent of KRAS mutation. As adhesion molecules FAK and EpCAM (Fig 3.16I and P) did not show any significant effect under any conditions. MMPs are central mediators in penetration and invasion. Although KRAS mutation alters MMPs, we failed to observe any significant changes induced by KRAS mutation. MMP1 and MMP3 (Fig 3.16R-T) are highly expressed on HSCs therefore, in contact culture conditions, we observed an increasing trend in expression. MMP3 is found to be significantly high in HepG2 G12V compared to no transduction when the cells are cultured in conditioned medium of HSC. In normal condition, HepG2 G12V induce higher MMP3 in cells, but it failed to reach significance. Contrary to MMP1 and MMP3, MMP7 is expressed in cancer cells, and the expression increases gradually when cells have closer contact with HSCs. L1CAM is another vital molecule for attachment to the mesothelial layer. L1CAM (Fig 3.16U) expression increased when the cells were co-cultured with HSC but not significantly. TGF-β expression is found to be slightly lower in HepG2 G12V and G12D compared to no transduced HepG2 and HepG2 BB. The decline is significant in HepG2 G12V when incubated with conditioned medium. TGF-β (Fig 3.16U) expression increases in all cells when the cells are co-cultured with HSC directly or indirectly. Yet, in contact culture, HepG2 BB and no transduction express significantly higher TGF-β compared to HepG2 and HSC controls. TNF-α (Fig 3.16W) expression is increased when cells are directly or indirectly cultured with HSCs. TNF-α mainly expressed from cancer cells; however, being in contact with the HSCs increase the expression further, especially for no transduced HepG2, HepG2 BB and HepG2 G12V compared to HepG2 controls. IL-1α and IL-1β (Fig 3.16X-Y) have not altered between different culture conditions. However, cancer cells and HSCs induce IL-1β expression when they have direct contact. IL-6 (Fig 3.16Z) as an inflammatory cytokine and an inducer of desmoplasia is found to increase in HepG2 when cultured with HSCs directly or indirectly. Since HSCs express IL-6 abundantly, it is expected to see increased expression of IL-6 in contact culture.

However, the results we gathered from indirect culture shows that HSCs are also capable of inducing IL-6 expression in a paracrine manner. IL-8 (Fig 3.16AB) is also showed increased expression in contact culture while HepG2 and HSCs alone have low expressions. Additionally, IL-8 slightly increased in HepG2 G12V and HepG2 G12D cells compared to no transduced HepG2 and HepG2 BB under normal condition. In angiogenic factors, VEGF (Fig 3.16AC) seem to increase overall under co-culture conditions however could not reach significance. Although PDGFB (Fig 3.16AD) showed a slightly different pattern than VEGF, it increased dramatically when the cancer cells co-cultured with HSCs directly and indirectly. The paracrine effect seems to have more impact on inducing PDGFβ. Unfortunately, we failed to observe significant changes in ITGA molecules. Some of the ITGA genes (ITGA3,4,5,6,8,9,11) were not amplified in HepG2. The ones that have expressions ITGA1, ITGA2, ITGA7, ITGA10 and ITGAV (Fig 3.16AE-AI) have not changed in different conditions. We had observed that ITGAV expression decreased slightly when in contact with HSCs, and ITGA10 significantly upregulated in HepG2 G12V when directly cultured with HSCs when compared to HepG2 and HSC controls. Lastly, we checked ITGB (Fig 3.16AJ-AN) genes, except for ITGB3, and saw that all have expressions in HepG2 cells although ITGB1, ITGB2, and ITGB5 had not altered in different culture conditions ITGB4 significantly decreased in HepG2 cells when cultured with HSC medium it did not seem to be KRAS dependent decrease. ITGB6 is also slightly reduced when co-cultured with HSC secretome or directly with HSCs.

Figure 3.16: Individual gene expressions in KRAS mutation-induced HepG2 cells under normal and co-cultured conditions

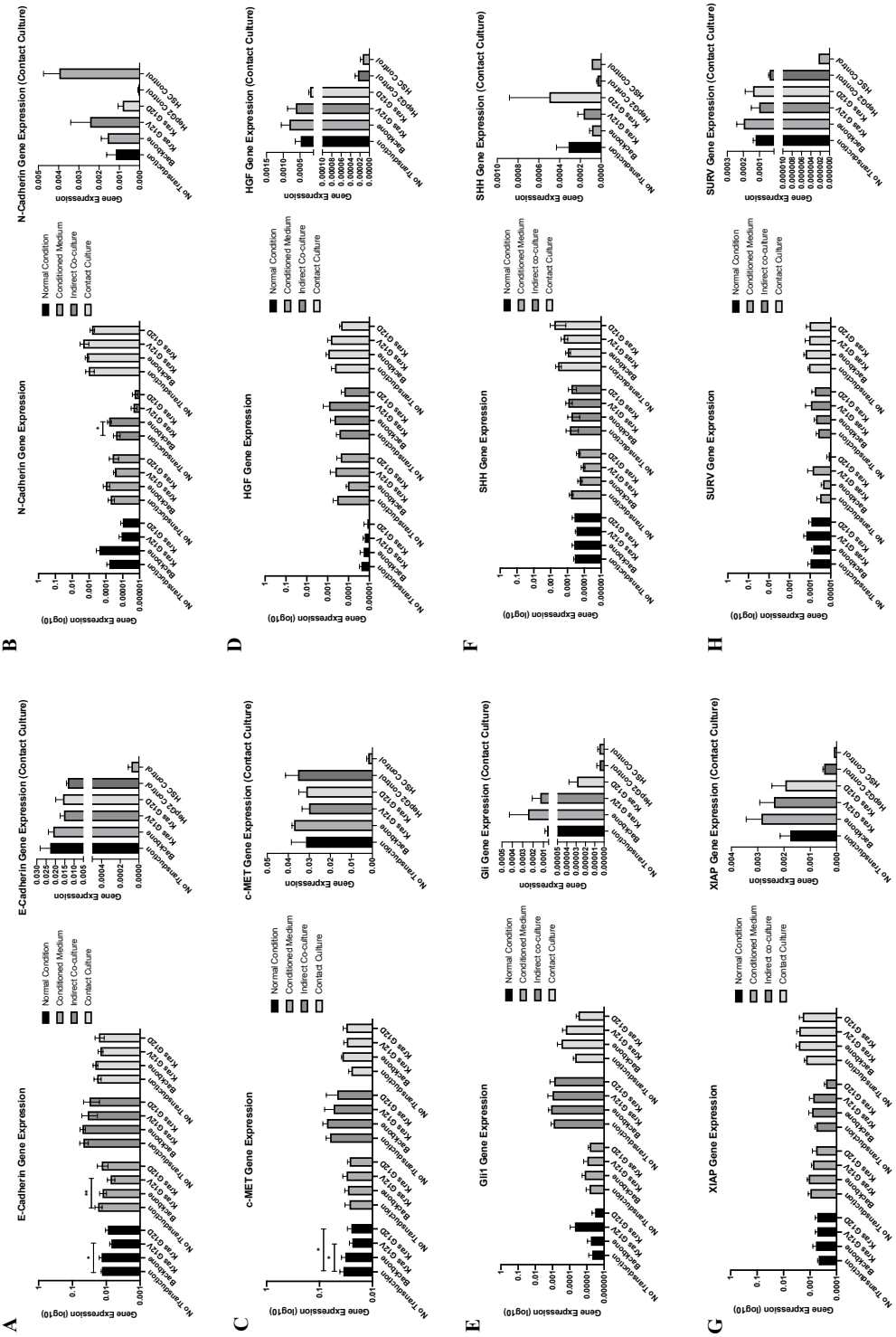

Figure 3.16 continues:

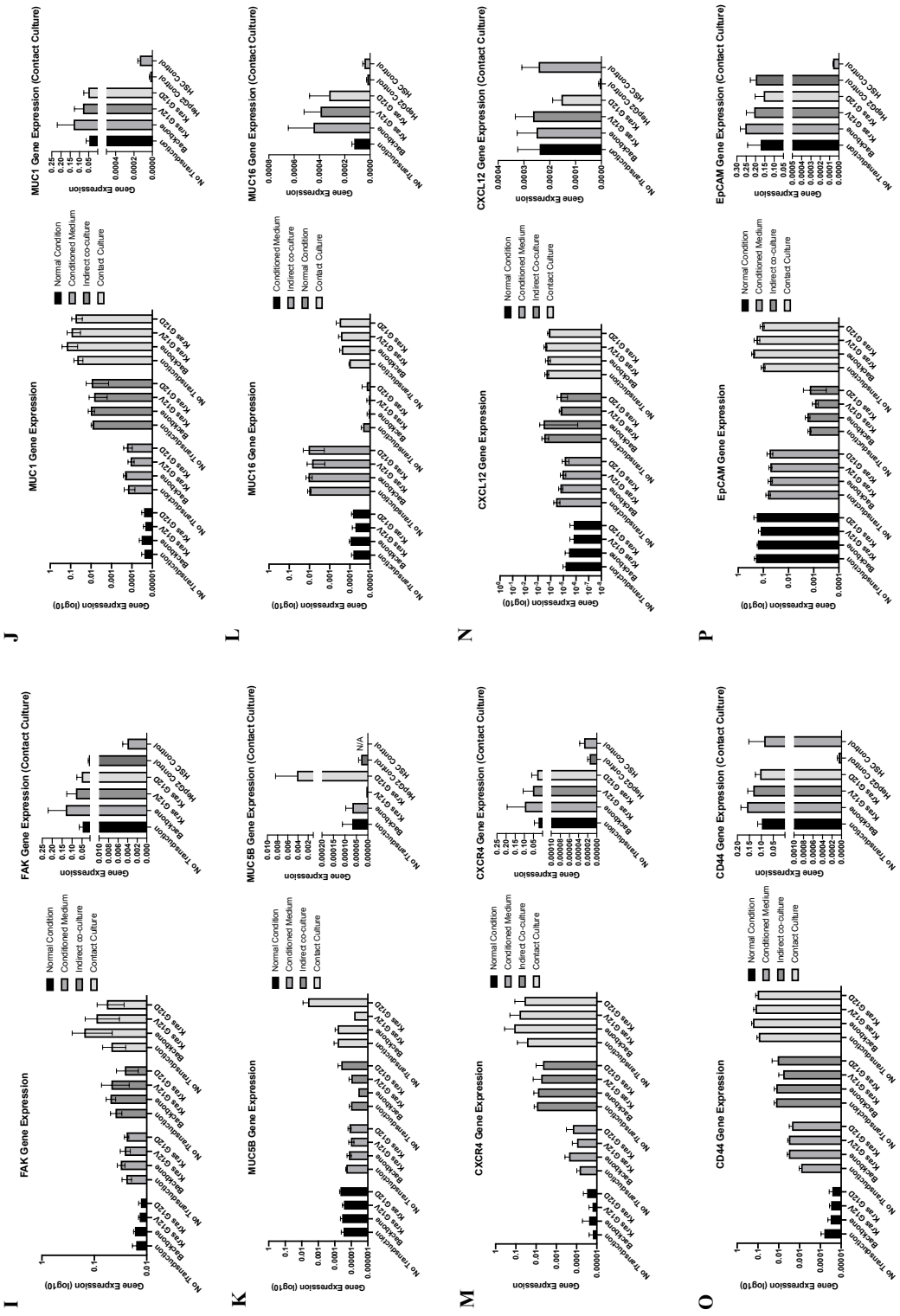

Figure 3.16 continues:

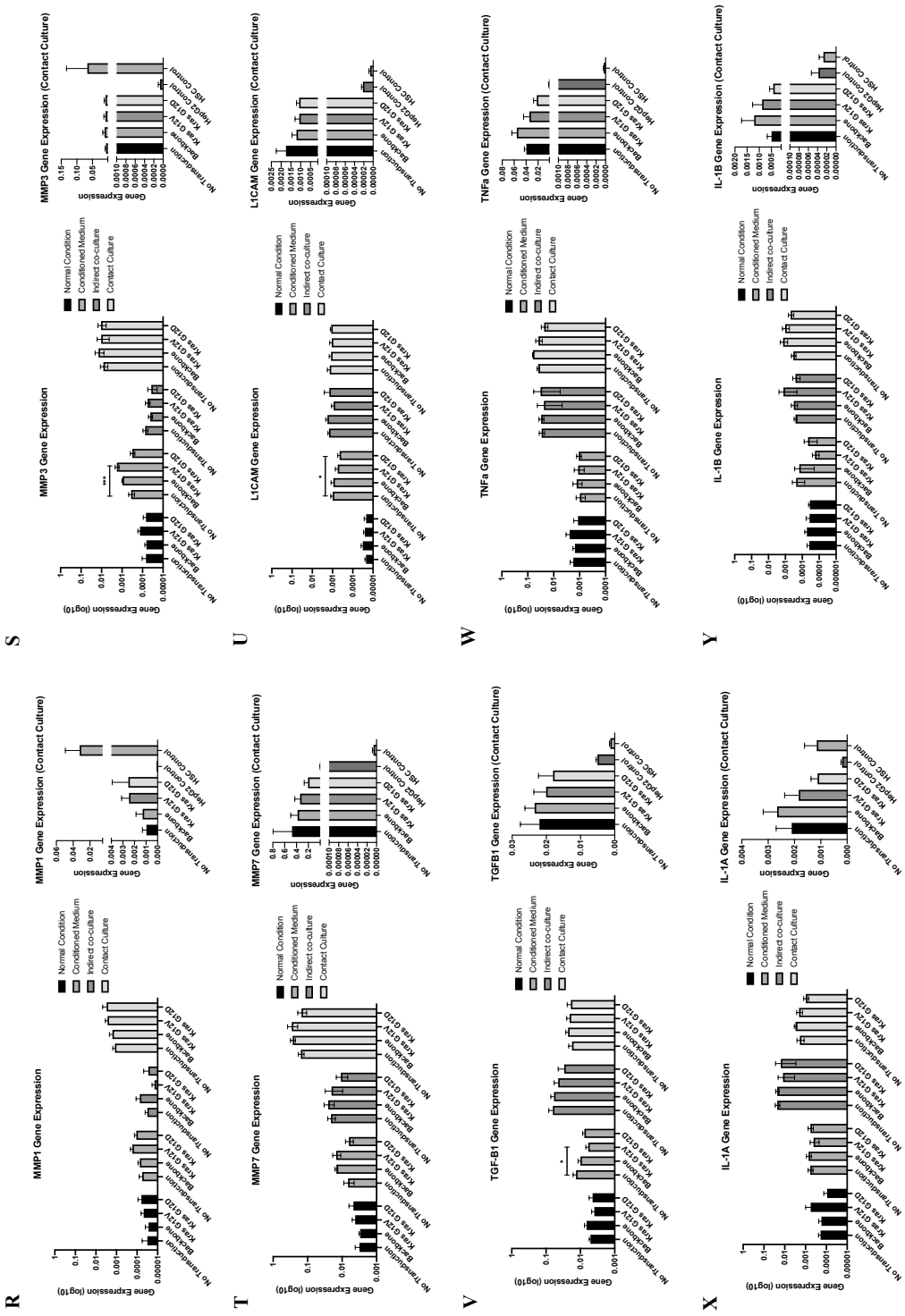

Figure 3.16 continues:

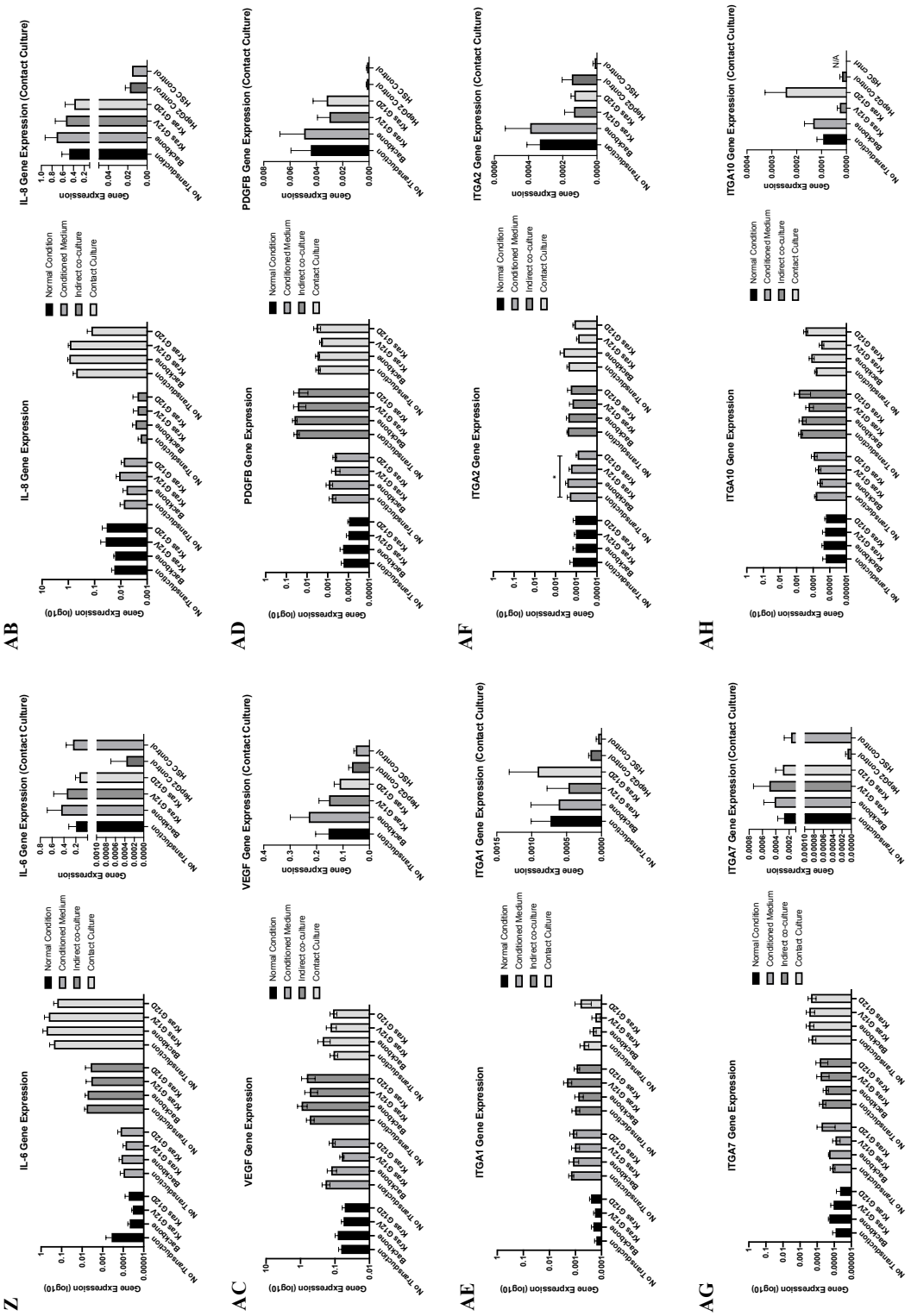

Figure 3.16 continues:

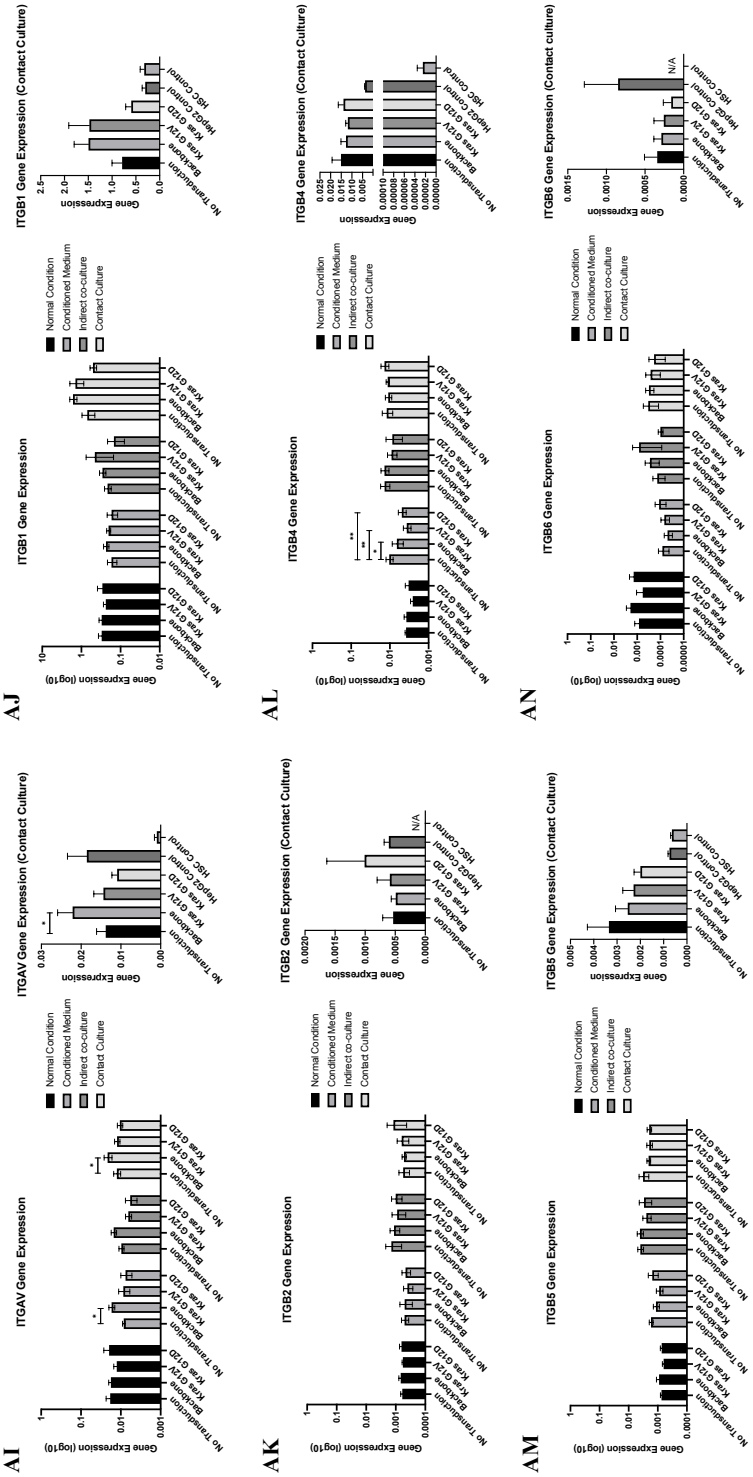

Figure 3.15 shows the gene expression pattern in Huh7 under normal conditions and when co-cultured with HSCs or its secretome. To sum up, the individual graphs that are shown in Figure 3.17 below E-cadherin (Fig 3.17A) is significantly decreased in Huh7 G12V compared to no transduced Huh7 under normal condition. However, the expression increases among transduced and non-transduced cells when co-cultured with HSCs. Particularly in contact culture E-cadherin in Huh7 G12D is significantly higher than no transduced Huh7 and Huh7 control. On the contrary, N-Cadherin (Fig 3.17B) did not show any changes between culture conditions, but interestingly N-Cadherin is expressed slightly higher than HSCs which shows that they might be in a differentiated state. In support of that is vimentin expression. Huh7 cells express a high level of vimentin. This is independent of KRAS mutation. Vimentin (Fig 3.17R) expression generally dropped among transduced and non-transduced cells when they were directly cultured with HSCs, but the reduction was only significant in no transduced Huh7 and Huh7 G12V compared to Huh7, and HSC controls. c-Met and HGF (Fig 3.17C-D) have not shown any alterations between conditions. Compared to HepG2, Huh7 cells express a higher level of HGF. Gli (Fig 3.17E) also did not show any significant expression differences between conditions except when Huh7 cells are in contact with HSCs. Huh7 G12V significantly higher Gli expression than its no transduced counterparts and Huh7 controls in contact culture. However, Gli's upstream mediator SHH was not amplified in Huh7 cells at all. FAK (Fig 3.17F) expression is found higher in conditioned medium and contact culture conditions than the normal and indirect culture conditions. Compared to Huh7 alone, FAK was slightly higher in Huh7 G12V when the cells were in contact with HSCs. Similar to HepG2, we did not observe any significant alterations in MUC1 and MUC16 (Fig 3.17G-H) expressions regarding KRAS mutation. However, we observed that MUC1 expression increases when co-cultured with HSC. Additionally, under contact culture conditions Huh7 G12D express significantly higher MUC1 and MUC16 compared to no transduced Huh7, Huh7 and HSC controls. In the CXCR4-CXCL12 axis (Fig 3.17I-J), Huh7 cells showed the higher CXCR4 expression in indirect culture condition. CXCL12 also slightly increased when Huh7 cells were co-cultured with HSCs or their secretome.

As mentioned before, CXCL12 is mainly expressed from mesenchymal cells. Under contact culture conditions, this expression increased further when Huh7 cells were cultured with HSCs. CD44 (Fig 3.17K) expression increased overall when Huh7 cells were co-cultured with HSCs, predominantly Huh7 G12D significantly increased in contact culture conditions when compared to no transduced Huh7. MMP1 and MMP3 (Fig 3.17 L-M) expressions showed a similar pattern in Huh7 cells and did not alter significantly under different culture conditions. Though, both decreased when Huh7 cells were cultured directly with HSC compared to HSC control. MMP7 (Fig 3.17N) has shown an increased pattern in contact culture, and when compared to Huh7 and HSC controls, the expressions seem to increase overall, again, independent from KRAS transduction. L1CAM and EpCAM (Fig 3.17O-P) expressions have not changed in different culture conditions with the exceptions of a slight increase in indirect co-culture for L1CAM and a significant increase of Huh7 G12D for EpCAM in contact culture when compared to no transduced Huh7 and Huh7 alone. TGF-β (Fig. 3.17S) expression did not differ between conditions. TNF-α (Fig 3.17T) expression slightly increased when Huh7 cells were co-cultured with HSC or its secretome. For IL-1α (Fig. 3.17U) expression, Huh7 cells have shown an increasing pattern overall in co-culture conditions. Particularly Huh7 G12D, when cultured with HSC, expressed higher IL-1α but it failed to reach significance. IL-1β (Fig. 3.17V) expression have not shown significant changes between culture conditions, but in contact culture, while Huh7 and HSC alone have a low expression when they have contacted, the expression increases especially for Huh7 G12D. IL-6 (Fig 3.17W) expression also did not show an increasing pattern under co-culture conditions similar to HepG2 cells; however, in contact culture, IL-6 expression in Huh7 G12D increased significantly compared to no transduced Huh7 and Huh7 control. IL-8 (Fig. 3.17X) expression, on the contrary, slightly dropped when cultured with HSCs apart from Huh7 G12D in contact culture. It increased significantly when compared to no transduced Huh7 and Huh7 control. Different from than HepG2 screen, ANGPTN1 (Fig. 3.17Y) has expressed in Huh7 cells. Yet neither different culture conditions nor KRAS mutation caused any changes in its expression. VEGF and PDGFβ (Fig 3.17Z-AB) did not show substantial changes among different culture conditions except VEGF.

It significantly dropped in Huh7 G12V under normal conditions compared to no transduced Huh7 and PDGFβ showed a slight increase in expression pattern when indirectly co-cultured with HSC. Similar to HepG2, we failed to observe significant changes in ITGA molecules. Some of the ITGA genes (ITGA3,4,5,6,8,10,11) were not amplified in Huh7 either. The ones that have expressions ITGA1, ITGA2, ITGA7, ITGA9 and ITGAV (Fig 3.17AC-AG) have not changed in different conditions. Contrarily, we have observed that ITGAV expression had not changed in different conditions except when directly cultured with HSC; we observed a slight decrease in Huh7 G12V and G12D compared to Huh7 controls. Different from HepG2, ITGA9 was expressed in Huh7, yet we did not observe any significant changes among different conditions. Lastly, we checked ITGB (Fig 3.17AG-AL) genes except for ITGB2, which all have an expression in Huh7 cells. ITGB1 expression is higher in Huh7 compared to HepG2 cells. The expression further increases when in contact with HSC or cultured with its secretome. In contact culture, ITGB1 expression increased significantly in Huh7 BB compared to Huh7 and HSC control. ITGB3 expression has not changed overall in different conditions. In contact culture, ITGB3 is substantially higher in Huh7 G12D compared to no transduced Huh7, Huh7 and HSC controls. While ITGB4 slightly increased when co-cultured with HSCs, ITGB5 is significantly reduced in Huh7 G12V under normal conditions, but the expression pattern has not changed among different conditions. ITGB6 expression also did not show any changes under different culture conditions.

Figure 3.17: Individual gene expressions in KRAS mutation-induced Huh7 cells under normal and co-cultured conditions

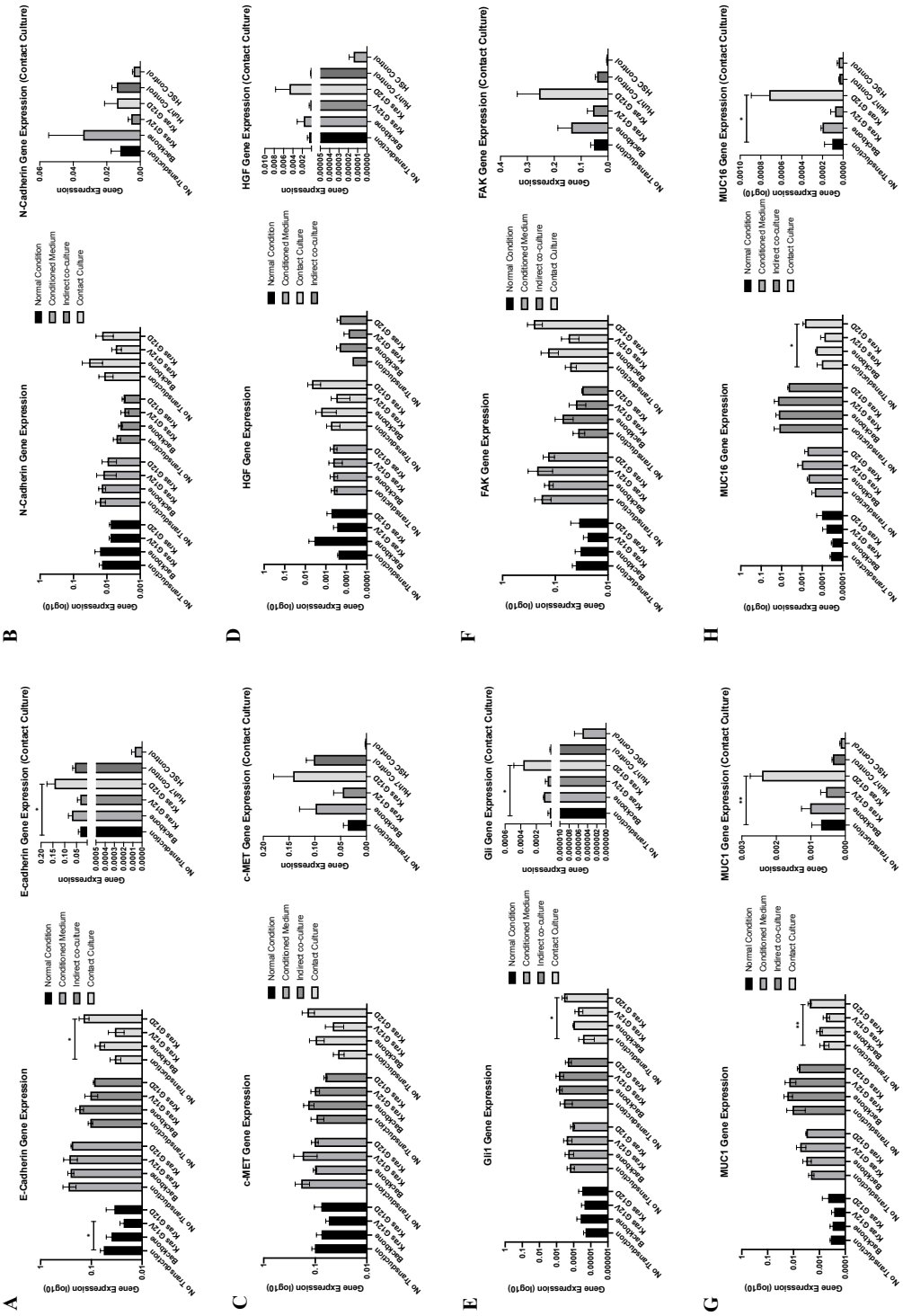

Figure 3.17 continues:

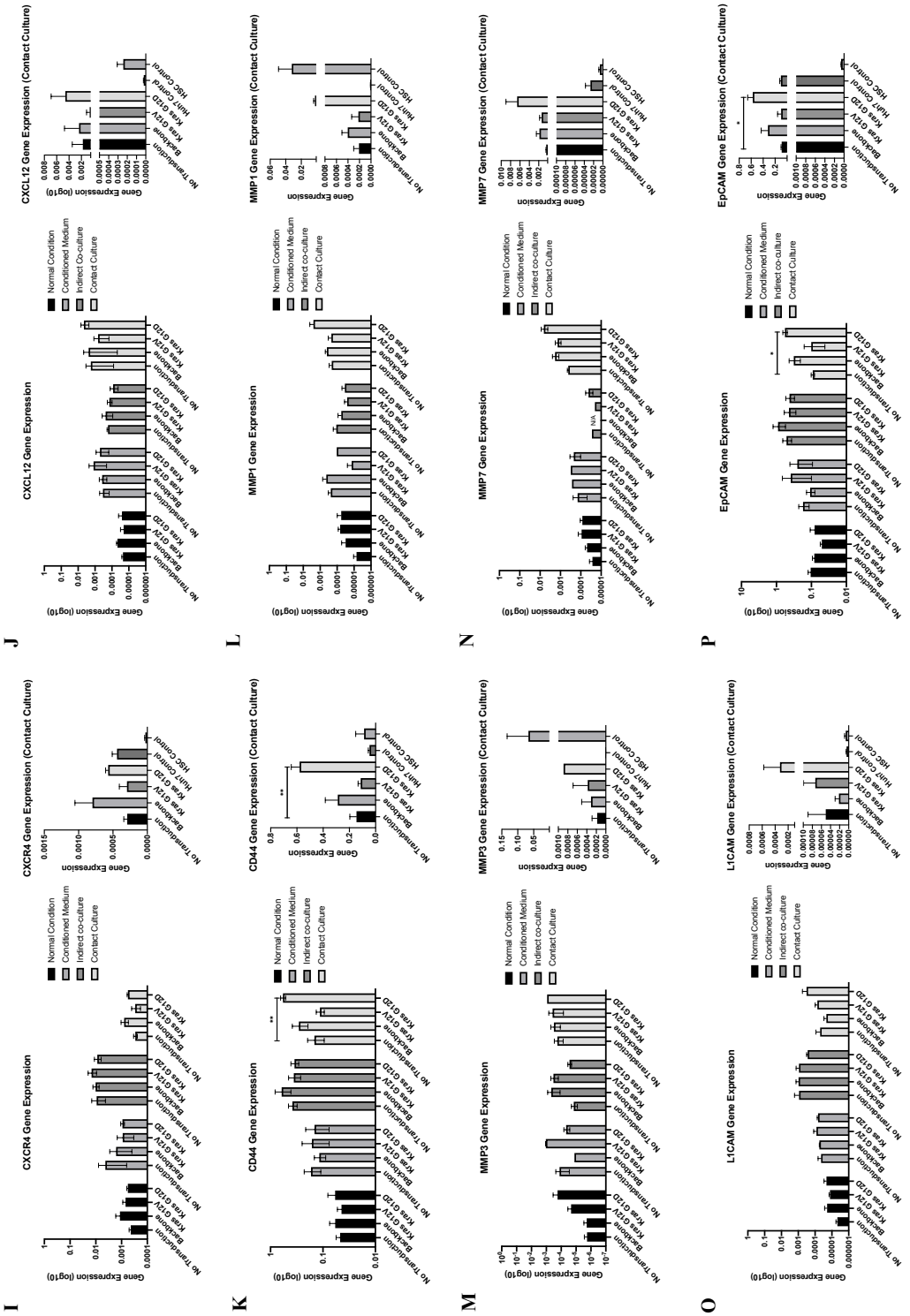

Figure 3.17 continues:

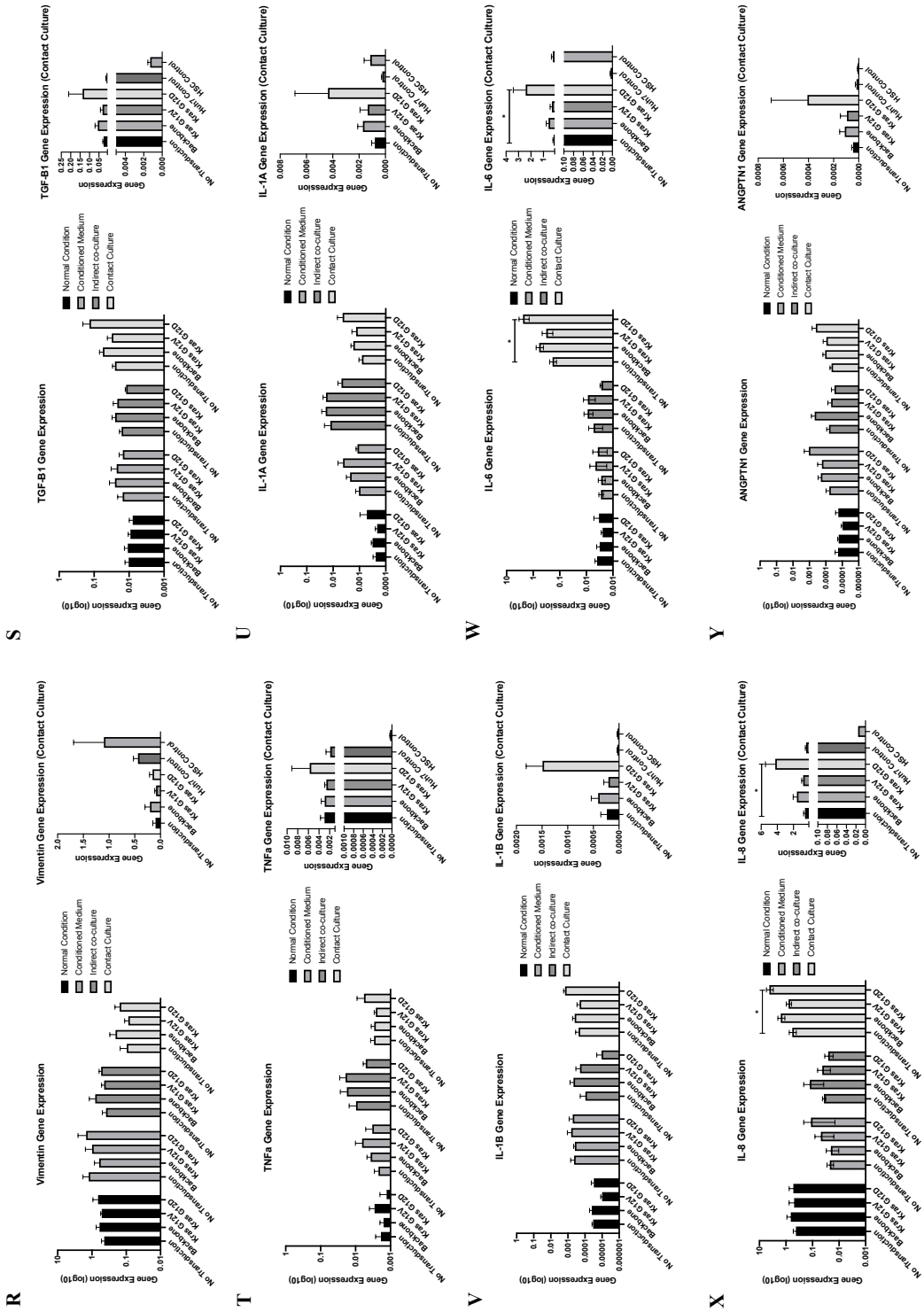

Figure 3.17 continues:

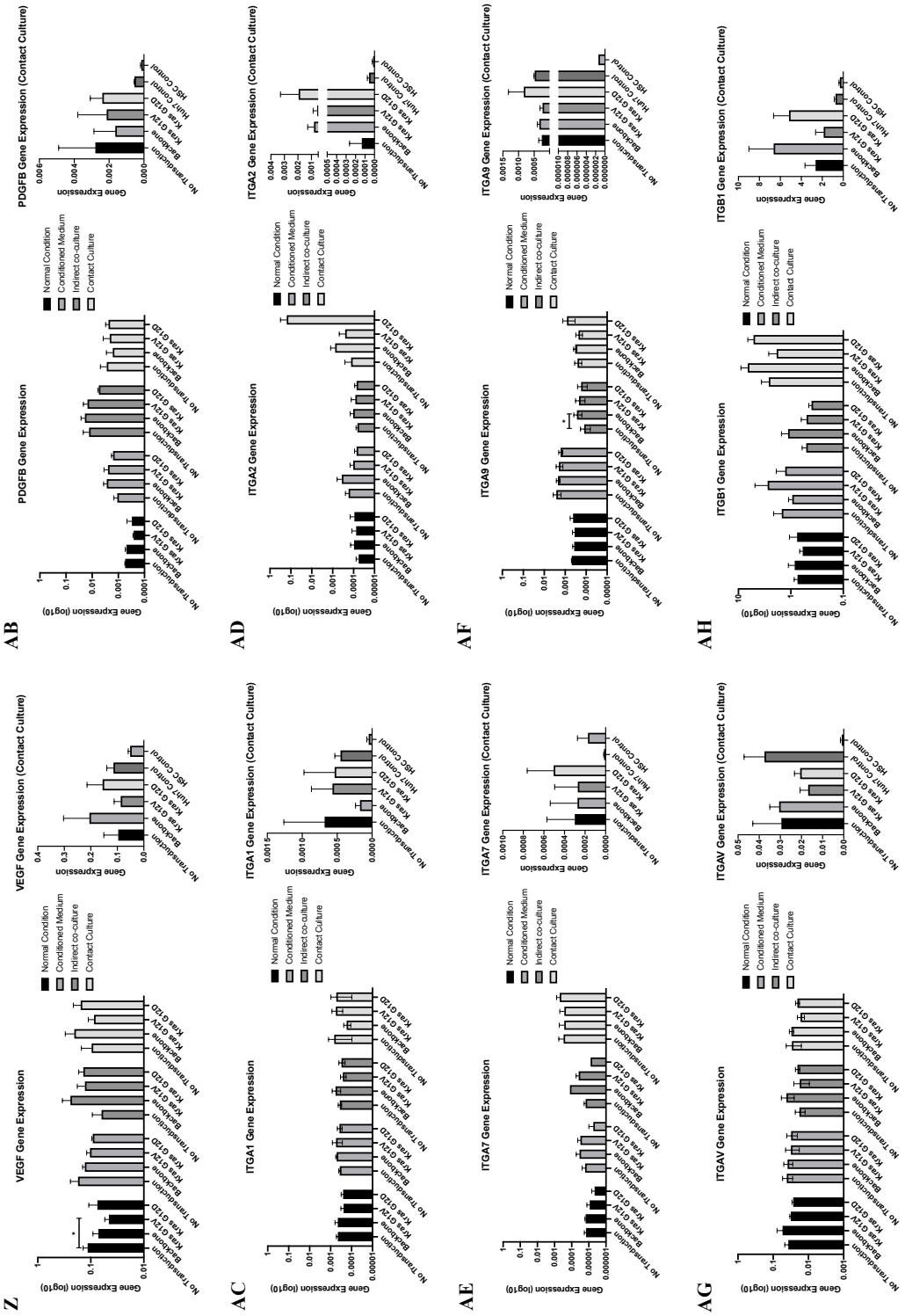

Figure 3.17 continues:

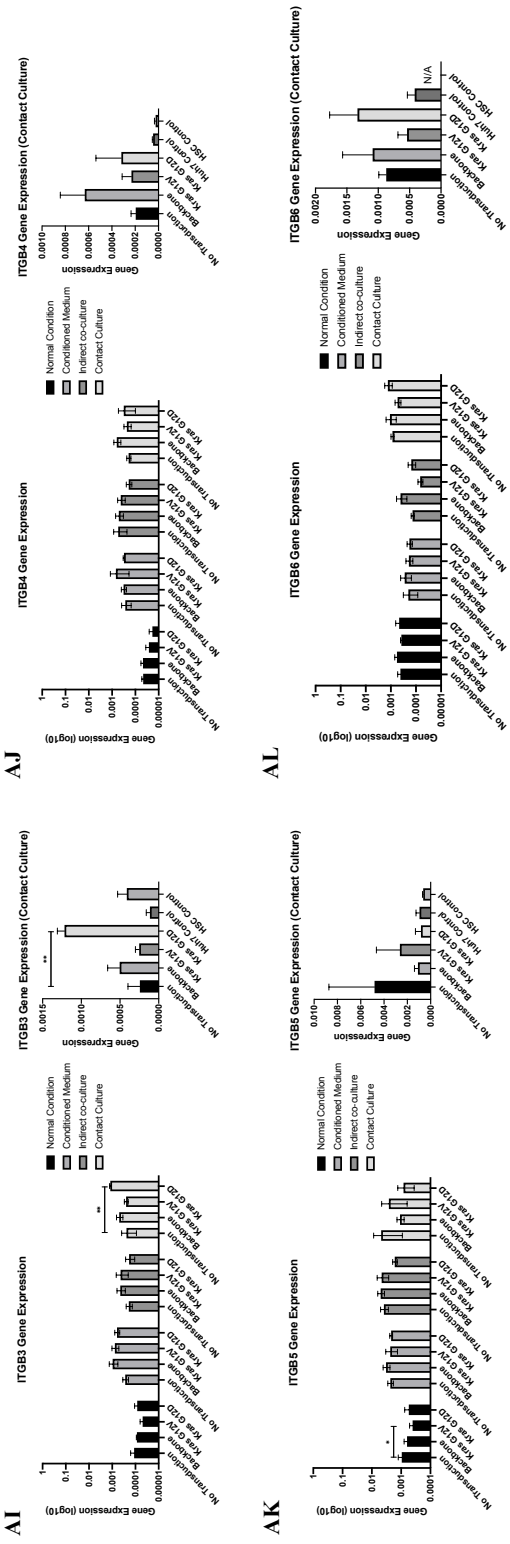

HSC gene expression profile when indirectly co-cultured with HepG2 (left) and Huh7 (right) is shown in Figure 3.18 below. Due to a limited amount of RNA isolated from the co-culture experiment, we were not able to run a large screen in HSC cells. In general, HepG2 and Huh7 almost show a very similar pattern of gene expression induced in HSCs. TGF-β is used as a positive control to increase ECM secretion. Negative control represents the basal level of HSC cells (cultured in serum-free DMEM-F12). Individual gene expressions are shown in Figure 3.19. Since some of the genes, particular to HSCs, were not screened for contact cultures previously, such as α-sma, Col1α1, FN1 and HAS1, their graphs are also included here.

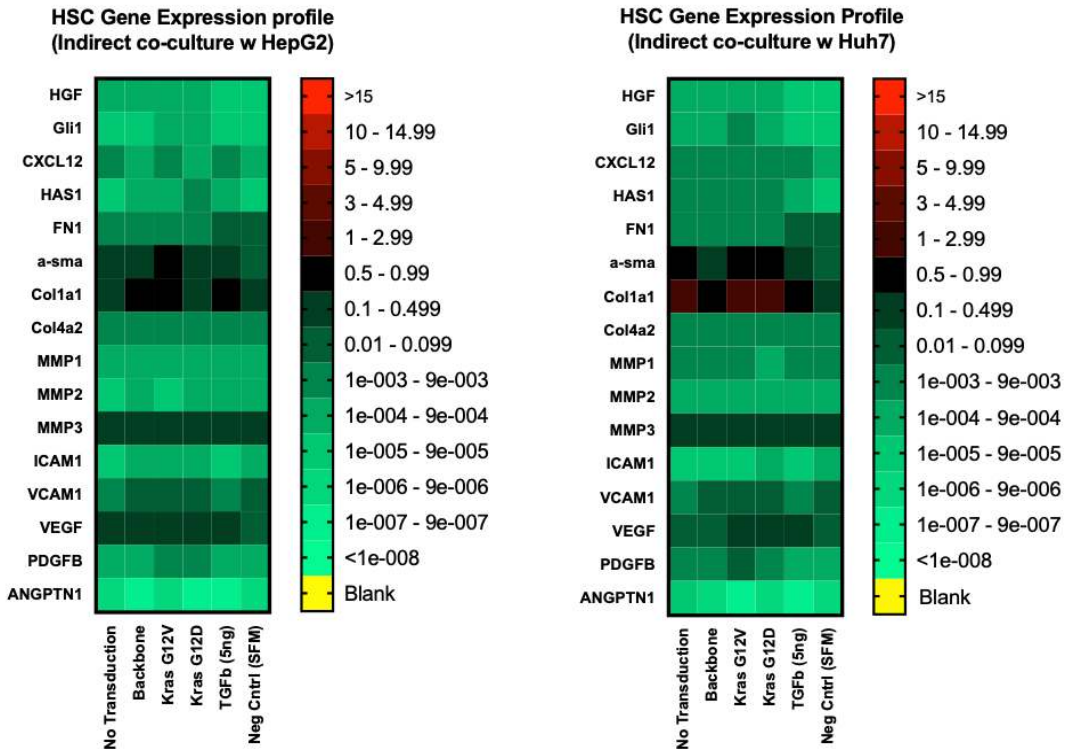

Figure 3.18: HSC gene expression profile co-cultured with HepG2 (left) and Huh7 right)

At first α-sma, col1α1, FN1 and HAS1 (Fig. 3.19 A-D) are investigated to see the fibrotic reaction. α-sma expression in HSC cells when co-cultured with HepG2 G12V is significantly increased compared to HSC negative control.

When HSCs are co-cultured with Huh7, they did not show the same increase, but Huh7 G12V cells, when directly cultured with HSC, showed an increase in α-sma expression compared to HSC control. There is an increase in Col1α1 expression in HSCs when co-cultured with HepG2 G12V compared to the basal level of Col1α1 expression in HSCs. Again, similar to the α-sma pattern, we failed to observe the same effect when HSCs are co-cultured with Huh7 cells. However, when Huh7 G12D and HSC are cultured together, there is a significant increase in Col1α1 expression of Huh7 G12D. FN1 expression is significantly increased in HSCs that are co-cultured with HepG2 G12D compared to HSCs with no transduced HepG2. Interestingly though, FN1 expression is a lot higher at the basal level. Still, we observed a further increase in FN1 expression when HSCs were stimulated with TGF-β. Another interesting result is when HSCs and Huh7 G12D co-cultured FN1 expression has dropped dramatically. HAS1 amplification results in HSC contact cultured with Huh7 were inconclusive; therefore, the data is not included. HAS1 expression is slightly increased when HSCs co-cultured with HepG2 G12V and G12D but did not reach significance. Also, under contact culture conditions, HAS1 expression seemed to increase compared to HSC control, but it was also not significant. When HSCs are co-cultured with Huh7, increased expression was observed, but it appeared to be independent of KRAS transduction. No significant difference is observed in HGF (Fig. 3.19E) expression in HSCs when co-cultured with either HepG2 or Huh7. However, in comparison to HepG2, Huh7 cells seem to be more capable of inducing HGF expression. Gli (Fig. 3.19F) has a very low expression in unstimulated HSCs. Huh7 G12V increased the expression of Gli in HSC cells but not significantly. MMP1 and MMP3 (Fig. 3.19G-H) showed similar patterns when HSCs are co-cultured with HepG2 or Huh7 cells, and neither MMP1 nor MMP3 expression was related to the presence of KRAS mutation. Likewise, VEGF and PDGFβ (Fig. 3.19I-J) showed no significant expression difference between different co-culture conditions.

Figure 3.19: Individual gene expressions in HSCs when indirectly co-cultured with KRAS mutation-induced HepG2 and Huh7 cells. Graphs A, B and C also include contact culture results of HepG2 and Huh7 with HSC.

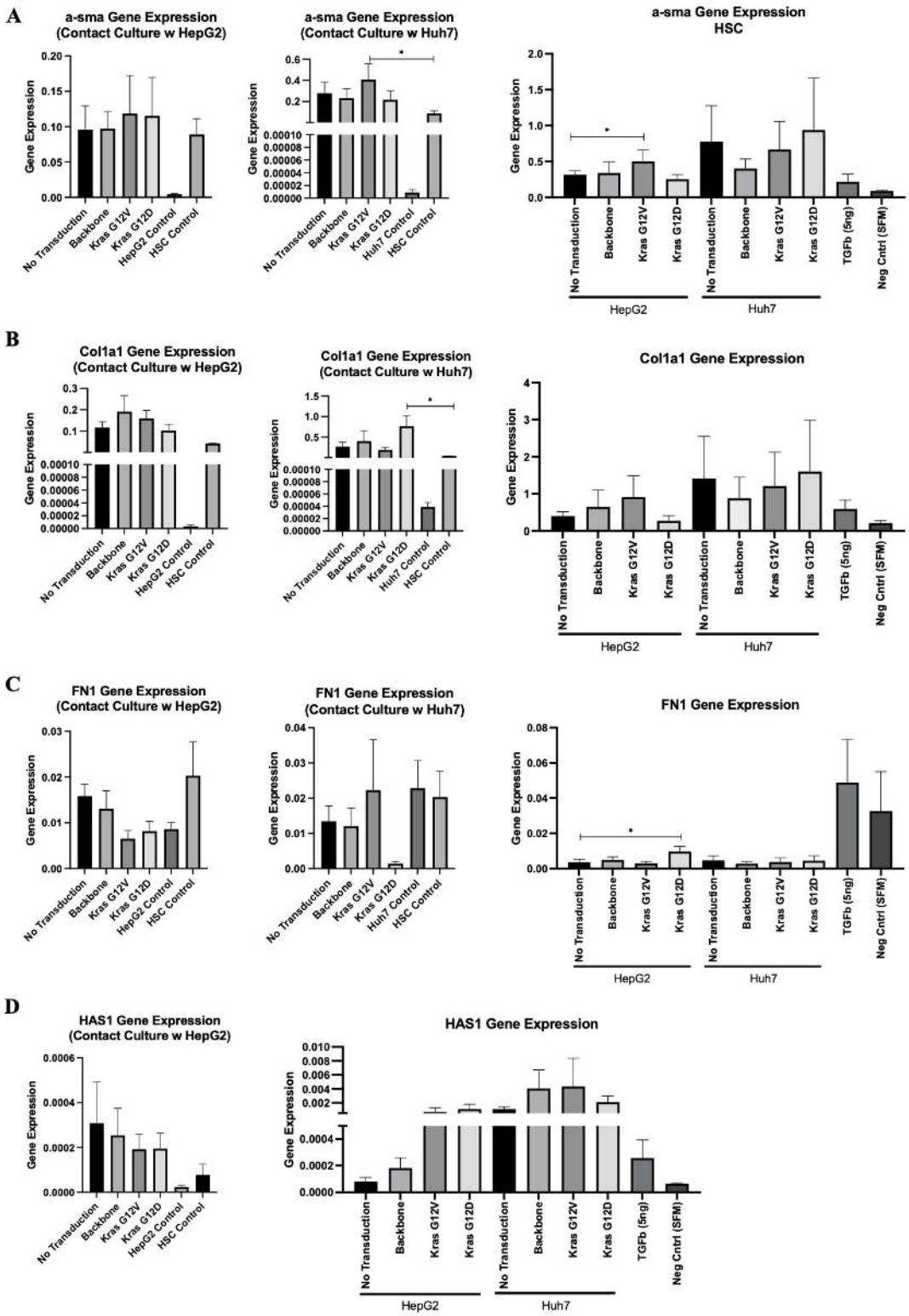

Figure 3.19 continues:

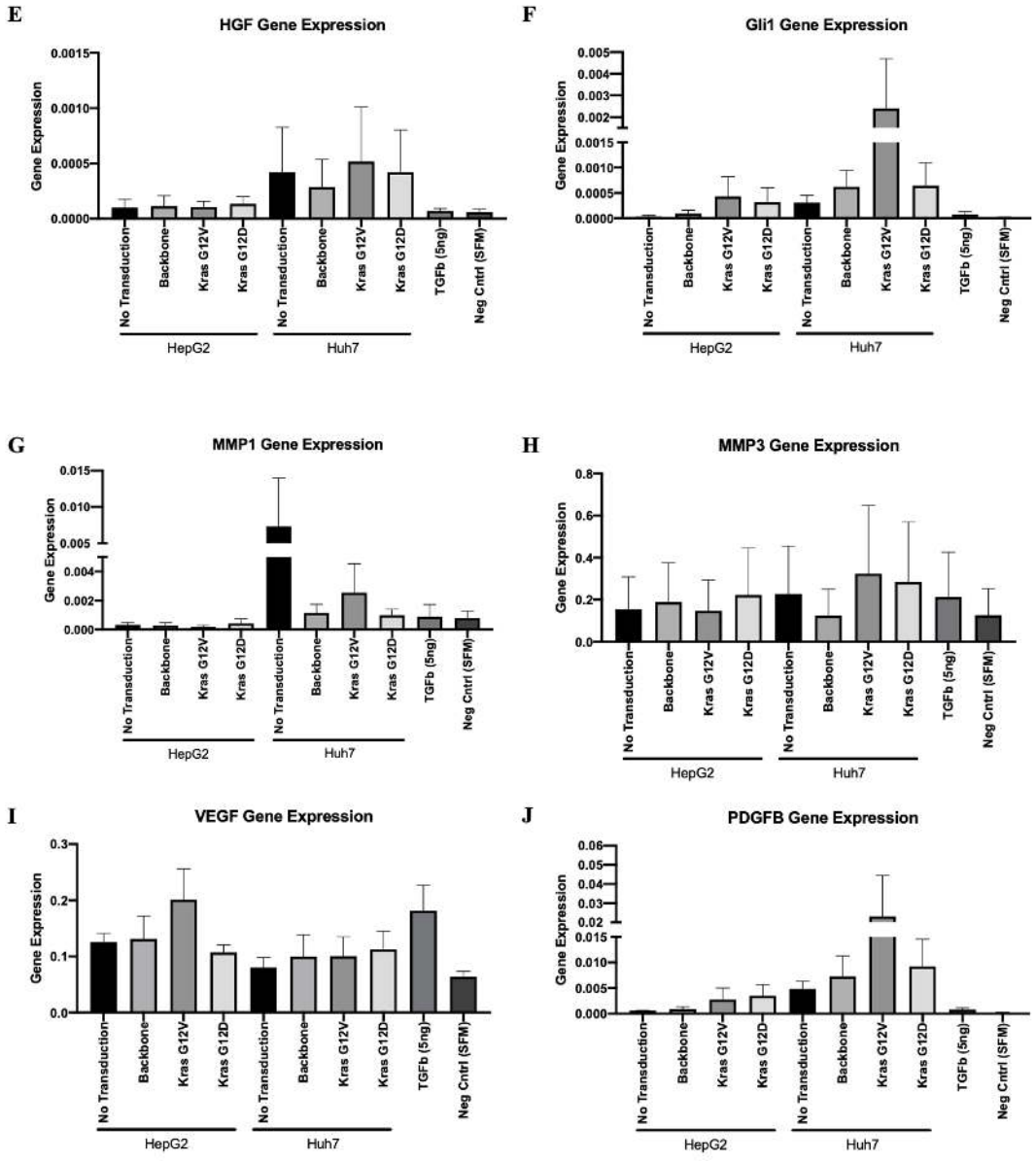

Chapter 4

DISCUSSION

The peritoneum is the site of homing for gastrointestinal cancers such as PDAC, CRC, gastric cancer and gynaecological cancers, mainly ovarian cancer. Since peritoneal mesothelial cells display continuity with ovarian epithelium, ovarian cancer is an example of direct intraperitoneal seeding. However, in case of the gastrointestinal cancers, the cancer cells must go through various biological changes for successful implantation[1]. In literature, peritoneal carcinomatosis steps are divided into four categories: tumour detachment from its primary site, whether spontaneously or iatrogenically, adherence to the surface of the peritoneum, penetration into mesothelial cell surface and invasion of the submesothelial space.

Peritoneal metastasis is often related to disease recurrence and poor prognosis, and yet there is no standardised treatment to eliminate it[43]. Even though the overall mechanism of disease occurrence is known, underlying molecular mechanisms remain vague.

In this project, we formed our hypothesis based on a clinical case of an HCC patient with a tumour rupture. A viable bulk of tumour floated in the peritoneal cavity until it was found during his surgery; however, no peritoneal dissemination was observed at the time of the surgery or in the three years follow-up after the surgery. This clinical case was a great example to illustrate that some cancers might have a predisposition to the peritoneum while others do not. Over a century ago, Paget proposed a theory that cancer, the seed, instead of constituting a random event, predetermined to find its most suitable secondary location, the soil[15]. Premetastatic niche formation is a critical process that cancer uses to prepare its secondary location before arrival. This is accomplished by secreting cytokines, recruiting stromal cells that could help them to proliferate and by hijacking immune responses to survive.

The pre-metastatic niche formation vastly overlaps with the concept of desmoplasia formation in terms of secretion of ECM molecules, forming new blood vessels via recruiting bone-marrow-derived cells or secreting growth factors such as VEGF and CTGF[3]. Therefore, we have investigated what causes these alterations in cancers that frequently metastasise to the peritoneum.

KRAS mutation is frequently seen event in nearly 95% of PDAC and up to 50% of CRC cases[44,45]. It is an initiating event in PDAC, and it induces desmoplasia in the tissue at early stages[44]. KRAS mutation is a widely researched phenomenon in cancer, and the biological changes that it causes in the cancer cells are well known[24,30,31]. KRAS mutation is associated with increased adhesion molecules, activated stromal cells to induce ECM secretion, causing EMT in cells to be more motile and many other documented effects[30,31,36,46,47]. Therefore, we wanted to investigate the role of KRAS mutation in peritoneal dissemination. There have been studies based on clinical evidence that correlates KRAS mutation and pleural dissemination for lung cancer, but there is a gap in the literature for gastrointestinal cancers metastasising to the peritoneum[33,34]. In this research, we investigated the molecular alterations that KRAS mutation cause in the cells to make them more suitable to adhere to peritoneal surfaces. Drawing inspiration from the clinical case mentioned above, along with the peritoneal metastatic cascade, we formed our hypothesis. To test our hypothesis, we induced KRAS mutation in two different HCC cell lines and investigated the biological changes.

KRAS mutation did not affect the cell proliferation, migration, or resistance to anoikis

According to what we observed with the patient, HCC is capable of surviving without attachment to ECM or basement membrane as the tumour, which ruptured from its primary site, stayed viable in the peritoneal cavity. In our model, we expected to see no impact from KRAS induction on the proliferation, migration and anoikis resistance. Through our experiments, we did not observe any significant differences in proliferation, anoikis resistance, colony formation or migration caused by KRAS mutation. Nonetheless, we have observed a significantly higher proliferation rate in cells that are transduced with or without mutation at 48h (Fig 3.4).

This is likely caused by the retroviral transduction itself, in which the viral DNA integrates itself randomly into the cells' chromosomes[48]. When this random integration disrupts a vital gene, these cells induce apoptosis. However, when the viral DNA integrates somewhere less significant for the cell's survival, these cells rescue themselves from apoptosis and may show irregularities, as we observed[48]. We also measured higher sensitivity to anoikis in transduced cells (Fig. 3.4). It is also likely that transduced cells, regardless of the mutation, proliferate at a higher rate compared to non-transduced counterparts, which cause high competition for the resources. The cells that could not access essential supplies eventually would die.

As the first step of the peritoneal metastatic cascade, we often see a decrease or loss of E-Cadherin[11,49]. However, in our case, the tumour exfoliation was caused by forced detachment due to the increased size of the tumour instead of being a spontaneous exfoliation. According to the results we gathered from the screening assay, KRAS transduced cells had decreased expression of E-cadherin (Fig. 3.16A and 3.17A). This indicates that the presence of KRAS mutations in HCC could make cells more motile.

KRAS mutation-induced ECM secretion but not so significantly

HepG2 and Huh7 cells, when co-cultured with HSCs, showed increased collagen and fibronectin secretion compared to the basal level of HSC. According to the results from western blot experiments using HSC supernatants, HSCs that are co-cultured with HepG2 G12D secrete an increased amount of collagen and fibronectin proteins, almost as much as when HSCs are induced with TGF-β (Fig. 3.13). In Huh7 cells, dissimilar to HepG2 cells, Huh7 G12V mutation increased collagen and fibronectin secretion as much as TGF-β. However, we failed to observe the same pattern in gene expression analyses (Fig. 3.19B-C). In contrast to secreted collagen, we observed increased Col1α1 gene expression in HepG2 G12V instead of G12D. Similarly, in Huh7 cells, Huh7 G12D seemed to increase Col1α1 gene expression more than G12V. α-sma as a transdifferentiation marker in HSCs are significantly increased when HSCs are co-cultured with HepG2 G12V when compared to no transduced counterparts (Fig 3.19A). Yet for Huh7, the increase in α-sma appeared to be the same among transduced and no transduced cells.

Interestingly TGF-β highly induced secreted collagen and fibronectin at the protein level, and although it also increased Col1α1 and FN1 gene expression, it was not as pronounced (Fig 3.19C). Another surprising aspect of the initiating desmoplastic reaction in HSCs was that neither HepG2 nor Huh7 cells showed an increased amount of TGF-β expression in our experiment (Fig. 3.16V, 3.17S). Therefore, induction of fibrosis could be mediated by other factors, perhaps by an inflammatory mediator such as IL-1α, IL-1β and IL-6, which all have shown some elevations in Huh7 G12V under contact culture conditions (Fig 3.17U-W). Similarly, HepG2 G12V also induce the expression of IL-1β and IL-6 under contact culture conditions (Fig 3.16Y-Z).

KRAS mutation did not alter adhesion molecules significantly

Integrins are important players for adhesion in peritoneal carcinomatosis. We screened HepG2 and Huh7 cells with or without KRAS mutation for integrin expressions, but we did not observe any significant difference between integrin expression patterns. We included almost all integrins into our panel, but we could not obtain amplification for every one of them because a majority of alpha subunits either was not expressed in HCC cell lines of the primers, we chose for those genes could not be optimised. We also set up all experiments with HSCs instead of mesothelial cells, so that might be the reason we did not observe increased integrin expression. It is unlikely this would be the case because there are a number of similarities between HSCs and mesothelial cells, such as expression of surface adhesion markers ICAM-1 and VCAM-1 and, when activated by a stimulus, the production of cytokines IL-1β, IL-6, VEGF, PDGF, MMPs and the secretion of ECM molecules such as collagen I, III, IV, elastin, fibronectin, laminin, proteoglycans[3].

Evaluation of the pre-metastatic niche formation and desmoplasia formation

The findings obtained in this project gave us information about KRAS mutation and molecular alterations in both HSCs and HCC cells when co-cultured. We employed different co-culture techniques in this project to investigate the effect of proximity between tumour and stromal cells. We observed various trends in gene expressions when different co-culture techniques were involved.

For example, expression of FAK, which is an important determinant for adherence, increased gradually when the interaction with HSCs improved by the proximity in various culture techniques (Fig. 3.16I, 3.17F). Another example is the expression of CXCR4, which is a chemokine receptor that is associated with cancer cell migration and metastasis, dramatically increased when co-cultured with HSCs or its secretome (Fig. 3.16M). Likewise, compared to CD44 expression under normal conditions, its expression increases prominently when co-cultured with HSC or HSC's medium (Fig. 3.16O, 3.17K). These findings were independent of KRAS mutation as all the cells, whether it is transduced or not, showed the same increasing pattern. It is also interesting to observe the TNF-α expression in HepG2 cells where TNF-α increased only when cancer cells were in close contact with HSCs, but not with its secretome (Fig. 3.16W, 3.17T). On the contrary, MMP1 slightly decreased in the cells when they were co-cultured with HSC directly and indirectly (Fig. 3.16R, 3.17L). Analysing the IL-8 expression, we see a decreasing pattern when the cancer cells are incubated with HSC medium or co-cultured with HSCs indirectly. Yet we observe an almost 10-fold increase in the expression when they co-cultured with HSCs directly (Fig. 3.16AB, 3.17X). So even though HSCs and HepG2 alone have a minimal expression of IL-8, when they are in contact, the expression elevates. We were also able to see the different expressions between two HCC cell lines using a variety of co-culture techniques. The CXCR4 expression Huh7 cells have a decreasing pattern when directly cultured with HSCs, while in HepG2, there was a substantial increase.

Chapter 5

CONCLUSION, FUTURE PERSPECTIVES AND WINDOW OF IMPROVEMENTS

The peritoneal carcinomatosis comprises a sequence of complex events starting from tumour detachment from its primary site, surviving in the peritoneal cavity, adherence to mesothelial surface, penetration, and invasion into submesothelial space where it can form a secondary tumour. Since gastrointestinal cancers, particularly PDAC and CRC, have tendencies to metastasise to the peritoneum, we investigated the underlying reasons of this proclivity in our project. We focused on the effect of KRAS mutation, as it is seen in the majority of PDAC and CRC cases, and transduced KRAS mutation to HCC cell lines that lack KRAS mutation to investigate the molecular alterations. Our data partially supported the clinical case we formed our hypothesis, but we were not able to observe definite information about the role of KRAS mutation in HCC cells. Although we investigated a relatively large panel of genes to see the molecular changes in HCC cells, most of the genes were selected from previous reports that studied peritoneal carcinomatosis in other cancer. Our results were difficult to relate to the original studies because our cell line origins were different. In addition to that, we transduced KRAS mutation, which regulates various pathways in the cells, to HCC cells lines that presumably changes cells' behaviour even further. Therefore, a larger screen, even an RNA sequencing (RNAseq), could be more informative about KRAS mutation's real impact on HCC cells. We could not perform RNAseq in this project due to a lack of resources, but it could be something that could be applied later in this project

There were some interesting outcomes of this project, particularly the observing of how stromal cells and cancer cells crosstalk under different conditions.

Even though some of the results we obtained could not reach statistical significance, it provided us with a pattern for future investigation while we improve this project further.

This thesis covers just the *in vitro* part of a larger project. *In vivo* experiments need to be performed to see KRAS transduced cells' behaviour in a permissive host. Extracting the tumour from the host animals would draw a better conclusion about the cell-cell and cell-to-ECM interaction.

REFERENCES

1 Mikula-Pietrasik, J., Uruski, P., Tykarski, A. & Ksiazek, K. The peritoneal "soil" for a cancerous "seed": a comprehensive review of the pathogenesis of intraperitoneal cancer metastases. *Cell Mol Life Sci* **75**, 509-525, doi:10.1007/s00018-017-2663-1 (2018).

2 diZerega, G. S. & Rodgers, K. E. in *The Peritoneum* 1-25 (Springer New York, 1992).

3 Kawanishi, K. Diverse properties of the mesothelial cells in health and disease. *Pleura Peritoneum* **1**, 79-89, doi:10.1515/pp-2016-0009 (2016).

4 Yung, S. & Chan, T. M. Pathophysiological changes to the peritoneal membrane during PD-related peritonitis: the role of mesothelial cells. *Mediators Inflamm* **2012**, 484167, doi:10.1155/2012/484167 (2012).

5 Sugarbaker, P. H. Peritoneum as the first-line of defense in carcinomatosis. *J Surg Oncol* **95**, 93-96, doi:10.1002/jso.20676 (2007).

6 Cortes-Guiral, D. *et al.* Primary and metastatic peritoneal surface malignancies. *Nat Rev Dis Primers* **7**, 91, doi:10.1038/s41572-021-00326-6 (2021).

7 Kranenburg, O., van der Speeten, K. & de Hingh, I. Peritoneal Metastases From Colorectal Cancer: Defining and Addressing the Challenges. *Front Oncol* **11**, 650098, doi:10.3389/fonc.2021.650098 (2021).

8 Jayne, D. Molecular biology of peritoneal carcinomatosis. *Cancer Treat Res* **134**, 21-33, doi:10.1007/978-0-387-48993-3_2 (2007).

9 Ceelen, W. P. & Bracke, M. E. Peritoneal minimal residual disease in colorectal cancer: mechanisms, prevention, and treatment. *Lancet Oncol* **10**, 72-79, doi:10.1016/S1470-2045(08)70335-8 (2009).

10 Lengyel, E. Ovarian cancer development and metastasis. *Am J Pathol* **177**, 1053-1064, doi:10.2353/ajpath.2010.100105 (2010).

11 Sawada, K. *et al.* Loss of E-cadherin promotes ovarian cancer metastasis via alpha 5-integrin, which is a therapeutic target. *Cancer Res* **68**, 2329-2339, doi:10.1158/0008-5472.CAN-07-5167 (2008).

12 Mendonsa, A. M., Na, T. Y. & Gumbiner, B. M. E-cadherin in contact inhibition and cancer. *Oncogene* **37**, 4769-4780, doi:10.1038/s41388-018-0304-2 (2018).

13 Kim, Y. N., Koo, K. H., Sung, J. Y., Yun, U. J. & Kim, H. Anoikis resistance: an essential prerequisite for tumor metastasis. *Int J Cell Biol* **2012**, 306879, doi:10.1155/2012/306879 (2012).

14 Kumar, S. *et al.* A pathway for the control of anoikis sensitivity by E-cadherin and epithelial-to-mesenchymal transition. *Mol Cell Biol* **31**, 4036-4051, doi:10.1128/MCB.01342-10 (2011).

15 Paget, S. The distribution of secondary growths in cancer of the breast. 1889. *Cancer Metastasis Rev* **8**, 98-101 (1989).
16 Lessan, K., Aguiar, D. J., Oegema, T., Siebenson, L. & Skubitz, A. P. CD44 and beta1 integrin mediate ovarian carcinoma cell adhesion to peritoneal mesothelial cells. *Am J Pathol* **154**, 1525-1537, doi:10.1016/s0002-9440(10)65406-5 (1999).
17 Yasumoto, K. *et al.* Role of the CXCL12/CXCR4 axis in peritoneal carcinomatosis of gastric cancer. *Cancer Res* **66**, 2181-2187, doi:10.1158/0008-5472.CAN-05-3393 (2006).
18 Cooper, J. & Giancotti, F. G. Integrin Signaling in Cancer: Mechanotransduction, Stemness, Epithelial Plasticity, and Therapeutic Resistance. *Cancer Cell* **35**, 347-367, doi:10.1016/j.ccell.2019.01.007 (2019).
19 Schlaeppi, M. *et al.* Role of integrins and evidence for two distinct mechanisms mediating human colorectal carcinoma cell interaction with peritoneal mesothelial cells and extracellular matrix. *Cell Adhes Commun* **4**, 439-455, doi:10.3109/15419069709004460 (1997).
20 Takatsuki, H., Komatsu, S., Sano, R., Takada, Y. & Tsuji, T. Adhesion of gastric carcinoma cells to peritoneum mediated by alpha3beta1 integrin (VLA-3). *Cancer Res* **64**, 6065-6070, doi:10.1158/0008-5472.CAN-04-0321 (2004).
21 Ziprin, P., Ridgway, P. F., Pfistermuller, K. L., Peck, D. H. & Darzi, A. W. ICAM-1 mediated tumor-mesothelial cell adhesion is modulated by IL-6 and TNF-alpha: a potential mechanism by which surgical trauma increases peritoneal metastases. *Cell Commun Adhes* **10**, 141-154 (2003).
22 Yonemura, Y. *et al.* A possible role of cytokines in the formation of peritoneal dissemination. *Int J Oncol* **11**, 349-358, doi:10.3892/ijo.11.2.349 (1997).
23 Heath, R. M., Jayne, D. G., O'Leary, R., Morrison, E. E. & Guillou, P. J. Tumour-induced apoptosis in human mesothelial cells: a mechanism of peritoneal invasion by Fas Ligand/Fas interaction. *Br J Cancer* **90**, 1437-1442, doi:10.1038/sj.bjc.6601635 (2004).
24 Buscail, L., Bournet, B. & Cordelier, P. Role of oncogenic KRAS in the diagnosis, prognosis and treatment of pancreatic cancer. *Nat Rev Gastroenterol Hepatol* **17**, 153-168, doi:10.1038/s41575-019-0245-4 (2020).
25 Alamo, P. *et al.* Higher metastatic efficiency of KRas G12V than KRas G13D in a colorectal cancer model. *FASEB J* **29**, 464-476, doi:10.1096/fj.14-262303 (2015).
26 Hunter, J. C. *et al.* Biochemical and Structural Analysis of Common Cancer-Associated KRAS Mutations. *Mol Cancer Res* **13**, 1325-1335, doi:10.1158/1541-7786.MCR-15-0203 (2015).
27 Pylayeva-Gupta, Y., Grabocka, E. & Bar-Sagi, D. RAS oncogenes: weaving a tumorigenic web. *Nat Rev Cancer* **11**, 761-774, doi:10.1038/nrc3106 (2011).
28 Lohr, M., Kloppel, G., Maisonneuve, P., Lowenfels, A. B. & Luttges, J. Frequency of K-ras mutations in pancreatic intraductal neoplasias associated with pancreatic ductal adenocarcinoma and chronic pancreatitis: a meta-analysis. *Neoplasia* **7**, 17-23, doi:10.1593/neo.04445 (2005).
29 Thayer, S. P. *et al.* Hedgehog is an early and late mediator of pancreatic cancer tumorigenesis. *Nature* **425**, 851-856, doi:10.1038/nature02009 (2003).

30 Collins, M. A. *et al.* Oncogenic Kras is required for both the initiation and maintenance of pancreatic cancer in mice. *J Clin Invest* **122**, 639-653, doi:10.1172/JCI59227 (2012).
31 Tape, C. J. *et al.* Oncogenic KRAS Regulates Tumor Cell Signaling via Stromal Reciprocation. *Cell* **165**, 910-920, doi:10.1016/j.cell.2016.03.029 (2016).
32 Ihle, N. T. *et al.* Effect of KRAS oncogene substitutions on protein behavior: implications for signaling and clinical outcome. *J Natl Cancer Inst* **104**, 228-239, doi:10.1093/jnci/djr523 (2012).
33 Raparia, K., Villa, C., Raj, R. & Cagle, P. T. Peripheral lung adenocarcinomas with KRAS mutations are more likely to invade visceral pleura. *Arch Pathol Lab Med* **139**, 189-193, doi:10.5858/arpa.2013-0759-OA (2015).
34 Agalioti, T. *et al.* Mutant KRAS promotes malignant pleural effusion formation. *Nat Commun* **8**, 15205, doi:10.1038/ncomms15205 (2017).
35 Bissell, M. J. & Hines, W. C. Why don't we get more cancer? A proposed role of the microenvironment in restraining cancer progression. *Nat Med* **17**, 320-329, doi:10.1038/nm.2328 (2011).
36 Macias-Perez, I. *et al.* Loss of integrin alpha1beta1 ameliorates Kras-induced lung cancer. *Cancer Res* **68**, 6127-6135, doi:10.1158/0008-5472.CAN-08-1395 (2008).
37 Zhang, K. *et al.* Oncogenic K-Ras upregulates ITGA6 expression via FOSL1 to induce anoikis resistance and synergizes with alphaV-Class integrins to promote EMT. *Oncogene* **36**, 5681-5694, doi:10.1038/onc.2017.177 (2017).
38 Cox, T. R. & Erler, J. T. Molecular pathways: connecting fibrosis and solid tumor metastasis. *Clin Cancer Res* **20**, 3637-3643, doi:10.1158/1078-0432.CCR-13-1059 (2014).
39 Bachem, M. G. *et al.* Identification, culture, and characterization of pancreatic stellate cells in rats and humans. *Gastroenterology* **115**, 421-432 (1998).
40 Bachem, M. G. *et al.* Pancreatic carcinoma cells induce fibrosis by stimulating proliferation and matrix synthesis of stellate cells. *Gastroenterology* **128**, 907-921 (2005).
41 Schneider, E. *et al.* Identification of mediators stimulating proliferation and matrix synthesis of rat pancreatic stellate cells. *Am J Physiol Cell Physiol* **281**, C532-543, doi:10.1152/ajpcell.2001.281.2.C532 (2001).
42 Vis, M. A. M., Ito, K. & Hofmann, S. Impact of Culture Medium on Cellular Interactions in in vitro Co-culture Systems. *Front Bioeng Biotechnol* **8**, 911, doi:10.3389/fbioe.2020.00911 (2020).
43 Sun, F., Feng, M. & Guan, W. Mechanisms of peritoneal dissemination in gastric cancer. *Oncol Lett* **14**, 6991-6998, doi:10.3892/ol.2017.7149 (2017).
44 Waters, A. M. & Der, C. J. KRAS: The Critical Driver and Therapeutic Target for Pancreatic Cancer. *Cold Spring Harb Perspect Med* **8**, doi:10.1101/cshperspect.a031435 (2018).
45 Zocche, D. M., Ramirez, C., Fontao, F. M., Costa, L. D. & Redal, M. A. Global impact of KRAS mutation patterns in FOLFOX treated metastatic colorectal cancer. *Front Genet* **6**, 116, doi:10.3389/fgene.2015.00116 (2015).
46 Brannon, A., 3rd *et al.* Beta 1 integrin signaling mediates pancreatic ductal adenocarcinoma resistance to MEK inhibition. *Sci Rep* **10**, 11133, doi:10.1038/s41598-020-67814-9 (2020).

47 Pollock, C. B., Shirasawa, S., Sasazuki, T., Kolch, W. & Dhillon, A. S. Oncogenic K-RAS is required to maintain changes in cytoskeletal organization, adhesion, and motility in colon cancer cells. *Cancer Res* **65**, 1244-1250, doi:10.1158/0008-5472.CAN-04-1911 (2005).

48 Skalka, A. M. & Katz, R. A. Retroviral DNA integration and the DNA damage response. *Cell Death Differ* **12 Suppl 1**, 971-978, doi:10.1038/sj.cdd.4401573 (2005).

49 Pecina-Slaus, N. Tumor suppressor gene E-cadherin and its role in normal and malignant cells. *Cancer Cell Int* **3**, 17, doi:10.1186/1475-2867-3-17 (2003).

Appendix A

Rumelifeneri Yolu Sarıyer 34450 İstanbul T: 0212 338 10 00 F: 0212 338 12 05 www.ku.edu.tr

KOÇ ÜNİVERSİTESİ

ETİK KURUL KARARI

Toplantı Tarihi:	14.06.2017
Karar No:	2017.085.IRB2.026
Sorumlu Araştırıcı:	Burcu Akpınar
Araştırma Başlığı:	Translational Assessment Of Echionococcus Granulosus Elicited - Host Mediated Fibrogenic And Immunogenic Responses
Başlangıç tarihi:	20.06.2017
Etik Kurul izninin süresi:	1 yıl (Uzatma hakkı mevcut olarak)

Koç Üniversitesi Etik Kurulu'na değerlendirilmek üzere başvuruda bulunduğunuz yukarıda künyesi yazılı projenizin başvuru dosyası ve ilgili belgeleri, Üniversitemiz **"Biyomedikal Araştırmalar Etik Kurulu"** tarafından araştırmanın gerekçe, amaç, yaklaşım ve yöntemleri dikkate alınarak incelenmiştir.

Yapılan inceleme sonucunda çalışmanın gerçekleştirilmesinde etik ve bilimsel sakınca bulunmadığına karar verilmiştir.

Notlar:

- Araştırma başlangıç tarihinin 6 aydan daha fazla gecikmesi durumunda Etik Kurul'a başvurularak tarihlerin değiştirilmesi gereklidir.
- Etik Kurul incelemesi ve onayı olmadan bu araştırmada kullanılan prosedürler, formlar ya da protokollerde herhangi bir değişiklik yapılamaz.
- Etik bakımdan sorun çıkması ya da şüpheli bir olay/beklenmeyen etki görülmesi durumunda derhal etik kurul bilgilendirilmelidir.
- Araştırmanın gerçekleştirileceği birimlerin yöneticilerinden de ayrıca izin alınması gerekli olabilir.

Saygılarımla,

Hakan S. Orer
Başkan

Koç Üniversitesi Etik Kurulları Sekreteryası T: 0212 338 11 76 chr@ku.edu.tr

Appendix B

Stellate cell isolation- Nycodenz density gradient centrifugation

Mince the tissue with scalpels until the tissue completely disintegrate.
Prepare the transfer medium for digestion. Add:
- 0.1% Collagenase P (for pancreas); 0.01% Collagenase IV (for liver)
- 0.1% Pronase
- 0.1% DNAse I
(See the enzyme preparation below)*

Filter through 0.22um filters into a sterile beaker with glass beads and a magnet.

Add minced tissues into a beaker and seal well with paraffin.

Digest tissues at 37C incubator on a magnetic stirrer for 30 mins. (The duration of the digestion can vary depending on tissue size, texture or stiffness, and type).

Prepare Nycodenz and BSA solutions. (See the method below)**

By the end of digestion, add 10ml PSC medium to inactivate enzyme activity and filter through a nylon mesh (sterile, attached to a beaker). Use a cell scraper to create a well to strain all the liquid.

Transfer supernatant into a 50ml falcon tube, top-up to 50 ml with GBSS-positive and centrifuge at 600g for 10mins at 4C (AC:10 DC:10)

Aspirate the supernatant. Wash the pellet with 50ml GBSS-positive and centrifuge at 600g for 6mins at 4C (AC:10 DC:10).

Aspirate the supernatant completely and add:

- 4.75ml BSA solution to the cell pellet and mix well. Make sure the mixture is homogenous looking.
- 4ml Nycodenz solution slowly.

Transfer cell suspension to 15ml falcon tube. (Better layer can be obtained with small tube).

On top of this mixture, add 3ml 0.3% BSA with a plastic Pasteur pipette dropwise, very slowly and carefully, as this step will create the gradient for the cell separation.

Centrifuge the tubes at 1400g for 20mins at 4C (AC:5 DC:0, brakes off).
By the end of centrifugation, there will be a pellet in the bottom of the tube and a layer as a buffy coat that contains PSC-HSC.

We collect the cells from the layer with a plastic Pasteur pipette in a 15ml falcon tube. Also, aspirate all supernatant collect pellet. (Pellet also contains stellate cells although when we culture these cells, we need to separate them as pellet and layer)

Wash pellet and layer with 15ml GBSS-positive twice and centrifuge at 600g for 5 mins at each time.

Suspend cells in 2.5ml pre-warmed PSC medium (7.5ml for T75 flasks) and seed into gelatine-coated T25 flasks.

NOTE: Gelatine coating improved PSC-HSC attachment to the flasks' surface; therefore, we coat flasks 1% gelatine prior to use.

Gey's Balanced Salt Solution (GBSS+ and GBSS-):

Chemical		**1L solution**	**2L solution**
$MgCl_2.6H_20$	Magnesium chloride hexahydrate	0.21 g	0.42 g
$MgSO_4$	Magnesium sulphate	0.0342 g	0.0684 g
KCl	Potassium chloride	0.37 g	0.74 g
KH_2PO_4 (anhydrous)	Potassium phosphate monobasic	0.03 g	0.06 g
Na_2HPO_4 (anhydrous)	Sodium phosphate dibasic	0.1196 g	0.2392 g
$NaHCO_3$	Sodium bicarbonate	2.27 g	4.5 g
D-Glucose	Glucose	1	2 g
NaCl*	Sodium chloride	7	14 g
$CaCl_2$**	Calcium chloride	0.2252 g	0.4504 g

* **NaCl** is **ONLY** used in **GBSS-positive.**

** Mix all substances in distilled water and then add **$CaCl_2$** dissolved in 2ml ddH_2O **dropwise and carefully** with a plastic Pasteur pipette. If not, $CaCl_2$ precipitates. Be extra careful when preparing GBSS-negative, as its pH is more sensitive to $CaCl_2$ addition.

Adjust the pH of the solutions between 7.3 - 7.4 and store at 4C fridge. Use within a month.

Solutions for gradient:

Nycodenz solution (28.3%):

Dissolve 5.74g Nycodenz completely in 20ml GBSS-negative.
Filter through 0.22um filter and store at 4C until use.
Prepare freshly and use within 24h.

BSA solution (0.3%)

Dissolve 60mg BSA in 20ml GBSS-positive.
Filter through 0.22um filter and store at 4C until use.
Prepare freshly and use within 24h.

Enzymes:

Collagenase P
Conc: 100mg/ml
Dissolve in GBSS+ and aliquot as 20uL per vial.

Collagenase IV
Conc: 10mg/ml
Dissolve in dPBS and aliquot as 20uL per vial.

Pronase
Conc: 100mg/ml
Dissolve in nuclease-free water and aliquot as 20uL per vial.

DNAse I
Conc: 10mg/ml
Dissolve in nuclease-free water and aliquot as 20uL per vial.